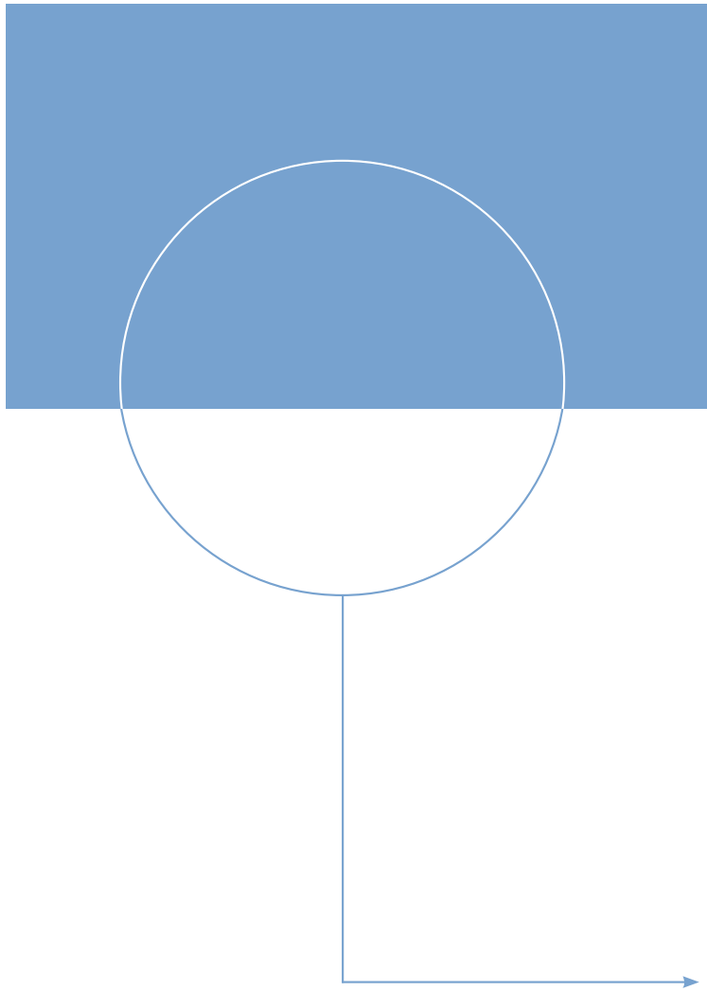

Master's thesis

2020

Bjarte Grindheim

**NTNU**
Norwegian University of
Science and Technology
Faculty of Engineering
Department of Geoscience and Petroleum

Bjarte Grindheim

# Mapping of Shrinkage Cracks with Dye Penetrant on Sprayed Concrete Cores

July 2020

NTNU
Norwegian University of
Science and Technology

NTNU
Norwegian University of
Science and Technology

NTNU
Norwegian University of
Science and Technology

# Mapping of Shrinkage Cracks with Dye Penetrant on Sprayed Concrete Cores

Bjarte Grindheim

Geotechnology
Submission date: July 2020
Supervisor: Eivind Grøv

Norwegian University of Science and Technology
Department of Geoscience and Petroleum

**Norges teknisk-naturvitenskapelige universitet**
**NTNU**

**Fakultet for ingeniørvitenskap og teknologi**
**Studieprogram Geofag og petroleumsteknologi**

## *MASTEROPPGAVEN*

***Kandidatens navn:*** Bjarte Grindheim

***Oppgavens tittel:*** Kartlegging av svinnriss med dye penetrant på sprøytebetongkjerner

***English title:*** Mapping of Shrinkage Cracks with Dye Penetrant on Sprayed Concrete Cores

***Utfyllende tekst:*** I oppgåva skal ein ny metode for å kartlegge svinnriss på overflata til sprøytebetongkjernar testast. Svinnriss kan oppstå når betong krympar under herdinga og ikkje får deformera seg fritt. Dette er svakheita i sprøytebetongen som kan minke styrken og haldbarheita. Metoden som vert nytta er dye penetrant som har vorte brukt på kjernar frå berg med godt hell i doktorgrada til Solveig Vassenden.

Riss kartlegginga skal prøvast å koplast opp mot trykkfastheita og fiberinnhaldet til sprøytebetongkjernane. Dette for å sjå om mengda riss avhenger av fiberinnhaldet i sprøytebetongen og om styrken avhenger av mengda riss eller storleiken på rissa.

Arbeidet skal gjerast i laboratoria åt NTNU IGP.

Oppgåva utførast saman med utvalde samarbeidsgrupper i det NFR-støtta prosjektet SUPERCON.

Ansvarlig faglærer og hovedveileder for oppgaven er prof. II Eivind Grøv, Institutt for geologi og bergteknikk.

***Studieretning:*** Teknisk geologi

***Hovedprofil:*** Ingeniørgeologi/bergteknikk

***Tidsrom:*** 15.01.2020-10.07.2020

Grøv Eivind
Digitally signed by Grøv Eivind
DN: cn=Grøv Eivind
Date: 2020.05.18 18:40:16 +02'00'

*Eivind Grøv*
*Faglærer*

***SKJEMAET TAS INN SOM SIDE 1 I MASTEROPPGAVEN***
***NTNU, 16 mai 2020***

# Abstract

A new method to map shrinkage cracks on sprayed concrete cores has been tested in this master's thesis. This was done with dye penetrant. The method is a non-destructive test method on sprayed concrete cores. All the testing was done on sprayed concrete cores from the road project Nordøyvegen. It was done in cooperation with the research project SUPERCON.

Chapter 2 is a literature review on sprayed concrete and shrinkage cracking. It starts with constituents of sprayed concrete, spraying technique, and hardening. This builds up an understanding of what factors affects the sprayed concretes abilities. Then it looks on how and why sprayed concrete starts to shrink and crack. The section shows the different ways concrete shrinks. The different types of shrinkage are plastic-, autogenous-, thermal- and drying shrinkage. The adhesion between sprayed concrete and the rock surface was investigated. The investigation showed how the bond strength affected the cracking. In the end of the chapter, it looks on self-healing and how to mitigate shrinkage.

The methods used are explained in chapter 3. It starts with a description of the project the sprayed concrete cores came from, Fv. 659 Nordøyvegen. The method used for sampling the cores is explained. The mix design of the sprayed concrete is presented. Then all the lab tests are described. The tests conducted were dye penetrant inspection, uniaxial compressive strength, density, and fibre content measurements. It ends with an explanation on how the rock mass under the sprayed concrete was classified.

The testing showed that the dye penetrant had low sensitivity to mapping cracks in sprayed concrete. Only a few cracks became visible. The compressive strength testing showed the sprayed concrete had a strength much higher than the strength class. The fibre content and density in the cores was lower than in the mix design. The rock mass was of good quality at the locations where the cores were taken from.

The test results were analysed. The analysis indicated that the number of cracks and rock mass affected the compressive strength of the sprayed concrete. More cracks or a better rock mass quality lowers the strength of the sprayed concrete. The rock mass influenced the density and the fibre content of the sprayed concrete. Higher rock mass qualities gave lower densities and fibre content in the sprayed concrete cores.

It was concluded that the dye penetrant test method is not suitable for mapping shrinkage cracks on sprayed concrete cores. Higher rock mass qualities gave lower sprayed concrete strength, compared to lower rock mass qualities.

The last chapter comes with suggestions on further work. The suggestions are things that can be done to increase the understanding of shrinkage cracks in sprayed concrete.

# Samandrag

Ein ny metode for kartlegging av svinnriss på sprøytebetongkjernar blei testa i denne masteroppgåva. Dette vart gjort med penetrantvæske med fargemiddel. Metoden er ein ikkje-destruktiv test metode på sprøytebetongkjernar. All testing vart utført på sprøytebetongkjernar frå Nordøyvegen. Dette vart gjort i samarbeid med forskingsprosjektet SUPERCON.

Kapittel 2 er eit litteraturstudie på sprøytebetong og svinnriss. Det startar med å sjå på bestanddelane til sprøytebetong, sprøyteteknikk og herding. Dette er for å bygge opp ei forståing på kva faktorar som påverkar eigenskapane til sprøytebetong. Deretter ser det på korleis og kvifor sprøytebetong startar å krympe og sprekke opp. Ulike typar svinn vert vist. Dei forskjellige typane svinn er plastisk-, autogent-, termisk- og uttørkingssvinn. Ein ser på korleis sprøytebetong festar seg til overflata og korleis dette påverkar rissa. På slutten av kapitelet vert det sett på sjølvlæking og måtar å minke svinn.

Metodane som vart nytta er forklart i kapittel 3. Det startar med ei beskriving av prosjektet sprøytebetongkjernane kom frå, Fv. 659 Nordøyvegen. Metoden brukt for å ta ut kjernane vert forklart. Resepten til sprøytebetongen vert presentert. Deretter vert alle testane beskriven. Testane som vart utført var penetrantvæske med fargemiddel, einaksiell trykkfastheit, måling av tettleik og fiberinnhald. Det vert avslutta med å forklara korleis bergmassen under sprøytebetongen vart klassifisert.

Testinga viste at penetrantvæska med fargemiddel hadde lite sensitivitet til å kartlegge sprekker i sprøytebetong. Berre nokre få sprekker vart synlege. Einaksielle trykktestinga viste at sprøytebetongen hadde ein styrke som var mykje høgare enn fastheitsklassen. Fiberinnhaldet og tettleiken i kjernane var lågare enn i resepten. Bergmassen hadde god kvalitet på lokasjonane kjernane vart tatt ut.

I analysen av test resultata kom det indikasjonar på at mengda riss og bergmassen påverka fastheita til sprøytebetongen. Fleire riss eller ein betre bergmassekvalitet minka fastheita til sprøytebetongen. Bergmassen påverka tettleiken og fiberinnhaldet i sprøytebetongen. Betre bergmassekvalitet gav lågare tettleik og fiberinnhald i sprøytebetongkjernane.

Det vart konkludert med at testinga med penetrantvæske ikkje var egna for å kartlegge svinnriss på sprøytebetongkjernar. Betre bergmassekvalitet gav lågare styrke på sprøytebetong, samanlikna med dårlegare bergmassekvalitet.

Det siste kapitelet kjem med forslag til vidare arbeid som kan bli gjort for å betra forståinga av svinnriss i sprøytebetong.

# Preface

This master's thesis is the last project of a five-year master's program at NTNU in geotechnology. The writhing has been a long and at times frustrating process, especially with the COVID-19 pandemic that happened during the semester. The pandemic delayed the progress. Norway went into lockdown, and the labs were closed for over a month. The re-opening of the labs had strict restrictions to whom could get access.

The topic in this thesis is sprayed concrete. Sprayed concrete is very much used in tunnelling, but the topic sprayed concrete had little emphasis in the master's program. Therefore, it was interesting to specialise in this topic. My knowledge on the topic has increased drastically through the work on this project.

Hopefully, this project can help the SUPERCON research project. It also aims to help the understanding of other engineering geologists on sprayed concrete. The thesis shows that sprayed concrete is a complicated topic, and that the quality of the tunnel lining is affected by many factors.

I want to thank my supervisor Eivind Grøv for including me in the research program SUPERCON. He helped me through his network. This gave me relevant contacts for my work. He always answered the questions I had along the way. I also want to thank Nicholas Henry Trussel, for taking time to help me during his PhD-studies.

The research would not have been possible without the sprayed concrete cores from Nordøyvegen. I must thank Jan-Erik Hetlebakke and Entreprenørservice for getting me the cores. The guys at the rock mechanics lab at NTNU, Gunnar Vistnes and Jon Runar Drotninghaug, deserves a big thanks for conducting all the lab tests.

Written in cooperation with SUPERCON.

Bjarte Grindheim, Trondheim, July 7, 2020

# Contents

# Figures

# Tables

# Legend

| | | |
|---|---|---|
| **1** | | |
| c/c | = | Center to center |
| ø20 | = | Diameter of 20 mm |
| SUPERCON | = | Sprayed sUstainable PErmanent Robotized CONcrete tunnel lining |
| UCS | = | Uniaxial compressive strength |
| **2.1** | | |
| ACI | = | American Concrete Institute |
| OPC | = | Ordinary Portland cement |
| w/b | = | Water-binder ratio |
| **2.2** | | |
| EFNARC | = | European Federation of National Associations Representing producers and applicators of specialist building products for Concrete |
| **2.3** | | |
| S | = | Silica, $SiO_2$ |
| C | = | Calcium oxide, CaO |
| A | = | Aluminate, $Al_2O_3$ |
| F | = | Iron oxide, $Fe_2O_3$ |
| H | = | Water, $H_2O$ |
| **2.4** | | |
| w/c | = | Water-cement ratio |
| $\epsilon_T$ | = | Strain from temperature change |
| $\alpha_C$ | = | Coefficient of thermal expansion (1/°C) |
| $\Delta T$ | = | Temperature change (°C) |
| $T_i$ | = | Initial placing temperature (°C) |
| $T_{ad}$ | = | Adiabatic temperature rise (°C) |
| $T_{env}$ | = | Temperature change from heat added/removed from environment (°C) |
| $T_f$ | = | Final stable temperature (°C) |
| $r_m$ | = | Radii meniscus ($\mu m$) |
| $r_L$ | = | Radii of large pore ($\mu m$) |
| $\delta$ | = | Thickness of liquid film on pore wall ($\mu m$) |
| **2.5** | | |
| E | = | Evaporation rate ($kg/m^2/h$) |
| $T_c$ | = | Concrete temperature (°C) |
| $T_a$ | = | Air temperature (°C) |
| r | = | Relative humidity (%) |
| V | = | Wind velocity (km/h) |

**2.6**

| | | |
|---|---|---|
| v | = | Flow rate (m/s) |
| q | = | Crack transmissivity ($m^2/s$) |
| e | = | Crack width (m) |
| i | = | Effective hydraulic gradient |
| $\rho$ | = | Density of fluid ($kg/m^3$) |
| g | = | Gravity ($m/s^2$) |
| $\mu$ | = | Viscosity of fluid (Pa*s) |
| $\nu$ | = | Kinematic viscosity of fluid ($m^2/s$) |

**2.8**

| | | |
|---|---|---|
| SRA | = | Shrinkage reducing admixtures |
| CRA | = | Crack-reducing admixtures |
| SAP | = | Superabsorbent polymers |

**3.1**

| | | |
|---|---|---|
| NOK | = | Norwegian Krone |

**3.2**

| | | |
|---|---|---|
| L/d | = | Length-diameter ratio |

**3.5**

| | | |
|---|---|---|
| TBM | = | Tunnel boring machine |

**3.6**

| | | |
|---|---|---|
| $f_{c,cyl}$ | = | Compressive strength cylinder (MPa) |
| $\chi_{c,cyl}$ | = | Correction factor |
| F | = | Maximum load during compression (N) |
| $A_C$ | = | Pressed area of cylinder ($mm^2$) |
| L | = | Cylinder length (mm) |
| d | = | Cylinder diameter (mm) |

**3.7**

| | | |
|---|---|---|
| D | = | Density ($kg/m^3$) |
| m | = | Mass (g) |
| V | = | Volume ($cm^3$) |

**3.8**

| | | |
|---|---|---|
| $C_f$ | = | Fibre content ($kg/m^3$) |
| m | = | mass of fibre (g) |
| V | = | Volume of test sample ($cm^3$) |

**3.9**

| | | |
|---|---|---|
| RQD | = | Rock quality designation |
| $J_n$ | = | Joint set number |
| $J_r$ | = | Joint roughness number |
| $J_a$ | = | Joint alteration number |
| $J_w$ | = | Joint water reduction factor |
| SRF | = | Stress reduction factor |

# 1 Introduction

This master's thesis in engineering geology and rock mechanics investigates sprayed concrete, with emphasis on cracking in sprayed concrete lining in tunnels. Sprayed concrete is part of the concrete field. Many of the users are part of other fields as construction or engineering geology (NB 2011). Today, sprayed concrete is one of the most important elements for rock support when building underground tunnels and caverns (NFF 2008).

Sprayed concrete is a big part of the price when building a tunnel. Nilsen (2016) investigated prices of different rock support methods. These are gathered in figure 1. The prices should be considered as average numbers. The numbers may deviate a lot in some circumstances as costs deviate from tender offer to tender offer. Figure 1 shows that 10 cm of reinforced sprayed concrete on average costs 1.6 - 1.8 times the blasting costs. Large amounts of sprayed concrete are used in Norwegian road tunnels. Table 1 presents the permanent rock support categories in Norwegian road tunnels. The table shows that 8 cm of reinforce sprayed concrete should always be used, and if the rock mass quality is bad a larger thickness should be used. It can be seen that sprayed concrete is a larger cost than blasting in Norwegian road tunnels if figure 1 and table 1 is combined. From this information an assumption can be made, that sprayed concrete is one of the largest costs in tunnelling.

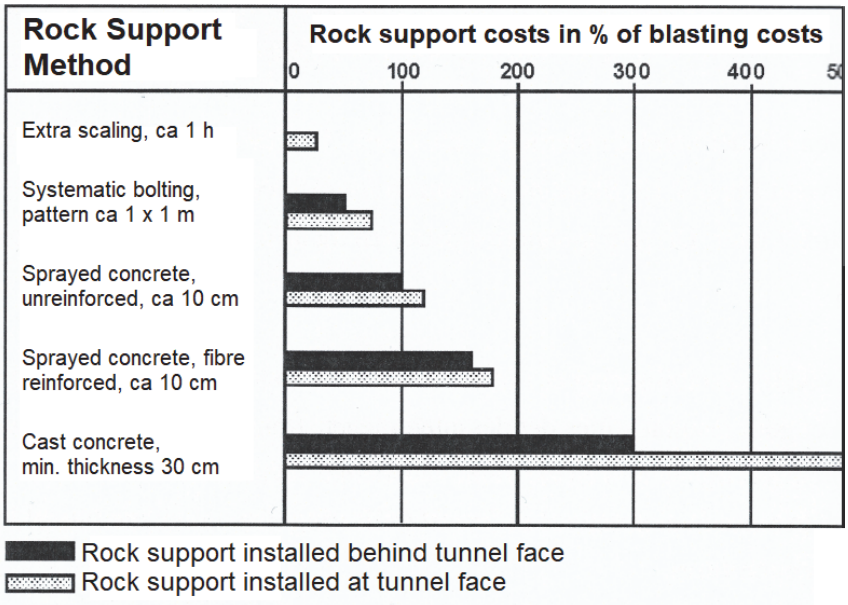


**Figure 1:** Comparison of relative costs for some commonly used rock support methods. Translated from Nilsen (2016).

This information got me interested in learning more about sprayed concrete. It is such a big part of engineering geology and rock mechanics, without the field having a lot of emphasis on it. This combined with my supervisor, Eivind Grøv, being leader of a large research project, SUPERCON, on sprayed concrete. All of this made me pick this topic for the master's thesis. I wrote a specialisation project on the durability of sprayed concrete

during the fall semester of 2019. This project demonstrated the influence of cracks on the durability of sprayed concrete. An increasing number of cracks makes the durability lower (Grindheim 2019). From this information it was decided to investigate shrinkage cracking in sprayed concrete. The decision was made together with my supervisor and Nicholas Henry Trussel, a PhD student. This would be done in association with the research project SUPERCON.

**Table 1:** The support categories for permanent rock support in Norwegian road tunnels based on the rock mass quality (Q-system). Translated from NPRA (2020*b*).

| **Rock Mass Quality** | **Rock condition**<br>**Q-value (blasted rock)** | **Support categories**<br>**Permanent rock support** |
|---|---|---|
| A/B | Rock mass with little jointing.<br>Mean joint distance >1 m.<br>Q = 100 - 10 | Support category I<br>- Spot bolting<br>- Sprayed concrete<br>B35 E700, thickness 80 mm |
| C | Rock mass with moderate jointing.<br>Mean joint distance 0.3 - 1 m.<br>Q = 10 - 4 | Support category II<br>- Systematic bolting, c/c 2 m<br>- Sprayed concrete<br>B35 E700, thickness 80 mm |
| D | Highly jointed rock mass or<br>stratified schistous rock mass.<br>Mean joint distance <0.3 m.<br>Q = 4 -1 | Support category III<br>- Systematic bolting, c/c 1.75 m<br>- Sprayed concrete<br>B35 E1000, thickness 100 mm |
| E | Very poor rock mass.<br>Q = 1 - 0.2<br>---<br>Q = 0.2 - 0.1 | Support category IV<br>- Systematic bolting, c/c 1.5 m<br>- Sprayed concrete<br>B35 E1000, thickness 150 mm<br>---<br>- Systematic bolting, c/c 1.5 m<br>- Sprayed concrete<br>B35 E1000. thickness 150 mm<br>- Reinforced ribs of sprayed concrete<br>Ribs dimensions E30/6, ø20 mm, c/c ribs 2-3 m,<br>Systematic bolting in ribs,<br>c/c bolt = 1.5 m, bolt length 3 - 4 m<br>- Cast concrete footing should be considered |
| F | Extremely poor rock mass.<br>Q = 0.1 - 0.001 | Support category V<br>- Systematic bolting, c/c 1.0 - 1.5 m<br>- Sprayed concrete<br>B35 E1000, thickness 150 - 250 mm<br>- Reinforced ribs of sprayed concrete<br>Ribs dimensions D60/6+4, ø20 mm, c/c ribs 1.5-2 m,<br>Systematic bolting in ribs,<br>c/c bolt = 1 m, bolt length 3 - 6 m<br>- Double ribs can be replaced by lattice arches<br>- Reinforced cast concrete footing,<br>bow min. height 10% of tunnel width |
| G | Exceptionally poor rock mass,<br>mostly soils, Q <0.01 | Support category VI<br>- Tunneling and permanent rock support<br>is dimensioned specifically |

SUPERCON stands for Sprayed sUstainable PErmanent Robotized CONcrete tunnel lining. The research program aims to increase knowledge on new eco-friendly materials in spayed concrete, robotized application methods, new approach for structural analysis and design, and improved durability to ensure the service life requirement of a 100 years (Grøv 2019). This master's thesis tries to contribute to the durability goal of SUPERCON. The contribution comes from improved knowledge on shrinkage cracking in sprayed concrete.

A new non-destructive method for mapping shrinkage cracks on the surface of sprayed concrete cores is tested in this master's thesis. The method is dye penetrant. This method is used for mapping cracks in metals and welding. It has also been tested on rock cores by Solveig Vassenden with good results (Vassenden 2019). After the dye penetrant testing, the cores were crushed to measure the uniaxial compressive strength (UCS) and the in-situ fibre content.

The lab results are used to see if the UCS is affected by the number of cracks in the core. There are many articles on how fibres decrease the cracking in concrete. Therefore, the in-situ fibre content was measured. The measurement was done to check if the cracking decreases with a higher fibre content. The density of the sprayed concrete was also measured. These measurements were used see if the cracking changed with the density. The rock mass classification from the locations were collected. The classification was used to see, if the cracking was affected by the quality of the substrate surface.

During the period, this master's thesis was written a global pandemic due to the virus COVID-19 happened. Norway went into lockdown. This set restraints to what could be done. All the sampling and lab tests had to be conducted by others. This was to limit the interaction with other people. This was to avoid spreading of the virus. The situation made it hard and time consuming to get samples from Nordøyvegen. The project was struggling at times to keep their operation going. They had a lack of manpower, because of local quarantine rules (Ålesund muncipality 2020). It was planned to try some mitigating measures in one or two tunnel sections in the original plan. This was to see if the cracking would decrease with the measures, but this had to be dropped because of the lockdown. The lockdown set restrictions to whom could get access to the labs. The restrictions stopped me form using the concrete lab. Therefore, the testing was conducted in the rock mechanics lab. The equipment in the rock mechanics lab set limitations to what tests that could be conducted. UCS, measurement of density and fibre content was selected to be done in addition to the dye penetrant testing. This was based on the equipment in the laboratory.

The thesis starts with a theory section. The section is done as a literature review. The literature review starts with the basics on sprayed concrete, which is the constituents, spraying technique, and hardening, to make sure the reader has a good enough understanding for the rest of the section. This is knowledge most engineering geologist does not have. Then it goes through how shrinkage cracks develop in concrete and spayed concrete.

The end of the theory section introduce some methods to mitigate shrinkage cracks.

The methods used are explained in the next section. The section starts with the location where the test samples came from and how they were gathered. Then the different tests are explained. The explanation starts with dye penetrant, then UCS, density and in-situ fibre content measurements. Finally, the method for rock mass classification is explained.

The results section presents the results from all the tests. They also show how some of the results affect each other. The results are discussed in the discussion section, and the last section comes with a conclusion based on the discussion of the results.

# 2 Theory

Cracking of concrete and sprayed concrete is a problem a lot of concrete structures experiences. Different types of cracking can occur. They can come from loads, deterioration over time or shrinkage (Bažant 1985). This master's thesis investigate shrinkage and how it effects sprayed concrete. The theory looks at the constituents and spraying technique of sprayed concrete and how they affect the properties of the concrete. Then shrinkage is explained. The explanation examines how shrinkage occurs during the hydration and drying of the concrete, and what this does to the concrete. It looks at how the adhesion between the sprayed concrete and the rock surface affects the cracking. In the last two sections methods to heal and mitigate shrinkage are looked at.

## 2.1 Sprayed Concrete Constituents

Sprayed concrete is mortar and concrete transported through a hose and sprayed with a high velocity on a surface. The high velocity of the sprayed concrete through the nozzle compresses the concrete when it hits the surface it is used on. This can be used on any kind of surfaces, including vertical and overhead surfaces (Khitab 2015).

Concrete is a composite material. It mainly consists of aggregates, water, and cement. The way these materials are mixed determine the properties of the concrete. It is also common to add additives and reinforcement to develop special properties in the concrete (Newmann & Choo 2003). Sprayed concrete is a high performance concrete (Hemphill 2012). A definition of high performance concrete is concrete with strength and durability significantly beyond those obtained by normal means (Leung 2001). Normally, the water-cement ratio is low in sprayed concrete. The low water-cement ratio is possible because of additives (Hemphill 2012). The different constituents of sprayed concrete are mentioned in this section. The main contribution of the constituents to the concrete abilities is explained.

### 2.1.1 Aggregates

Aggregates are sand and gravel material. It makes up the biggest part of concrete. Usually aggregates occupy between 70 to 80% of the volume of a normal concrete (Newmann & Choo 2003). The aggregates can come from natural deposits or it can be crushed from rock (Jacobsen et al. 2015).

Kozul & Darwin (1997) tested how different types of aggregates affected the strength properties in concrete. The tests showed that aggregates of stronger rock types increased the strength of high-strength concrete. ACI defines high-strength concrete as concrete with a compressive strength that exceeds 41 MPa. In other regions, high-strength concrete is defined as concrete with a greater uniaxial compressive strength than what is ordinarily

obtained in that region. The strength used may vary from region to region (Beshr et al. 2002). Wu et al. (2001) saw that high-strength concretes made with crushed quartzite gained 10-20% higher compressive and splitting tensile strength, than high-strength concrete made with marble coarse aggregate. The differences between the types of coarse aggregates were reduced in concrete with a lower target strength, 30 MPa.

The size of the aggregates in sprayed concrete is limited by the size of the nozzle. The nozzle clogs if the largest aggregates are too large. 8 mm are often used as the largest aggregate size in sprayed concrete. The rebound during the spraying increases with larger aggregates sizes. It is recommended to have less than 10% of the aggregates larger than 8 mm (Lundgren et al. 2018).

The grading of the aggregates is important for the concrete properties. Unsatisfactory gradation can lead to multiple bad effects on the concrete properties. It may lead to segregation of coarse aggregates and the mortar. The unsatisfactory grading could also lead to excessive bleeding around and below the large aggregates and on the surface. The aggregates may settle and leave the paste in the top layer. This makes a need for extra cement and water. The concrete may develop a high porosity and a bad air-void distribution. All of this increases the material costs and reduce the service life (Andersen & Johansen 1993). Richardson (2005) recommended to use well graded aggregates to elude all the bad effects mentioned above. This could be done by choosing a fine, an intermediate and a coarse aggregate and mix them together in concrete. Pawar et al. (2016) tested the effect of different grading on compressive strength. The tests showed that gap graded aggregates developed a slightly higher strength than well graded aggregates in concrete.

### 2.1.2 Cement

Cement together with water are the materials that binds all the constituents in the concrete together. The water and cement react and harden to a solid mass. The section on hardening explains this closer. Ordinary Portland cement (OPC) consists of different constituents. Together the different constituents give cement its properties which is used in concrete. The most important constituents in cement are alite, belite, aluminate and ferrite (Lea & Mason 2019). It is also common to use waste materials with similar properties as cement as replacement materials for parts of the cement. There are different reasons for doing this. The most important reasons are to reduce the carbon dioxide emissions and reduce the cost of the concrete (Claisse 2016). This thesis only goes through the constituents of cement and their properties. Under the different constituents are described as they were in Jacobsen et al. (2015). The replacement materials are not described more in detail, but it is important to know that they are being used in concrete at that they affect the cement properties.

**Alite** reacts fast with water. Most of the early settlement and early strength in concrete comes from the hardening of alite. It is sulphate resistant and makes up 50-70% of a

Portland clinker. The reaction between alite and water releases 500 kJ/kg heat in total.

**Belite** reacts slower with water. This means it contributes little to the early strength gain in concrete. The contribution from belite is significant in the long-term mechanical strength gain. It makes up 15-30% of a Portland clinker. This is also sulphate resistant. Full hydration of belite releases 260 kJ/kg heat.

The reaction between **aluminate** and water is very rapid. It releases a lot of heat, 870 kJ/kg at full hydration. The aluminate content in Portland clinker is 5-10%. Aluminate is not sulphate resistant.

**Ferrite** reacts much slower with water than aluminate. The typical grey colour of concrete comes from ferrite. The reaction releases 420 kJ/kg heat. The ferrite content in Portland clinker is 6-10%. Elakneswaran et al. (2019) described that by increasing the ferrite content in Portland clinker it is possible to lower the temperature in the kiln. This reduces the energy usage in cement production. The cement becomes more environmentally friendly with the reduced energy usage.

**Gypsum** is added to cement after it has been burned in the kiln. There are around 5% gypsum in cement. This is to avoid flash set during the hydration of the concrete (Lea & Mason 2019). Flash set is a very rapid reaction between water and aluminate. Gypsum participates in the reaction between water and aluminate, and flash set is avoided (Jacobsen et al. 2015).

The properties of the cement are changed by adjusting the content of the different constituents. This can be used to adjust the properties of the concrete. The amount of alite can be increased to gain high early strength. The ferrite content can be decreased if the grey colour is unwanted.

### 2.1.3 Water

Water is one of the most important materials in concrete. It is the chemical reaction between water and cement that makes the concrete harden into a solid mass. The reaction is called hydration. The water-cement ratio affects multiple abilities of the concrete. The most important ones are the compressive strength, permeability, and workability (CEMEX 2013).

### 2.1.4 Admixtures

An admixture is defined as "a material other than water, aggregates, hydraulic cement, and fibre reinforcement used as an ingredient of concrete or mortar, and added to the batch immediately before or during its mixing" (ACI 2010). There are several different admixtures that are used in sprayed concrete. Under the most important ones are described after Hewlett & Liska (2019). An own citation is given if other sources have been used.

**Accelerator** are chemicals that affects the hydration of cement. They increase the hydration rate and decrease the setting. Often, they increase the early strength gain in concrete. It is possible to divide accelerators in two.

The first group of accelerators affect aluminate ($C_3A$) in the Portland cement. The chemicals used for this is mainly chemicals with a high content of alkali metals. Examples of this is alkali hydroxides, carbonates, aluminates, and silicates. This leads to false set. The false set is when some of the aluminate hydrates immediately. The fast hydration releases a lot of heat and makes the concrete stiff, but with little strength. The heat can start the hydration of alite ($C_3S$). The hydration of alite contributes to the early strength gain. The process weakens the final strength in most cases. This type of accelerator has a limited range of application. It can be used to clog water leakages into basements, tunnels, or shafts before installing a permanent waterproof lining.

The other type of accelerator decreases the settlement and increase the hydration in concrete. They mostly affect the alite to increase the early strength gain. The chemicals used for this works as a catalyst that increases the hydration rate of alite. Mainly acids and the soluble salts of acids are used for this. The increase in reaction rate increases the amount of heat released at the early stages.

**Plasticising and superplasticising** admixtures are chemicals that increases the workability of a concrete mix without increasing the water content. They are also called water reducing admixtures. The reason for this is that the water-cement ratio can be lowered without lowering the workability with these chemicals. This leads to a stronger concrete. The workability increases because the chemicals disperse the cement particles in the water and flocculation is avoided.

**Retarding** admixture increases the settlement period or increases the hardening time of the concrete. Increasing the settlement period means that the time before the hydration starts is increased. Hansen (2017) described common applications of retarding admixtures. Settlement retarder is used if the concrete is going to be transported far or if it going to be pumped, to avoid clogging of the pipes. Hardening retarder is used to reduce the heat development in the concrete. This is used if concrete is going to be cast in warm weather or in thick concrete sections under construction.

**Air entraining** admixtures is surface active agents that affects the air-water interface in the cement paste. The chemicals stabilise the air that is mixed into the concrete. The air is distributed evenly in the concrete in small discreet air bubbles. Kumar et al. (2015) described how the entrained air affected the concrete properties. The addition of small evenly distributed air bubbles increases freeze-thaw resistance. It increases the workability. The strength is decreased. The bleeding and segregation are reduced. A study revealed that for every 1% the air content increases in concrete the compressive strength decreases by 4-6% (Zhang et al. 2018).

**Pump improving** admixture is stabilising on the concrete. It keeps the water in the concrete during pumping. The chemical slickens the concrete to avoid clogging of the pipes during pumping. This is the same chemicals that are used as stabilising admixture in normal cast concrete in constructions (NB 2011).

### 2.1.5 Fibre

Fibre is an important part of sprayed concrete. The properties of concrete improves with the addition of fibres. The fibres improve different properties. The most important ones are improved static and dynamic tensile strength, increased energy absorption and better fatigue strength (Mohod 2012). There are different types of fibres that can be used to improve different abilities in sprayed concrete. The two most common types of fibres are introduced in the paragraphs under.

**Steel fibres** are included in sprayed concrete to achieve a specific energy absorption class. The amount of fibres needed is specified in NS-EN 14889-1 class I (NB 2011). They improve different properties in addition to energy absorption in sprayed concrete. The other properties they improve are the toughness, shear strength, flexural strength, impact resistance and durability. The fibres increase the ductility of the sprayed concrete. The ductility changes the way the concrete fails. Sprayed concrete with fibres can endure large deformations before it cracks and after failure it can still bear loads (Henager 2003).

**Synthetic fibres** can be used in the same way as steel fibres for energy absorption. The amount needed and type of fibre is specified in NS-EN 14889-1 class II (NB 2011). There are different types of synthetic fibres. Some have similar abilities as steel fibres. Other are added to reduce plastic shrinkage cracking, increase the cohesion during pumping and to reduce rebound during the spraying (Laning 1992). Polypropylene fibres are added to help against explosive spalling during tunnel fires. Small cracks forms in the surface between the fibres and the cement matrix when the concrete is heated up. This creates space for the water vapour inside the concrete. This extra space lowers the vapour pressure. The lowering of the vapour pressure reduces the explosive spalling (Tatnall 2002).

### 2.1.6 Durability and Strength Classes

There are certain standards the sprayed concrete must fulfil. These standards set restrictions to how the constituents are mixed. The standards give specifications for the sprayed concretes abilities. These specifications are given through durability and strength classes. Specifications for sprayed concrete is given in NS-EN 14487-1 and NS-EN 206-1 (NB 2011). Here the durability and strength classes for sprayed concrete are shown and explained.

Table 2 is the durability classes given in NS-EN 206-1. The table shows that the durability classes is based on the water-binder ratio. A lower water-binder ratio means a higher durability. The ratio can be read directly from the durability class, as M40 is w/b = 0.40. b is the effective mass of binder. The table also shows the minimum binder content the concrete should contain (Jacobsen et al. 2015).

**Table 2:** Durability classes in NS-EN 206-1, with mass ratios and binder content. Modified from Jacobsen et al. (2015).

| | **Durability class** | | | | | |
|---|---|---|---|---|---|---|
| | **M90** | **M60** | **M45** | **MF45**[a)] | **M40** | **MF40**[a)] |
| Maximum mass ratio [b)] (w/(c + Σ k * p)) | 0.90 | 0.60 | 0.45 | 0.45 | 0.40 | 0.40 |
| Maximum air content in fresh concrete | - | - | - | 4% [c)] | - | 4% [c)] |
| Minimum effecient binder content (c + Σ k * p) (kg/m$^3$)[d)] | 225 | 250 | 300 | 300 | 330 | 330 |

[a)] For concrete composition MF40 and MF45 "frost resistant" aggregates shall be used.
[b)] The mass ratio is the ratio w/(c + Σ k * p) where c + Σk * p is denoted effective mass of binder.
[c)] Norwegian Standard does not give rules for production of frost resistant concrete without use of entrained air.
[d)] When adding fly ash, the amount of cement shal not be less than 200 kg/m$^3$.

Table 3 shows which durability class that must be used based on the exposure classes. The crosses marks which durability class that can be used with the specific exposure classes on the left (NS 2017). The exposure classes are explained in table 17 in appendix A. The durability classes for sprayed concrete used as rock support is specified in NS-EN 14487-1 and NS-EN 206-1. The specified durability classes are M40, M45 and M60. There sprayed concrete for rock support is specified as designed concrete (NB 2011).

The strength classes for normal and heavy weight concrete is shown in table 4. These strengths are the compressive strength of cylinder or cube specimens. The strength classes in Norway has the notation B for "betong" (Norwegian word for concrete) while in Europe they use the notation C, which stands for concrete. A B45 concrete cast as a cylinder should achieve a compressive strength of 45 MPa after 28 days, for a cube it should achieve a compressive strength of 55 MPa after 28 days (NS 2017). The strength class is specified for sprayed concrete used in tunnels. The specified strength classes are B30, B35 and B45 (NB 2011).

**Table 3:** Choice of durability class, depending on exposure class. Modified from NS-EN 206-1 (NS 2017).

| **Exposure class** | **Durability class** | | | | | |
|---|---|---|---|---|---|---|
| | **M90** | **M60** | **M45** | **MF45** | **M40** | **MF40** |
| X0 | X | X | X | X | X | X |
| XC1, XC2, XC3, XC4, XF1 | | X | X | X | X | X |
| XD1, XS1, XA1, XA2 [a)], XA4 [b)] | | | X | X | X | X |
| XF2, XF3, XF4 | | | | X | | X |
| XD2, XD3, XS2, XS3, XA3 [a)] | | | | | X | X |
| XSA [a)] | Concrete composition and protective measures to be determined separately. Composition of concrete shall at least satisfy the requirements of M40. | | | | | |
| [a)] If there is a possibility in exposure class XA2, XA3, XSA of contact with concentration of sulphates of limits exceeding XA2, the project sprecification shall state that sulphate resistant cement shall be used. [b)] The project specification shall specify at least 4% of silica fume for structures exposed to livestock manure. | | | | | | |

**Table 4:** Strength classes, characteristic cylinder and cube strength for normal and heavy weight concrete. Modified from NS-EN 206-1 (NS 2017).

| **Norwegian classes** | **B20** | **B25** | **B30** | **B35** | **B45** | **B55** | **B65** | **B75** | **B85** | **B95** |
|---|---|---|---|---|---|---|---|---|---|---|
| CEN classes | C 20/25 | C 25/30 | C 30/37 | C 35/45 | C 45/55 | C 55/67 | | | | |
| Char. cyl. $f_{ck,cyl}$ (MPa) | 20 | 25 | 30 | 35 | 45 | 55 | 65 | 75 | 85 | 95 |
| Char. cube $f_{ck,cube}$ (MPa) [1)] | 25 | 30 | 37 | 45 | 55 | 67 | 80 | 90 | 100 | 110 |
| [1)] For strength class B55 and higher, other values may be used, provided that the relationship between these and the reference strength for cylinders are established and documented with sufficient accuracy for the current concrete mix. | | | | | | | | | | |

## 2.2 Spraying Technique

The methods and procedure for spraying concrete is explained shortly in this section. The section also looks at what affects the rebound, quality and compaction of the spraying.

### 2.2.1 Spraying Methods

There are two ways to apply sprayed concrete to a surface. The two methods are wet mix and dry mix. Both methods are mentioned in this section. The focus in the rest of the text is on wet mix sprayed concrete. Here the wet and dry methods are explained according to the United States Patent of Bertoncini et al. (1999).

**Dry mix** process for spraying concrete starts by mixing all the dry components. The dry components are cement, fine and coarse aggregates, and additives in solid form. Then the mix is conveyed pneumatically to the nozzle. Water is added to the mix in the nozzle. Set accelerator is added in powder or liquid form. The accelerator is usually added upstream or at the nozzle. The mixture is then sprayed at the surface with the aid of compressed air.

The method has some disadvantages. The process creates a lot of dust and the rebound loss is high. The high rebound can be a risk for the operator. It increases the material needed. The spraying time to obtain the thickness needed in the concrete layer is increased by the high rebound loss.

The **wet mix** process adds water to the mix. This can be mixed at the site or come from a mixing plant. The mix is conveyed by a pump toward a spraying nozzle. Set accelerator in liquid form is added at the nozzle. The fact that water is added to mix sets new demands to the pumpability of the mix.

Jolin et al. (2009) studied the pumpability of concrete. Pumpability introduces notions as stability and mobility under pressure. The definition of pumpability is the capacity of concrete under pressure to be mobilised while maintaining its initial properties. Stability is the concretes ability to not segregate during pumping. Segregation gives the concrete a deficient particle size distribution or excessive water to cement ratio. Mobility is the concretes ability to move. It is important to know this to get a steady flow during pumping and spraying. These are important factors to control to get a homogeneous sprayed concrete lining.

Melbye et al. (2001) summarised the advantages of the wet mix method compared with the dry mix method. The method has a lot less rebound. This creates less dust and the working environment is improved. Thicker layers can be sprayed with the use of admixtures. The water dosage is controlled. The concrete is more homogeneous. The production is larger. The large production improves the economy. It is easier to add steel fibres and new advanced admixtures. There are some disadvantages with the method.

The conveying distance is limited, max. 300 m. The method demands a higher aggregate quality. The cleaning costs are higher.

### 2.2.2 Procedure

An important procedure before spraying a surface with concrete is treatment of the surface. The treatment increases the bond strength between the sprayed concrete and the substrate surface. There are several methods that are used for surface treatment. Some examples are mechanical scaling, scaling, high pressure water washing and water jet scaling. Mechanical scaling creates a lot of dust. Therefore, the surface must be cleaned after this method is used. It has been showed that when the surface is not cleaned, the occurrence of areas with sprayed concrete with low or no bond strength is higher (Bryne et al. 2014*b*).

The spraying starts at the lower sections and then moves upwards towards the crown. The thickness of the sprayed concrete should be applied on numerous thinner layers rather than to spray the entire thickness in one pass. The sprayed concrete should be given sufficient time to set, when more than one layer is needed, before the nest layer is applied (Melbye et al. 2001).

The nozzlemen have an important role in the spraying of concrete. The quality is highly dependent on the nozzlemen. Therefore, it is important that they have the skills to preform safe, high quality, efficient and cost-effective concrete spraying. EFNARC have a certification for robotic spraying to ensure that the nozzlemen have these skills. This certification is a quality assurance of the operators abilities (EFNARC 2019).

### 2.2.3 Rebound and Quality

Rebound is one of the main reasons for increased costs of sprayed concrete lining and the poor quality in some sections. There are four major factors in the spraying technique that affect the rebound and the quality of the sprayed concrete. These are summarised in figure 2. Each of the factors are explained as they are described in Melbye et al. (2001).

The angle of the nozzle to the substrate surface is the most significant factor for rebound. The compaction and orientation are affected by the nozzle angle. The nozzle should be held at right angles (90°) to optimise the compaction and fibre orientation. The angle should always be greater than 70°, if the angle becomes smaller the rebound is excessive. At smaller angles, the compaction is poor. The poor compaction leads to low strength and durability.

The dosage of accelerator also affects the rebound. Sprayed concrete with low dosages of accelerator does not set adequate and gain enough early strength. This may lead to the concrete being shot off the surface by the next pass of the nozzle. A too high dosage, above 10%, leads to flash setting. The flash setting creates a hard surface that causes

rebound of the larger aggregates. It also prevents complete compaction. A bad compaction leads to reduced strength and durability.

The nozzle should be held at the right distance to the surface. The optimum distance is 1 to 2 m as shown in figure 2. The projected concrete may tear off the freshly placed material when the nozzle is too close to the surface. The impact energy is lowered at distances more than 3 m from the surface. This leads to bad compaction and large amounts of rebound.

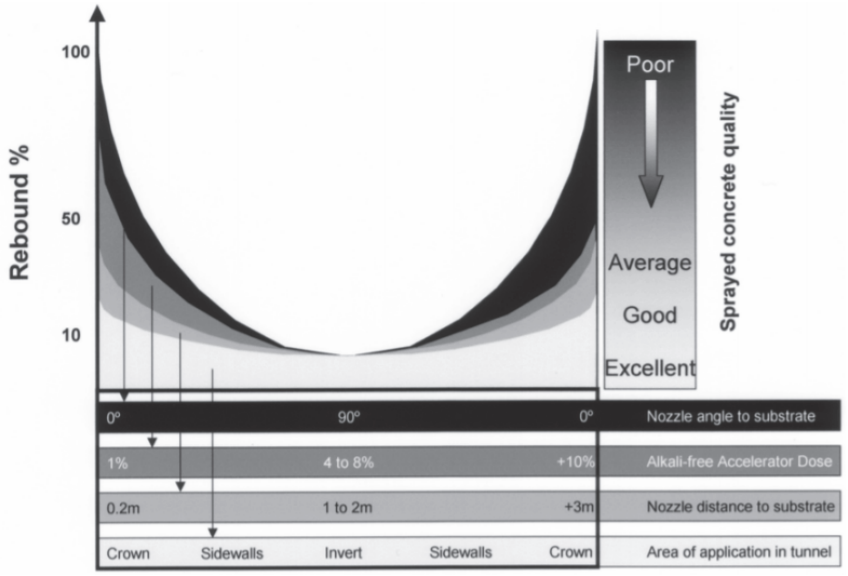


**Figure 2:** The effect of principal spraying parameters on rebound and concrete quality. Taken from Melbye et al. (2001).

The area of application in the tunnel must be taken into consideration around rebound. The rebound varies with the surface that is being sprayed. This is due to gravity. Gravity works against the bond strength in the crown.

Banthia et al. (1992) studied rebound of steel fibres in dry mix sprayed concrete. The testing showed a tendency that fibres rebound more than the rest of the materials in sprayed concrete. The rebound loss of fibres in the testing varied from 35% to 78% with different types of fibres. The rebound increased with an increasing area of the projected fibres. They stated that the loss is lower in wet mix sprayed concrete.

### 2.2.4 Compaction

Compaction of concrete is methods used on the fresh material to reduce the volume of voids in the material. This can increase the compressive strength of the concrete. It can magnify the strain capacity before collapse. The reduction of entrapped air contributes to reduce the thermal conductivity of the hardened concrete (Nguyen et al. 2011).

Banthia et al. (1994) showed that sprayed concrete does not achieve the same compressive strength as cast concrete. They saw that the pneumatic spraying does not achieve the same compaction as cast concrete compacted through external vibration. The pneumatic compaction of sprayed concrete gives a better alignment of the fibres. The alignment of the fibres in sprayed concrete gives a higher flexural strength than a cast concrete with the same mix design.

## 2.3 Hardening

Hardening of concrete is a chemical reaction between cement and water. The process is time consuming. It happens gradually as the water moves into the cement particles (Thue 2019). The chemical process under the hardening is explained shortly in this section. First there is a short introduction in chemical notations in concrete technology.

Portland cement consists mainly of four constituents, alite, belite, aluminate and ferrite as mentioned earlier. They have different chemical structure. It is these four constituents that reacts with water and creates the bonds that makes concrete into a solid mass. Table 5 shows the chemical formula of the four main clinker phases in Portland cement written with oxide form (Aïtcin 2016).

**Table 5:** The main clinker phases in Portland cement with chemical formula. Made from Aïtcin (2016).

| Name of clinker phase | Chemical name | Chemical formula (oxide form) |
|---|---|---|
| Alite | Tricalcium silicate | $3CaO * SiO_2$ |
| Belite | Dicalcium silicate | $2CaO * SiO_2$ |
| Aluminate | Tricalcium aluminate | $3CaO * Al_2O_3$ |
| Ferrite | Tetracalcium aluminoferrite | $4CaO * Al_2O_3 * Fe_2O_3$ |

It is common to simplify the chemical notation of oxides in concrete technology. This is to get shorter and more efficient chemical equations. S is used for silica, $SiO_2$. C for calcium oxide, CaO. A for aluminate, $Al_2O_3$. F for iron oxide, $Fe_2O_3$. This gives shorter chemical formulas for the clinker phases in cement. The shortened chemical notations of the clinker phases are given in table 6 (Aïtcin 2016).

**Table 6:** The main clinker phases in Portland cement with shortened chemical formula. Made from Aïtcin (2016).

| Name of clinker phase | Chemical formula (oxide form) | Shortened chemical formula |
|---|---|---|
| Alite | $3CaO * SiO_2$ | $C_3S$ |
| Belite | $2CaO * SiO_2$ | $C_2S$ |
| Aluminate | $3CaO * Al_2O_3$ | $C_3A$ |
| Ferrite | $4CaO * Al_2O_3 * Fe_2O_3$ | $C_4AF$ |

The hydration of cement is what makes concrete into a solid mass. The cement hydration is a chemical reaction between cement and water. It is mainly the hydration of alite and belite that contributes to the strength gain in concrete. Only the hydration of these two clinker phases are shown here. The reaction between water, aluminate and ferrite is much more complicated and a lot of the properties they give concrete is unwanted. They are included in cement for economic and technical reasons for the production. Equation i shows the hydration of alite. Water, $H_2O$, is written as H in the equation. Equation ii shows the hydration of belite (Jacobsen et al. 2015).

$$2C_3S + 6H \longrightarrow C_3S_2H_3 + 3CH. \quad \text{(i)}$$

$$2C_2S + 4H \longrightarrow C_3S_2H_3 + CH. \quad \text{(ii)}$$

By comparing the two equations, it is possible to see that belite ($C_2S$) produces more C-S-H ($C_3S_2H_3$), which is the binder in concrete, and less calcium hydroxide per reacted molecule. Calcium hydroxide is the weak part of the hydration reaction. This makes belite more efficient at complete hydration. The drawback is that hydration of belite is much slower than alite ($C_3S$) (Jacobsen et al. 2015). High early strength is wanted in sprayed concrete. Therefore, the alite content is high and belite content is low.

The hardening is usually divided into three periods. The reactions are slow in the beginning. This is called the dormant period. After a certain time, the cement reaction becomes rapid, the acceleration period. The acceleration slows down after some time and are followed by slower reactions that increases the strength, which is the late hardening. Figure 3 shows the different periods. It is possible to identify the different periods by isothermal calorimetry. Isothermal calorimetry measures the heat released from the exothermic cement hydration. A graph like the one at bottom of figure 3 can be plotted from the measurements of the released heat (Lagerblad et al. 2010).

The set accelerator reacts with components in the pore solution in the dormant period. The components of the pore solution in the dormant period are $Ca^{2+}$, $Na^{+}$, $K^{+}$, $OH^{-}$ and $SO_4^{2-}$. Normal cement reaction gets stifled by the early cement hydrates during the dormant period. The type of cement and temperature affects the length of the dormant period. The start of the acceleration period is often late in sprayed concrete in tunnels, due to the cool rock walls in the tunnel (Lagerblad et al. 2010).

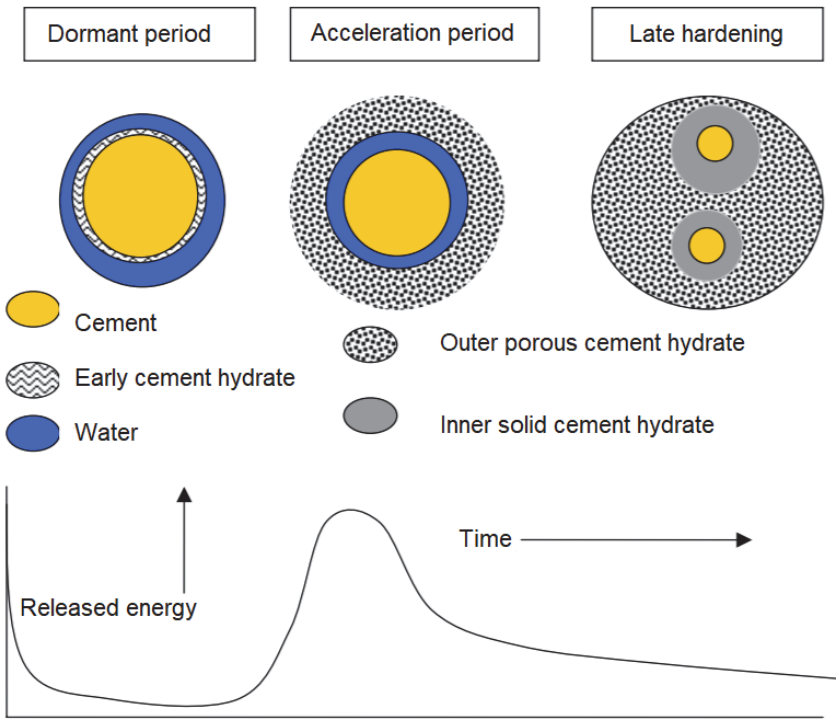


**Figure 3:** The different steps in cement hydration. The graph at the bottom shows the energy released at the different periods. Translated and modified from Lagerblad et al. (2006).

## 2.4 Shrinkage

Sprayed concrete starts to shrink when it hardens on the rock surface. The cement content is higher in sprayed concrete than in normal cast concrete. The shrinkage is greater with a higher cement content. The amount of shrinkage is increased even more with the usage of accelerator in sprayed concrete (Ansell 2010). Four types of shrinkage are mentioned here in this section. They occur at different stages of the hardening. Each one is described here.

### 2.4.1 Plastic Shrinkage

This subsection on plastic shrinkage is based on Sayahi (2019). Plastic shrinkage is something that happens in concrete straight after casting before it hardens. The solid particles in concrete starts to settle when it has been cast. The settlement makes water rise in the concrete. This is called bleeding. It was mentioned that this process does not occur in all modern concretes with a high content of fines and a low inner permeability.

A water film forms on the concrete surface if the bleeding rate is higher than the evaporation rate. The water film decreases if the evaporation rate is higher than the bleeding rate. This makes the surface dry out. The capillary water starts to evaporate when the whole surface is dry. The reduction of capillary water starts the formation of water menisci in the pores and on the surface of the concrete. This creates a negative capillary pressure.

The curvature of the menisci increases as the water evaporates. An increased curvature of the menisci increases the negative capillary pressure. Large negative capillary pressure pulls the particles tighter together. Figure 4 illustrates this. This is the reason for the plastic shrinkage. The menisci break if the negative pressure gets too large when the curvature increases. The breaking of the menisci draws air into the concrete. This is called the time of air entry. The infiltration of air leaves the pores on the surface empty. This was described further in (Combrinck & Boshoff 2013). The air entry is the event that initiates cracking. Cracking cannot develop where air have not entered the concrete. The positions with air entry are weak spots in the concrete where cracking is likely to develop.

There are different actions that can be done to reduce the plastic shrinkage. Most of the actions tries to reduce the surface evaporation. The surface can be covered with plastic or tarpaulin. It is possible to wet the surface to replace the water that has evaporated. There could be set up wind stoppers to reduce the airflow above the surface and this reduces the evaporation. Sivakumar & Santhanam (2007) mentioned that fibres can be used as a secondary reinforcement mechanism to mitigate the stresses that are developed during the drying.

### 2.4.2 Autogenous Shrinkage

The hydration reaction between water and cement is shown in equation i and ii, in those equations the volume of the reaction products is smaller than the volume of the reactants. This comes from the water that is chemically bound to the cement takes up a smaller volume than the free water. That volume reduction is the chemical shrinkage in concrete (Essili 2017). Most of the water is bound to the binder when the water to binder ratio is low. This causes a volume change when the water reduces volume. Small pores start to develop in the cement paste if this volume reduction is restrained. The chemical reaction between the water and the binder use the free water in the concrete. The vapour and the relative humidity decrease when the water is used. The reduction mechanism of vapour and humidity in concrete is known as self-desiccation. It is this mechanism that induces the shrinkage known as autogenous shrinkage (Yoo et al. 2012).

The mechanism that causes autogenous shrinkage in concrete can be explained by capillary tension. The hardening of the cement paste consumes water. The consumption of water reduces the saturation. There is also formed pores in the cement paste during the hardening. The consumption of water changes the saturation of the capillary pores from saturated to unsaturated. The surface of the capillary pore water becomes more and more concave as the humidity decreases. Figure 4 demonstrates the concave surface of the capillary water. This leads to an increase in capillary tension. The capillary tension creates a negative internal pressure. This makes the pore diameter shorter and is the reason for autogenous shrinkage (Wu et al. 2017).

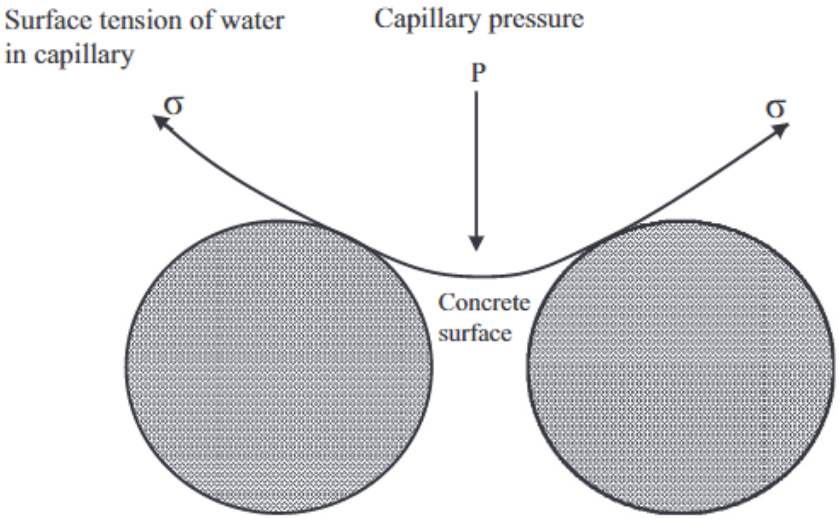


**Figure 4:** Capillary water tension demonstrated schematically. Taken from Wu et al. (2017).

Autogenous shrinkage is influenced by different factors. The autogenous shrinkage is very small compared to other types of shrinkage when the water to cement ratio (w/c) is over 0.42. It increases when the w/c is lowered. Micro strains in order of 50 to 400 can come from lowering the w/c. This could be around half the shrinkage in a concrete with w/c of 0.30 (Essili 2017). The cement fineness affects the hydration rate as the specific surface area increases. The increased hydration rate reduces the humidity in the concrete faster, intensifies the capillary pressure and the autogenous shrinkage. Admixtures that lowers the w/c ratio can increase the possibility for autogenous shrinkage. The addition of 1% superplasticizer in a concrete with w/c of 0.30 can increase the autogenous shrinkage by almost 30% (Wu et al. 2017). The curing temperature affects the amount of autogenous shrinkage in high performance concrete. The shrinkage increases with increasing temperature (Shen et al. 2015).

There are different actions that can be done to mitigate the autogenous shrinkage. The best way to avoid autogenous shrinkage is to avoid extremely low w/c ratios, lower than 0.40, and large volumes of cement paste. It can also be reduced by keeping the surface wet during the whole hardening process. Water is drawn into the capillary pores of the concrete if the surface it kept wet (Essili 2017).

### 2.4.3 Thermal Shrinkage

Concrete has a direct relation between temperature changes and length, and volume changes, like in most materials. This has been seen and recognised in highways, bridges, walls, and buildings. The relationship between temperature and volume changes is important to understand to be able to control the volume changes and the consequent concrete cracking (Tatro 2006).

The thermal conductivity is an important parameter when looking at thermal shrinkage. Thermal conductivity is how the material conducts heat. A material with low thermal conductivity has a slow heat transfer across the material. Materials with high thermal conductivity has a fast heat transfer. The property is temperature dependant (Huang 2017). There are three conditions that significantly influence the thermal conductivity in concrete. They are the water content, density, and temperature. Thermal conductivity in normal weight concrete is determined by the mineralogical character of the aggregates. Light weight concrete is filled with more air voids and the moisture content is higher. This mask the effect of aggregate types on the thermal conductivity. Table 7 shows some typical variation of the thermal conductivity of concrete with moisture. The unit of thermal conductivity is watts per meter Kelvin, as seen in the table (Tatro 2006).

The thermal expansion of concrete for a given temperature change is determined by the coefficient of thermal expansion, $\alpha_C$. The risk of early-age thermal cracking can be reduced significantly by producing concretes with a low coefficient of thermal expansion. The coefficient of thermal expansion can be estimated from the knowledge of the coefficients of thermal expansion for aggregates. Figure 5 shows values for some aggregate types and with a proposed design value for concrete (Bamforth 2007).

**Table 7:** Typical variations in thermal conductivity with moisture at normal temperatures. Modified from Tatro (2006).

| **Moisture Condition** | **Conductivity (W/m * K)** |
|---|---|
| | Limestone Concrete |
| Moist | 2.2 |
| 50% relative humidity | 1.7 |
| Dry | 1.4 |
| | Sandstone Concrete |
| Moist | 2.9 |
| 50% relative humidity | 2.2 |
| Dry | 1.4 |
| | Quartz Gravel Concrete |
| Moist | 3.3 |
| 50% relative humidity | 2.7 |
| Dry | 2.3 |
| | Expanded Shale Concrete |
| Moist | 0.85 |
| 50% relative humidity | 0.79 |
| Dry | 0.62 |

| Coarse aggregate/ rock group | Thermal expansion coefficient (microstrain/°C) | | |
|---|---|---|---|
| | Rock | Saturated concrete | Design value |
| Chert or flint | 7.4–13.0 | 11.4–12.2 | 12 |
| Quartzite | 7.0–13.2 | 11.7–14.6 | 14 |
| Sandstone | 4.3–12.1 | 9.2–13.3 | 12.5 |
| Marble | 2.2–16.0 | 4.4–7.4 | 7 |
| Siliceous limestone | 3.6–9.7 | 8.1–11.0 | 10.5 |
| Granite | 1.8–11.9 | 8.1–10.3 | 10 |
| Dolerite | 4.5–8.5 | Average 9.2 | 9.5 |
| Basalt | 4.0–9.7 | 7.9–10.4 | 10 |
| Limestone | 1.8–11.7 | 4.3–10.3 | 9 |
| Glacial gravel | – | 9.0–13.7 | 13 |
| Lytag (coarse and fine) | – | 5.6 | 7 |
| Lytag coarse and natural aggregate fines | – | 8.5–9.5 | 9 |

**Figure 5:** Coefficients of thermal expansion. Taken from Bamforth (2007).

Moisture have a dominant influence on the coefficient of thermal expansion. The saturation of concrete effects the coefficient of thermal expansion. A higher saturation lowers the effect hydration has on the coefficient of thermal expansion. This means the coefficient of thermal expansion can be controlled by controlling the moisture content. The coefficient of thermal expansion is minimum in a saturated state. Concretes with internal water sources obtain two benefits during the curing. Autogenous deformation is reduced or eliminated and the coefficient of thermal expansion is minimised (Sellevold & Bjøntegaard 2006).

The strains induced in concrete from temperature changes can be calculated with equation iii.

$$\varepsilon_T = \alpha_C \Delta T. \tag{iii}$$

Where $\alpha_C$ is the coefficient of thermal expansion, $1/°C$, and $\Delta T$ is the temperature change in °C. The maximum temperature change in the concrete can be calculated with equation iv.

$$\Delta T = T_{max} - T_f = T_i + T_{ad} + T_{env} - T_f. \tag{iv}$$

Where $T_i$ is the initial placing temperature, $T_{ad}$ is the adiabatic temperature rise of the concrete, $T_{env}$ is the temperature change from heat added or removed from the concrete due to environmental conditions, $T_f$ is the final stable temperature of concrete. All have °C as unit. The thermal cracking in concrete results from the volume change at the maximum temperature difference, between the peak temperature during hydration and the minimum

temperature it is subjected to under service conditions (Knoppik-Wróbel & Klemczak 2015).

Thermal shrinkage can be mitigated with different treatments. One way to reduce the thermal shrinkage is by reducing the coefficient of thermal expansion. This can be done by using aggregates with a lower coefficient of thermal expansion, for example by replacing parts of the normal aggregates with light weight aggregates or keeping it moist. The shrinkage can be reduced by lowering the curing and placement temperature. The cracking during summer placing when the thermal stresses are largest can be reduced by replacing parts of the cement with fly ash or slag (Schindler et al. 2019).

### 2.4.4 Drying Shrinkage

Drying shrinkage is described in Naik et al. (2006). This is the basis for this subsection, where other sources have been used separate citations are given. Drying shrinkage occurs because of a reduction of the moisture in hardened cement paste. The reduction of the moisture happens through diffusion of water from the concrete to the surroundings with a lower relative humidity than the concrete.

The changes in the pores during drying can be explained with the illustration in figure 6. The figure shows two pores, one large and one small, that are connected. A meniscus is formed in the pores at the drying surface when the water evaporates. The radii is equal for all pores regardless of the size of the pore. The liquid would be drawn towards the smaller meniscus if the radii were to be different. This comes from the pressure differences. The water is drawn to the smaller radii until equilibrium is restored. The radii of the meniscus decrease during evaporation. The pore starts to drain when $r_m = r_L$ - $\delta$, $\delta$ is the thickness of the liquid film on the pore wall. This is the smallest the meniscus can get. The meniscus in the smaller pores can decrease from evaporation. This creates a pressure difference between the pores and water is drawn from the large pores to the smaller ones (Scherer 2015).

The loss of capillary water from evaporation can lead to tensile stresses in the concrete. The tensile stresses cause the concrete to contract (Zhang et al. 2013). It has been suggested that the tensile stresses come from hydro static tension exerted from the meniscus in small capillaries (5-50 nm). The removal of capillary water induces compressive stresses on the walls of the capillary pores. The compressive stresses contribute to the overall contraction of the concrete system. This contraction is the drying shrinkage (Goodwin 2006).

The size of the drying shrinkage is not the same as the volume of the evaporated water. The reason for this is that the water evaporated from large capillary pores (>50 nm) is considered as free water. The removal of water from all the large capillary pores does not cause any change in the concrete. It is the loss of water from the smaller capillary pores (5-50 nm) that is the cause of the change of volume in the concrete.

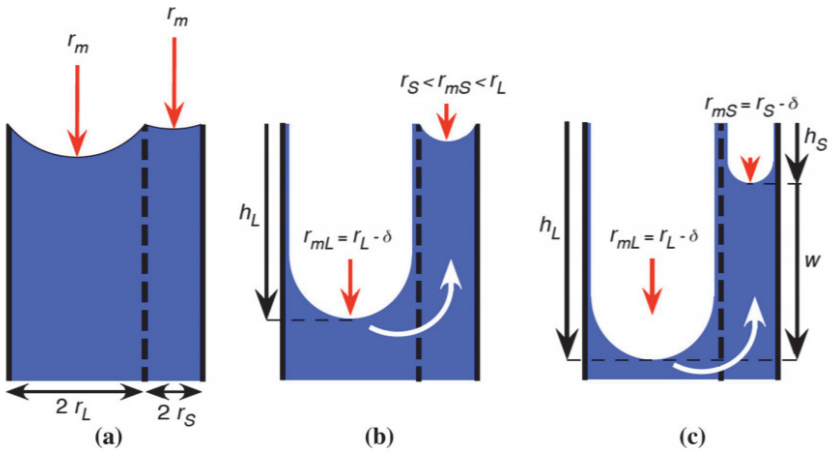


**Figure 6:** Illustrating the draining of pores. (a) Menisci of all pores have the same radii. (b) The meniscus in the smaller pore ($r_{mS} < r_{mL}$) draws liquid to the outer surface, while the larger pore is being drained. (c) The smaller pore starts to drain. Taken from Scherer (2015).

The drying shrinkage starts in the hardened cement paste on the surface and progresses gradually through the concrete. The rate it progresses depends on the relative humidity in the air around the concrete, the size and connection between the capillary pores. The drying happens fast in normal concrete with good connection between the capillary pores. The drying is slow in a high strength concrete with finer capillary pores and little connection between the pores.

Jacobsen et al. (2015) tells shortly on how to mitigate drying shrinkage. They mention a rule of thumb. The rule is that if less water (or binder) are used in the concrete mix then less drying shrinkage is expected. An even grading of the aggregates and a large biggest fraction in the aggregates helps to restrain the concrete. This is because the aggregates do not shrink when it dries out. Finally, it is mentioned that it is important to remember that the humidity of the air is the driving force behind drying shrinkage. This can be interpreted, that keeping the concrete moist keeps the drying shrinkage away.

## 2.5 Shrinkage Cracking

Cracks have a negative effect on the structural integrity, durability, and long-term service life in concrete structures. The development of early age cracks is a problem that arises from the interaction between the concrete and the environment, when the concrete experiences complex physical and chemical changes (Mihashi & de B. Leite 2004). The service life of any given structure gets shorter the earlier cracking occurs (Combrinck & Boshoff 2013). It is necessary for durability and functionality to be able to develop concrete structures without cracks. Cracks accelerate the flow of materials and fluids through the concrete. This may harm the concrete now or in the future. One example of this is chloride that can lead to corrosion of the reinforcement (Sayahi et al. 2014). Therefore, it is important to understand how cracks develop in concrete. It is possible to develop concrete with a

smaller risk of developing cracks and better durability with that understanding. Under the development of shrinkage cracks and some mitigating measures against shrinkage cracking are described.

### 2.5.1 Plastic Shrinkage Cracking

Plastic shrinkage cracks are often the first cracks to develop in concrete structures (Sayahi et al. 2014). Figure 7 shows the stepwise development of plastic shrinkage cracks in concrete. The first steps of the figure were explained in the development of plastic shrinkage. The rest of the steps are explained here.

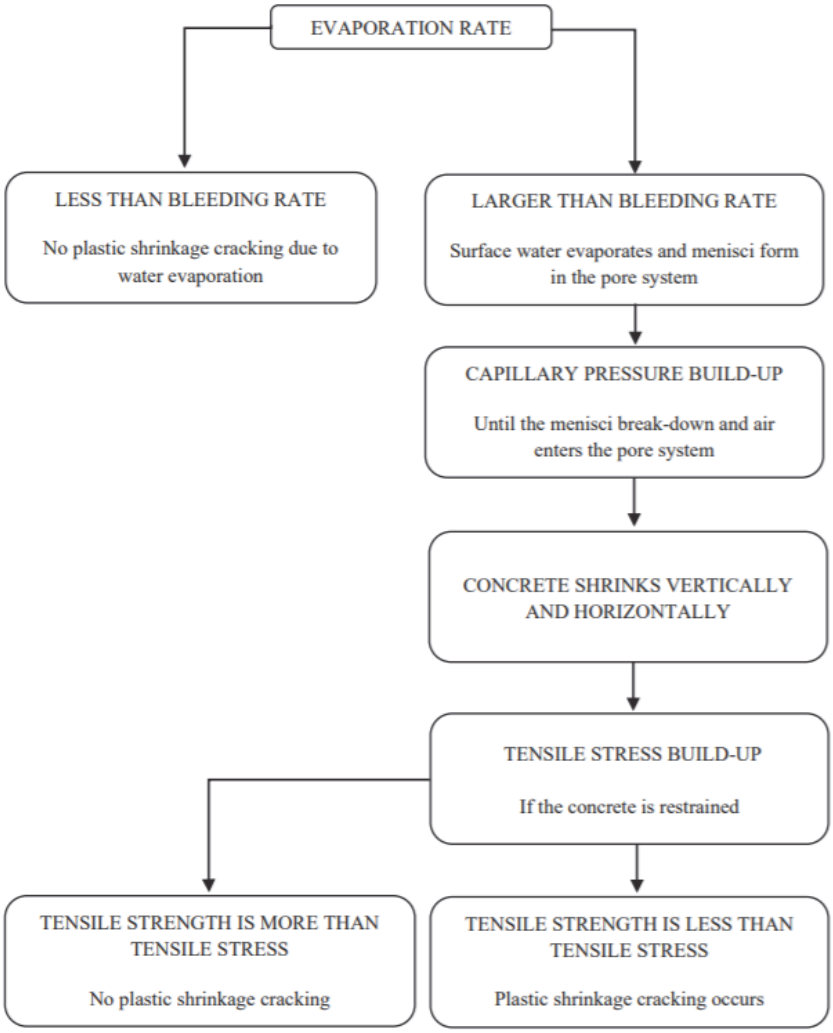


**Figure 7:** Stepwise development of plastic shrinkage cracks. Found in Sayahi (2019).

Plastic shrinkage can induce tension forces in the concrete if the concrete is restrained. The restraint can come from reinforcement, different thickness in the concrete, various shrinkage in different parts of the concrete, from friction from the formwork or from the rock surface. The tension starts on the surface. Cracks start to develop if the tension is larger than the tensile strength of the concrete. The tensile strength is very low in the early stages of the concrete. Plastic shrinkage cracks are often very thin and cannot be seen with the naked eye (Sayahi et al. 2014). The internal restrained shrinkage strains change rapidly during the first few hours after casting. The tensile strength and strain to failure also changes. These changes limit the times the restrained strains exceed the capacity of the concrete and cause plastic shrinkage cracks (Branch et al. 2002).

Figure 8 under shows how plastic shrinkage cracks normally develop. There plastic shrinkage cracks are mainly related to the evaporation and the bleeding rate of the concrete (Sayahi et al. 2014). A couple of ways to calculate the evaporation rate in concrete is explained here. There is not much bleeding water on the surface of sprayed concrete since the concrete hangs on vertical and overhead walls. Therefore, the focus is on evaporation.

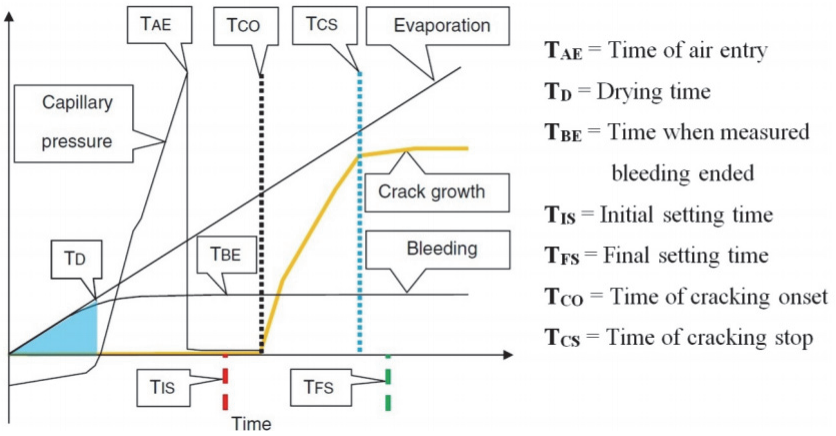


**Figure 8:** Typical development of plastic shrinkage cracks. Found in Sayahi et al. (2014).

**Evaporation** usually gets calculated with the diagram in figure 9. There the evaporation is calculated with four steps. First the air temperature is measured. From the air temperature one moves up in the diagram to the measured relative humidity. The next step is to move to the right to the measured concrete temperature. Then move down to the wind velocity. The evaporation can be read to the left of the wind velocity. Another way of calculating the evaporation is with equation v under. The diagram and the equation give almost identical results for the evaporation (ACI 2007).

$$E = 5([T_c - 18]^{2.5} - r[T_a + 18]^{2.5})(V + 4) * 10^{-6}. \quad \text{(v)}$$

Where E is the evaporation rate ($kg/m^2/h$), $T_c$ is the concrete temperature (°C), $T_a$ is the air temperature (°C), r is the relative humidity in percent and V is the wind velocity (km/h).

There are other factors that also affect the plastic shrinkage cracking, but it is emphasised that the main factor affecting plastic shrinkage cracking is evaporation. Higher concrete grade (high cement content or low w/c) increases plastic shrinkage. Air entraining and retarding admixtures generally increase plastic shrinkage. Replacement of cement with fly ash increases evaporation, reduces bleeding, increases cracking, and reduces the time to onset of cracking (Dias 2003).

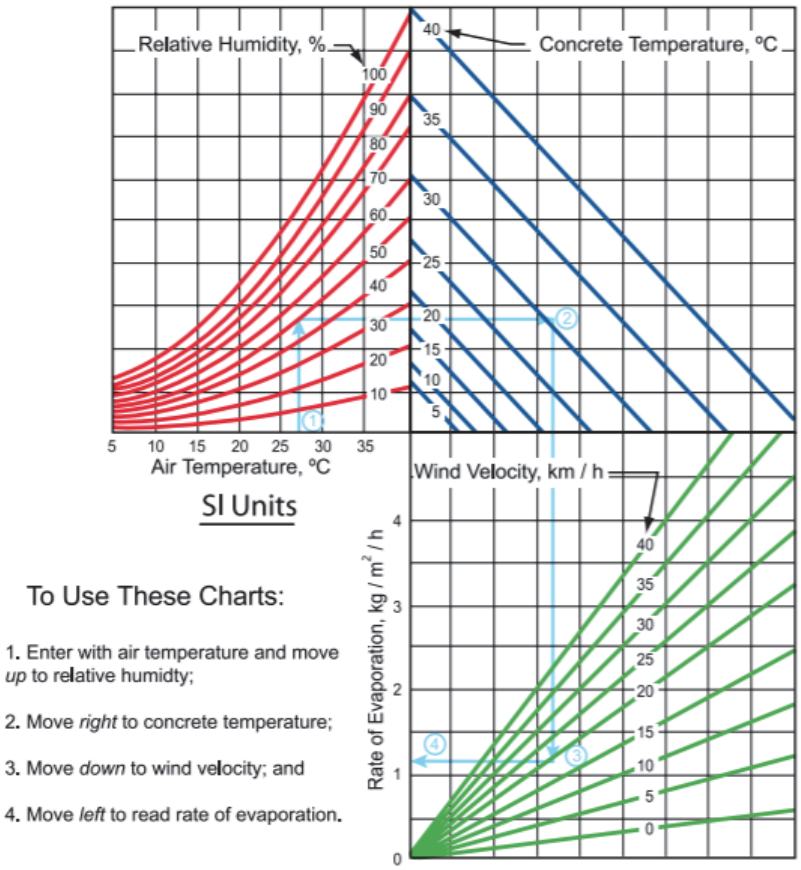


**Figure 9:** Evaporation diagram. The light blue arrows show an example. In the example, the air temperature is 27°C, the relative humidity is 50%, the concrete temperature is 31°C and the wind velocity is 19 km/h. That gives an evaporation of 1,2 kg/$m^2$/h. Found in ACI (2007).

### 2.5.2 Thermal Shrinkage Cracks

Thermal shrinkage is the main cause of cracking in massive concrete structures. This comes from the heat liberated during hydration. The peak temperature often exceeds 60 °C in mass concrete. Thermal shrinkage cracking develops due to external restrains, but also by internal restrains. The internal restrains are caused by the difference in thermal expansion coefficients of aggregates and cement (Liwu & Min 2006).

The restrains of the concrete may generate internal stresses. The behaviour of the cement matrix under thermal stresses can be estimated. This demands information on the heat liberated, temperature variation and thermal shrinkage. The thermal shrinkage is proportional to the coefficient of thermal expansion as mentioned earlier. Therefore, the thermal stress development is highly dependent on the coefficient of thermal expansion. It is important to understand the coefficient of thermal expansion to know if thermal shrinkage cracks can develop (Liwu & Min 2006).

### 2.5.3 Drying Shrinkage Cracks

Drying shrinkage cracks develop in concrete that experiences drying shrinkage. Concrete structures that cannot deform freely develop tension in the restrained concrete. The tension may lead to drying shrinkage cracks. Drying shrinkage cracks develop if the tension becomes larger than the tensile strength of the concrete (Topçu & Bilir 2010). The tension from the drying of concrete can also expand the plastic shrinkage cracks in the concrete (Sayahi et al. 2014).

The type of drying shrinkage cracking is determined by the restraints in the concrete. The restrains should be separated in external and internal. External restrain of the shrinkage is caused by surrounding structures, or the rock mass in tunnels. Cracks developed from this kind of restrains are generally visible to the unaided eye. These cracks are referred to as macro cracks. Internal restrains can happen from two mechanisms. The first one is called self-restraining of the material. This restraint comes from non-uniform shrinkage in the material. The non-uniform shrinkage is caused by a moisture gradient during the drying of the concrete. The shrinkage causes tensile stress near the surface that is drying and compressive stresses in the centre. Micro crack with little penetration develops if the tensile stresses exceed the tensile strength. The second type of internal restraints are caused by the stiff aggregate particles. Radial and bond cracks forms around the aggregate particles when the shrinkage is large enough. These are also small micro cracks (Shiotani et al. 2003).

### 2.5.4 Shrinkage Cracks in Sprayed Concrete

Cracking in sprayed concrete differs from normal cast concrete. This was investigated in Sweden. The wet mix sprayed concrete is like an ordinary concrete. The properties in the sprayed concrete changes from the ordinary cast concrete when the accelerator is added in the nozzle during the spraying. The accelerator stiffens the sprayed concrete. This makes the cement reactions happen in a stiff, not hardened, material. The hydration of the cement leads to shrinkage. The settlement in normal cast concrete compensates for the shrinkage. This is not possible in the stiff sprayed concrete. The pore structure is also changed because of the accelerator. The amount of coarse porosity is higher with an alkali free accelerator. The increased porosity makes the sprayed concrete susceptible to drying

(Lagerblad et al. 2010).

All concrete structures shrink. The shrinkage is not at problem if the concrete is not restrained. This is not the case for most structures. Most structures have restraints that hiders the volume changes. The bond to the rock surface is restraining the shrinkage in sprayed concrete. Restrained shrinkage leads to stresses building up. The stresses can result in the concrete cracking. It is there for a need to control the shrinkage properties better. This is especially important for sprayed concrete. Since the shrinkage is larger in sprayed concrete than in cast concrete, because of the large cement content and the use of set accelerator (Bryne et al. 2014*a*). An increasing degree of restraint induce more tensile stresses. This reduce the time to cracking, when the rest of the parameters are unchanged (Khan et al. 2017).

Lagerblad et al. (2010) mentioned that chemical shrinkage can cause considerable cracking in sprayed concrete. Chemical shrinkage comes from the products of the hardening process have a smaller volume than before the chemical reactions. The chemical reactions are shown in equation i and ii. This can cause cracking since the sprayed concrete is stiff when the chemical reactions happen. The sprayed concrete is not stiff enough to withstand the forces of the chemical shrinkage. The shrinkage cracking from chemical shrinkage can be averted by adding water during the hardening. The chemical shrinkage in the stiff sprayed concrete increases the porosity and makes it coarser than in cast concrete.

Aggregates may affect the cracking of the concrete. The aggregates work as internal restraints. This leads to micro cracks around the aggregates when the concrete shrinks. The size of the micro cracks is dependent on the aggregate size and volume fraction. A large aggregate diameter or volume fraction leads to a shorter length of the micro cracks. The crack width decreases with an increasing volume fraction and decreasing aggregate diameter. This affects the permeability of the concrete. The permeability increase with larger aggregates and a lower volume fraction, because of the increase of the micro crack width (Grassl et al. 2009).

Tensile creep behaviour is important for the understanding of stress development and prediction of early age cracking in restrained concrete. Tensile creep may lead to stress relaxation in the concrete. This delays shrinkage induced cracking (Khan et al. 2017). Creep is time- and stress dependent deformation. It can be defined as the difference in strain between a loaded and an unloaded specimen. Creep in concrete can be divided into two types depending on the ambient humidity. The types are basic creep and drying creep. Basic creep is creep that occurs when there is no moisture exchange between the concrete and the environment. Drying creep is creep with moisture exchange with the environment (Atrushi 2003). Under drying conditions, the creep increases sharply. The time of loading affects the creep. The creep increases with earlier loading of the concrete (Bissonnette et al. 2007).

Early age tensile creep together with shrinkage are important factors. Restrained shrinkage in concrete causes stresses, while tensile creep is a stress relaxation mechanism (Altoubat & Lange 2001). It is very important to be aware of the creep in concrete, when estimating the possibility of cracking in concrete due to restrained shrinkage and thermal stresses at early ages. There is considerable creep in hardening concrete. The creep can be as large as 30% to 70% of the autogenous shrinkage. The stress reduction due to creep can lead to a reduction of the restraining stresses by 50% in hardening concrete (Tao & Weizu 2005).

## 2.6 Adhesion

The adhesion between the sprayed concrete and the rock surface is an important property. This property is affected by the shrinkage. Tests have shown that the restrained shrinkage in sprayed concrete can destroy the bond between the sprayed concrete and the rock surface. The sprayed concrete loses its ability to distribute and control the crack width if the bond fails (Malmgren et al. 2005). Therefore, it is important to understand what affects the adhesion strength in sprayed concrete to have better crack control.

Traditionally, adhesion strength is defined as the strength of the surface between two materials. An example is between sprayed concrete and rock. Failures can develop in multiple places, where they develop varies depending on the strength of the contact zone, the tensile strength of the sprayed concrete and the rock (Malmgren et al. 2005).

The adhesion strength between rock and sprayed concrete is dependant of a few factors. The most important ones are the treatment (cleaning) of the surface, surface roughness, the mineral composition of the rock and the spraying technique (Malmgren et al. 2005).

Duan et al. (2019) studied the adhesion strength of sprayed concrete in tunnels with high terrestrial heat. They found out that the temperature and the humidity is the most important factors affecting the adhesion strength, when the tunnel temperature is above 35°C. The adhesion strength decreases with increasing temperature. This is shown in figure 10. It increases with higher humidity. Figure 11 demonstrates this. The water disperses quickly in a dry heat situation. The loss of water stops the hydration of cement early. This leads to a low density of the hydration product and an insufficient strength in the sprayed concrete. The dry heat lead to drying shrinkage. All of this leads to a low adhesion strength between the sprayed concrete and the rock in dry heat situations.

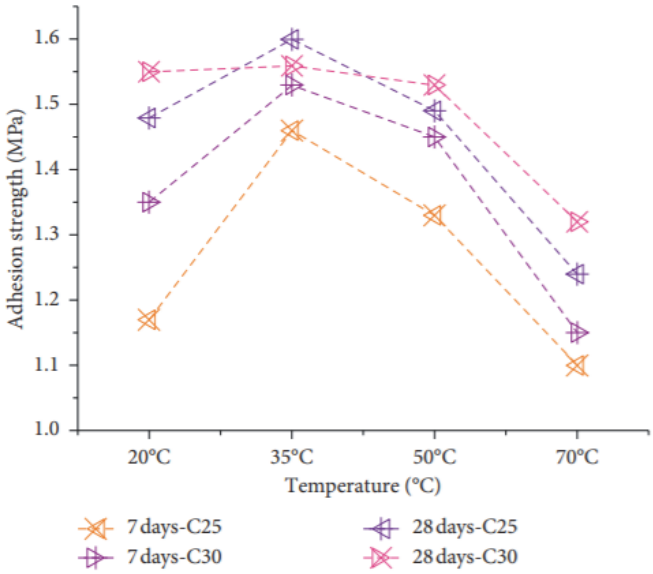


**Figure 10:** Rock-concrete adhesion strength of different concrete grades at different temperatures. Found in Duan et al. (2019).

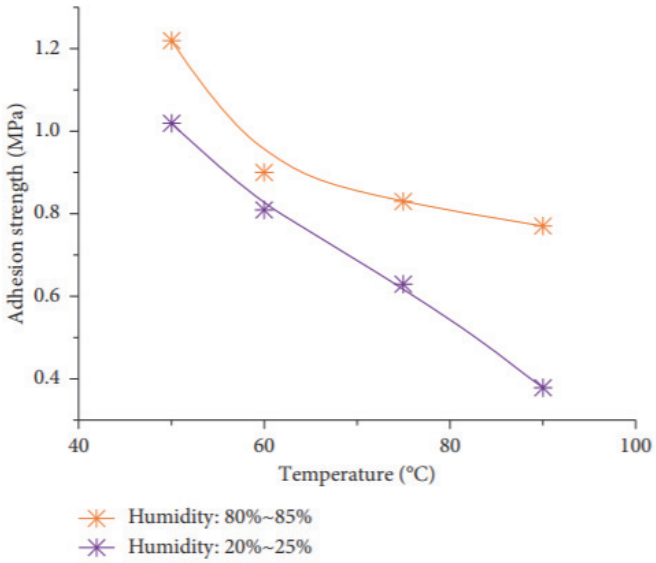


**Figure 11:** Rock-concrete adhesion strength at different humidity levels at different temperatures. Found in Duan et al. (2019).

Cleaning of the rock surface is important. Contamination on the surface reduces the adhesion strength (Son 2013). Therefore, it is important that the surface is free of dust, oil, grease, and other contaminants. The contaminants decrease the friction on the surface. They create a preventative layer for interlock between the sprayed concrete and the surface (Bakhsh 2010).

It is important to remove surface deterioration and damages before the sprayed concrete is applied. This is to gain proper bonding to the surface and to remove weak parts. Table 8 is a summary of different ways to prepare a surface for application of sprayed concrete.

The methods are developed to get a good bond between the concrete and the substrate surface. They work on different types of surfaces and to different depths. Some of the methods can remove materials to a significant depth and other methods can only remove thin layers of concrete (Bakhsh 2010). The most common way to prepare the rock surface for spraying in hard rock tunnelling is through mechanical scaling and cleaning with water. It was shown that rock surfaces treated with high pressure water gained increased adhesion strength (Son 2013). Malmgren et al. (2005) found out that scaling the rock surface with water jet gained a much greater adhesion strength compared to the commonly applied mechanical scaling.

Ozturk & Tannant (2011) looked at how rock properties and surface roughness affect the adhesion strength of a thin spray-on liner. The liner was applied to different rock types with different roughness. The results showed that the roughness of the substrate does not increase the adhesive strength. It was observed that the chemical reaction between the rock grains and the liner material was more important to get a high adhesive strength. This was more important than the mechanical interlocking.

**Table 8:** Methods to treat surfaces before applying sprayed concrete to improve bond strength. Modified from Bakhsh (2010).

| Removal method | Principle behaviour | Important advantages | Important disadvantages |
|---|---|---|---|
| **Sand-blasting** | Blasting with sands. | No micro cracking. | Not selective, leaves considerable sand. |
| **Scrabbling** | Pneumatically driven bits impaction. | No micro cracking, no dust. | Not selective. |
| **Shot blasting** | Blasting with steel balls. | No micro cracking, no dust. | Not selective. |
| **Grinding (planning)** | Grinding with rotating lamella. | Removes uneven parts. | Dust development, not selective. |
| **Milling ( scarifying)** | Longitudinal tracks are introduced by rotating metal lamellas. | Suitable for large volume work, good bond if followed by water flushing. | Micro cracking is likely, reinforcement may be damaged, dust development, noisy, not selective. |
| **Pneumatic (jack) hammers (chipping), hand-held or boom-mounted** | Compressed-air-operated chipping | Simple and flexible use, large ones are effective. | Micro cracking, damages reinforcement, poor working environment, slow production rate, not selective. |
| **Explosive blasting** | Controlled blasting using small, densely spaced blasting charges. | Effective for large removal volumes. | Difficult to limit to solely damaged concrete, safety and environmental regulations limit use, not selective. |
| **Water-jetting/ hydro demolition** | High pressure water jet from a unit with a movable nozzle. | Effective (especially on horizontal surfaces), selective, does not damage reinforcement or concrete, improved working environment. | Water handling, removal in frost degrees, costs for establishment. |

Movements in sprayed concrete due to shrinkage and thermal effects is restrained by the bond between the sprayed concrete and the rock. The sprayed concrete is expected to form several small cracks if the bond to the rock surface is complete. Local debonding in a section leads to severe cracking. The sprayed concrete has an end restrained situation if it debonds from the substrate surface. End restrained slabs are prone to cracking induced by

shrinkage. They develop one large crack due to the absence of other restraints (Sjölander & Ansell 2017). Several small cracks are better than one larger crack. This can be explained with the following equation vi. The equation has a basis in Darcy's equation for water flow between two parallel smooth plates.

$$v = \frac{e^2 * \rho * g}{12\mu} * i = \frac{g * e^2}{12\nu} * i$$
$$or \tag{vi}$$
$$q = \frac{e^3 * \rho * g}{12\mu} * i = \frac{g * e^3}{12\nu} * i$$

where v is the flow rate (m/s), q is the crack transmissivity ($m^2/s$), e is the crack width (distance between the plates) (m), i is the effective hydraulic gradient, $\rho$ is the density of the fluid ($kg/m^3$), g is the gravity ($m/s^2$), $\mu$ is the viscosity of the fluid (Pa*s), $\nu$ is the kinematic viscosity ($m^2/s$).

The flowing water volume increases if the crack width (e). The increase is by a factor of 1000 if the crack width is increased from 0.01 mm to 0.1 mm, when all other factors are kept constant. This can be said in another way. A single crack of 0.1 mm gives the same water leakage as 1000 cracks with width 0.01 mm (Nilsen 2016).

## 2.7 Self-healing

Some concretes can self-heal. Self-healing is when a material can repair itself to its original state. Concrete can self-heal in two ways, autogenic and artificial self-healing (Alhalabi et al. 2017). This is an important mechanism to prolong the service life of a concrete structure and to water-tighten structures (Li & Yang 2007). The mechanisms of autogenic and artificial self-healing is explained shortly under.

Autogenic or natural self-healing is something that has been observed in many old structures. These observations show cracks that have sealed themselves in structures that have had limited maintenance. The natural healing comes from non-hydrated cement clinker in cracks. The non-hydrated cement interacts with moisture when the cracks open. This can result in sealing of the cracks. The amount of cement used is lower in modern concrete. This means that there is less non-hydrated cement available and the autogenic self-healing is reduced (Alhalabi et al. 2017). In et al. (2013) wrote that natural self-healing in cracks in concrete could happen in three ways. The first one is formation of calcium carbonate or calcium hydroxide. The second one is sedimentation of particles in the cracks. The last is hydration and swelling of the cement matrix. Self-healing can only occur if there is presence of water, the crack is stable and the liquid in the crack does not lead to leaching or dissolution of the concrete.

Bacterial spores and calcium lactate embedded in expanded clay pellets is added to the concrete mix in artificial self-healing. They are uniformly distributed in the concrete during the mixing. The pellets break and release the spores and calcium lactate when cracks develop in the concrete. A favourable environment for the bacteria develops if moisture and air enter these cracks. The favourable environment makes them grow. These bacteria produce limestone that eventually seals the cracks. It has been shown that this technique of self-healing can repair cracks up to 0.5 mm (Ghodke & Mote 2018).

Self-healing with bacteria is an advantageous method. It seals of cracks in structures, lowers the permeability, which again reduces the corrosion of steel reinforcement and increases the durability. An increase in durability makes the concrete eco-friendlier. The increased durability lowers the need for repair works and replacement of the concrete. Therefore, it becomes eco-friendlier. There are also some disadvantages with the method. The pellets replace parts of the aggregates and occupy around 20% of the total volume of the concrete. This leads to a reduction in compressive strength of 20-25%. It is also costly to buy the healing agent, calcium lactate. This makes self-healing concrete more expensive than normal concrete (Ghodke & Mote 2018).

## 2.8 Shrinkage Mitigation

Formation of shrinkage cracks are unwanted in sprayed concrete. This is not because they cause failure of concrete constructions, but over time they might develop. The development of shrinkage cracks may lead to deterioration and failure. Aggressive agents may come into the concrete through the cracks. Examples of aggressive agents are chlorides, sulphates, and carbonates. They can deteriorate the concrete and shorten the durability of the concrete (Safiuddin et al. 2018). There are different actions that can be done to mitigate the shrinkage and cracking in sprayed concrete. Some mitigating actions are mentioned here.

### 2.8.1 Aggregates

The choice of aggregates can affect how much shrinkage there is in the concrete. The use of soft aggregates, like sandstone, may lead to increased drying shrinkage. The use of harder aggregates like quartz can decrease the shrinkage (TRB 2006). The size of the aggregate also affects the shrinkage. The shrinkage becomes smaller in the concrete by increasing the size of the coarse aggregate (Qiao et al. 2010).

Fujiwara (2008) looked at length changes in aggregates due to absorption and drying. The tests showed that the length change in aggregates is much smaller than in the cement paste. Most of the shrinkage happens in the cement paste during the drying of concrete. The length change in the aggregates is not necessarily small enough to be negligible, as it is often assumed. It was also showed that the length change in lightweight aggregates is

smaller than in normal aggregates.

Henkensiefken et al. (2009) tested the use of saturated lightweight aggregates to improve the internal curing in concrete. The tests demonstrated that this decreased the shrinkage. The shrinkage cracks could be delayed or prevented if a large enough amount of saturated lightweight aggregates were used. Plastic shrinkage cracking was reduced or eliminated. It was pinpointed that this had only been tested in the laboratory. There is still a lot of work needed before this could be used in practice.

### 2.8.2 Cement-Binder

A decrease in the cement content in concrete has a direct positive effect on reducing and controlling the cracking in concrete. It is generated less heat in concrete by using less cement. There is less thermal shrinkage with less heat. Thermal shrinkage is the contraction of the concrete when it is cooled down. Concretes with a lower cement content show lower autogenous- and drying shrinkage (TRB 2006).

Bentz & Peltz (2008) looked at how to reduce the autogenous shrinkage and the contribution this has on the early crack formation in concrete. They found out that there is three ways to reduce the autogenous shrinkage. The different ways were by increasing w/c, using coarser cement powder, or replacing parts of the cement with coarse limestone powder. All these measures reduce the early strength gain and heat that is developed in the concrete.

The cement can be replaced with replacement materials. The amount of plastic shrinkage cracks increases with high replacement amounts of ground granulated blast-furnace slag or fly ash. This is because the binder gets finer, the settlement slower and the early strength lower (Sirajuddin & Gettu 2018). It is therefore important to limit the replacement amount to lower the shrinkage.

### 2.8.3 Admixtures

Chemical admixtures can be used to reduce the amount of shrinkage cracks. Shrinkage reducing admixtures (SRA) changes the surface tension of the pore liquid in concrete. This reduces the shrinkage by reducing the capillary pressure through a lower tension in the pore water surface (Radlinska et al. 2008). This was tested by Sirajuddin & Gettu (2018). They saw an effect of SRA by adding a dosage of 1%, and by a dosage of 2% the shrinkage cracks was eliminated.

Crack-reducing admixture (CRA) is another chemical admixture that can be used to reduce cracks in concrete. The admixture has a similar effect on setting time and strength of concrete as SRA. It lowers the surface tension of the water in a similar way as SRA. This reduces the drying shrinkage in concrete the same way as SRA. The way CRA differs from SRA is that it changes the mode of failure. The mode of failure is changed from a sudden release of all the compressive strain to a gradual reduction in strain. This provides an

increased time to cracking. The reason for the increased time to cracking was attributed to a relaxation of the tensile stress (Nmai et al. 2014).

Essili (2017) compared the effect of CRA and SRA. The tests showed that CRA gave better results in reducing shrinkage and shrinkage cracks than SRA. The concrete with CRA also achieved better mechanical properties than the control mix. One side effect by using CRA is that the concrete can get extra spalling due to freeze-thaw. This can be reduced by adding fibres and by having a high enough air content.

### 2.8.4 Fibre

Fibres is another way of reducing shrinkage cracks in concrete. They work as millions of bridges that distribute the tension forces. This intercept and stops the growth and development of cracks in all directions by reinforcing the concrete in all directions (Ruiz-Ripoll et al. 2016). This is not new knowledge. The Romans used horsehair in their concrete to reduce the shrinkage over 2000 years ago (Pillar & Repette 2015). The effect different fibre types and lengths have on shrinkage and shrinkage cracks in concrete is explained in the next paragraphs.

The strength of concrete can be improved by adding steel fibres. A random distribution of steel fibres can delay the visible cracking and reduce the cracking. The steel fibres create a restraint inside the concrete. Mainly they contribute to crack control after cracking (Qiao et al. 2010). Pillar & Repette (2015) showed that steel fibres work efficient to reduce the plastic shrinkage cracking in concrete. The fibres tied up the water. A concrete with steel fibres keeps the water better than a concrete without fibres.

Synthetic fibres showed a lot of the same properties as steel fibres. Polypropylene and polyester fibres showed a little bit better water bearing capacity than other types of fibres. This could be because they hinder settlement in the concrete. This stops the water from moving upwards in the concrete (Sirajuddin & Gettu 2018).

Boghossian & Wegner (2008) tested to use a natural fibre, flax, to reduce the cracking in concrete. The tests showed that flax fibres preformed slightly better than other synthetic fibres, when optimal lengths were compared in terms of reducing total crack area and limit crack widths in fresh mortar specimens. This fibre is a waste by-product from industrial or agricultural processes. It would be a cheap alternative to the fibres used today.

The length of the fibres affects the concrete properties. Shorter fibres increase the amount of fibres in the concrete per kg added. They are used to decrease the cracking and increase the durability. Longer fibres are used to improve the mechanical properties. Macro polypropylene fibre have a negative effect on the shrinkage in concrete. An explanation for this may be that they increase the permeability of the concrete and this makes the concrete more exposed to drying (Qiao et al. 2010). Micro fibres reduce the early shrinkage cracks significantly. The efficiency of the micro fibres depends on the dosage (Ruiz-Ripoll

et al. 2016). It is therefore important to find the optimum amount for each mix design.

The control of plastic shrinkage cracking can be improved by choosing the right fibre diameter. A finer diameter can lead to substantial improvement. Fine diameter fibres, less than 0.04 mm, at a volume fraction of 0.2% can reduce the plastic shrinkage to approximately 10% of a concrete without fibres (Naaman et al. 2005).

The distribution of cracks is of importance for the sprayed concrete. It is better with several fine cracks than one wider. This was showed earlier in the section on adhesion. Wider cracks lead to faster deterioration. Fibres can be used to change the crack distribution. Steel fibres have a strain softening behaviour. This combined with the restrained shrinkage leads to an unfavourable crack formation. The addition of very fine fibre glass could be a possible solution. Ring tests have showed that very fine glass fibres can prevent macro cracks from forming. This is probably due to the fibre glass is stopping the micro cracks form expanding into larger cracks (Bryne et al. 2014*a*).

### 2.8.5 Curing

The goal of good curing is to keep the concrete saturated. The saturation keeps the hydration going and evaporation of the pore water is avoided. This reduces or removes the shrinkage. Figure 12 shows how the mechanical strength develop in concrete with w/c of 0.5 under different wet curing lengths. There the test specimens that had wet curing for the whole period gained the highest compressive strength (Neville & Brooks 2010).

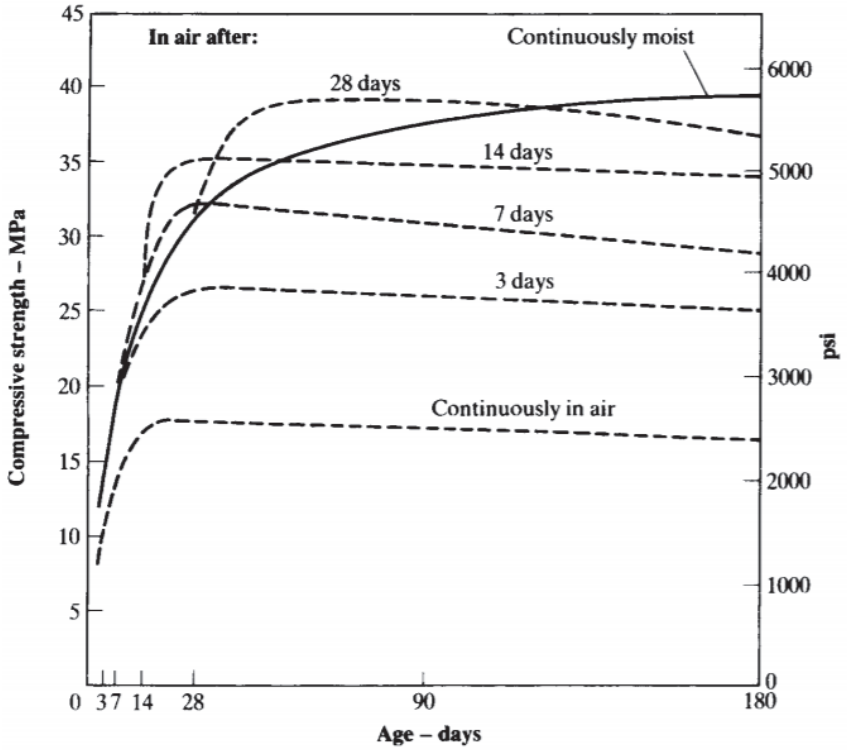


**Figure 12:** Influence of wet curing on compressive strength for a concrete with w/c ratio of 0.5. Taken from Neville & Brooks (2010).

Sprayed concrete must harden like normal cast concrete. It is important that it gets to harden properly to fully develop its mechanical strength and durability. This is especially important for thin sections, low w/c ratios and uneven surfaces (Bernard 2010). Curing is designed to hinder the loss of water in the sprayed concrete. The shrinkage and cracking can be minimised with proper curing (Schallom III 2006).

The final sprayed concrete is not better than the curing it has received. This process is much harder for sprayed concrete than for normal cast concrete. Sprayed concrete is exposed to drying, wind and loads from the rock mass during the first hours. Normal cast concrete often is enclosed within formwork shielded from the exposure (Höfler & Schlumpf 2004). Some measures to improve the curing of sprayed concrete are mentioned in the next paragraphs.

The goal is to achieve wet curing in sprayed concrete. It is possible to try to achieve this by covering up the sprayed concrete with wet burlap covered with plastic or tarpaulin. There can be installed a sprinkler system or water hose to spray water continuously on the sprayed concrete to keep it moist. The surface can be covered with a liquid membrane that helps the sprayed concrete to keep the water (Schallom III 2006).

Another option to wet curing is internal curing. Like the one that was mentioned with the lightweight aggregate or superabsorbent polymers. Superabsorbent polymers are explained later. The sprayed concrete gets water from the materials inside with internal curing. This improves the curing of the concrete.

The last curing option is natural curing. This can only be used if the atmospheric conditions are favourable. One example of favourable conditions is when the relative humidity is above 85%. It is important to monitor the relative humidity, temperature, and wind/air flow to see if it changes. These changes affect the natural curing (Bernard 2010).

### 2.8.6 Superabsorbent Polymers

An interesting alternative to reduce shrinkage and shrinkage cracking are superabsorbent polymers (SAP). This was described in Mignon et al. (2017). SAP are cross bindings of hydro gel networks that consists of water-soluble polymers. These can hold water solutions up to many hundred times its own weight. Figure 13 shows an example of this. Even under pressure they hold the water. This expansion is one of the most important properties for SAP in concrete usage.

SAP are used for multiple purposes. The biggest volume is used for single use diapers and sanitary napkins. They are used to absorb liquids from the body during surgeries and for treatment of edema in medicine. Agriculture uses SAP to retain water in the soil. Especially in arid areas, this is a significant improvement of the soil and makes the conditions much better for plants. They are also in use for other purposes like food packaging, artificial snow, toys and more (Zohuriaan-Mehr & Kabiri 2008).

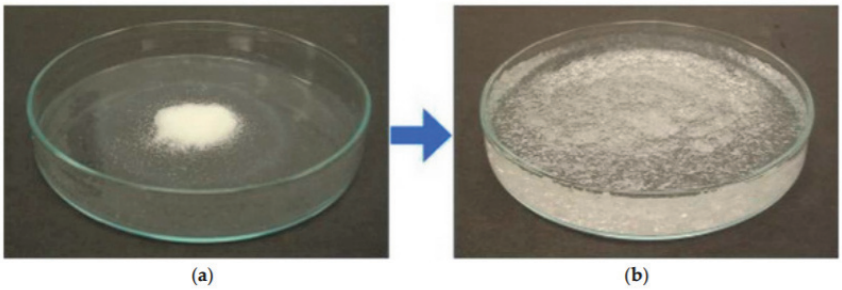


**Figure 13:** (a) Dry SAP powder and (b) swelled SAP. Taken from Mignon et al. (2017).

The way SAP works in concrete is that they absorb parts of the mixing water during the mixing of the concrete. This water may be released at a later stage within the matrix. The water works as an internal curing agent. This can reduce and in some cases eliminate the autogenous shrinkage. Elimination of the autogenous shrinkage improve the mechanical properties of the concrete. Unfortunately, they may form macro pores that have a negative effect on the compressive strength of the concrete. Schröfl et al. (2012) looked at this. Their tests revealed that the type of SAP and the water release kinetics of the SAP is important for the mechanical properties of concrete. SAP with a high density of anionic function groups that releases the water prematurely leads to a decrease in compressive strength. The early release of water increases the effective w/c and subsequently higher porosity of the mortar. Concrete mixtures with SAP with a lower anion concentration observed no decrease or a very moderate decrease in compressive strength. Here the SAP releases the water during the self-desiccation and truly works as an internal curing agent.

Internal curing agents are only effective when they increase the degree of hydration. The strength of the concrete increases when they increase the degree of hydration. SAP added beyond the point where they increase the degree of hydration lead to a decrease of strength. This happens in two situations. The first situation is when there is a high w/c ($> 0.42$) and the water from the reservoirs are not needed. The other situation is at low w/c and the reservoirs contains more water than can be used for hydration. Figure 14 shows an example on how SAP affects the degree of hydration. Case (B) in figure 14 there is added more internal curing water through SAP than what is needed. This leads to an increase of the pore volume. The rule of thumb says that each % of air added in the concrete reduces the compressive strength with 5% compared to air free concrete (Hasholt et al. 2012).

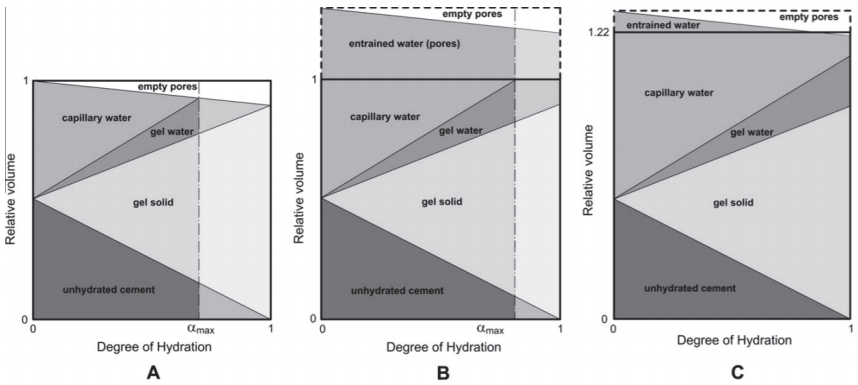


**Figure 14:** (A) Closed system, w/c = 0.32. The hydration stops when the free water is used. The maximum degree of hydration $\alpha_{max}$ is 0.71. (B) Closed system with reservoir with internal curing water, w/c = 0,32 and $w_e/c = 0.19$. The hydration stops when there is no more space for the gel to grow, even though there is access to free water. The maximum degree of hydration $\alpha_{max}$ is 0.83. The pore volume in this situation is more than three times larger. (C) Closed system with reservoir with internal curing water, w/c = 0,45 and $w_e/c = 0.06$. Since w/c is > 0.42 full hydration ($\alpha_{max} = 1$) is possible. In this situation there are no need for entrained water. The entrained water only contributes to creating a larger pore volume. (In both (B) and (C) it is assumed that the capillary pores are fully saturated if there is internal curing water in the reservoirs.) Taken from Hasholt et al. (2012).

SAP also affects other properties in concrete. The macro pores help to improve the freeze-thaw resistance in the concrete, in the same way as air entraining admixture. The SAP can swell in cracks and this lowers the water permeability. It has a self-sealing effect. This is very interesting for waterproof structures.

Even with all these good effects from SAP on concrete, it is pinpointed by Mignon et al. (2017) that this is still under development. There are still some challenges that needs to be overcome before it is used in construction. The need for extra water during mixing because of the swelling of the SAP need to be resolved and how to avoid clusters of SAP during mixing. It is also needed to find ways to reduce the formation of macro pores from the SAP.

# 3 Method

This section presents the location the sprayed concrete came from. How the sprayed concrete cores were sampled and the mix design of the sprayed concrete. Then there is a short description of the laboratories where all the testing was done. The method used for all the lab tests are described. The descriptions starts with the dye penetrant testing, then uniaxial compressive strength testing, density, and fibre content measurements. The section ends with a description on how the quality of the rock mass was classified, and how the test results were analysed.

## 3.1 Description of Test Site, Fv. 659 Nordøyvegen

A tunnel project with a high sprayed concrete usage was needed as a test site for this master's thesis. Fv. 659 Nordøyvegen was chosen as the test site for this master's thesis. Since the firm responsible for the sprayed concrete work, Entreprenørservice, is part of the SUPERCON research project. The project expected to use large amounts of sprayed concrete during the period this master's thesis had to be written. That was convenient for the work on the thesis.

Nordøyvegen is a road project connecting the old municipalities of Haram and Sandøy, now part of Ålesund municipality, with the mainland. The project was started in 2017 and expected to finish in 2022 with a total cost of 4,90 billion NOK. Figure 15 shows the planned new road with tunnels and bridges (NPRA 2020*a*).

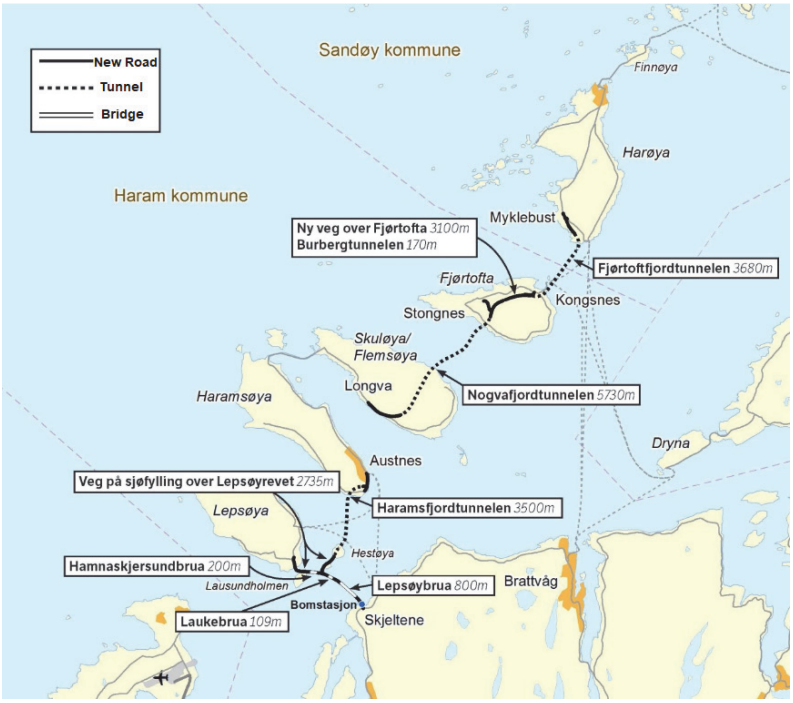


**Figure 15:** The planned route for Fv. 659 Nordøyvegen with tunnels and bridges. Taken from NPRA (2020*a*).

The main contractor in the project is Skanska Norge AS (NPRA 2020*a*). Entreprenørservice AS, a partner in SUPERCON, is responsible for all the sprayed concrete work. Large amounts of sprayed concrete is expected to be used as there is 4 tunnels with a total length around 13 km, that is going to be built (Steinstø & Hetlebakke 2020).

### 3.1.1 Geology

The geology at the Nordøyvegen project consists of metamorphic rocks. The rock is folded and the foliation changes fast. These changes in foliation can affect the tunnelling. Figure 16 gives an overview of the rock types in the area. The strength of the rock types is assumed to be similar. This comes from that all the rock types went through the same ductile transformation during the Caledonian orogeny (Ganerød & Lutro 2011).

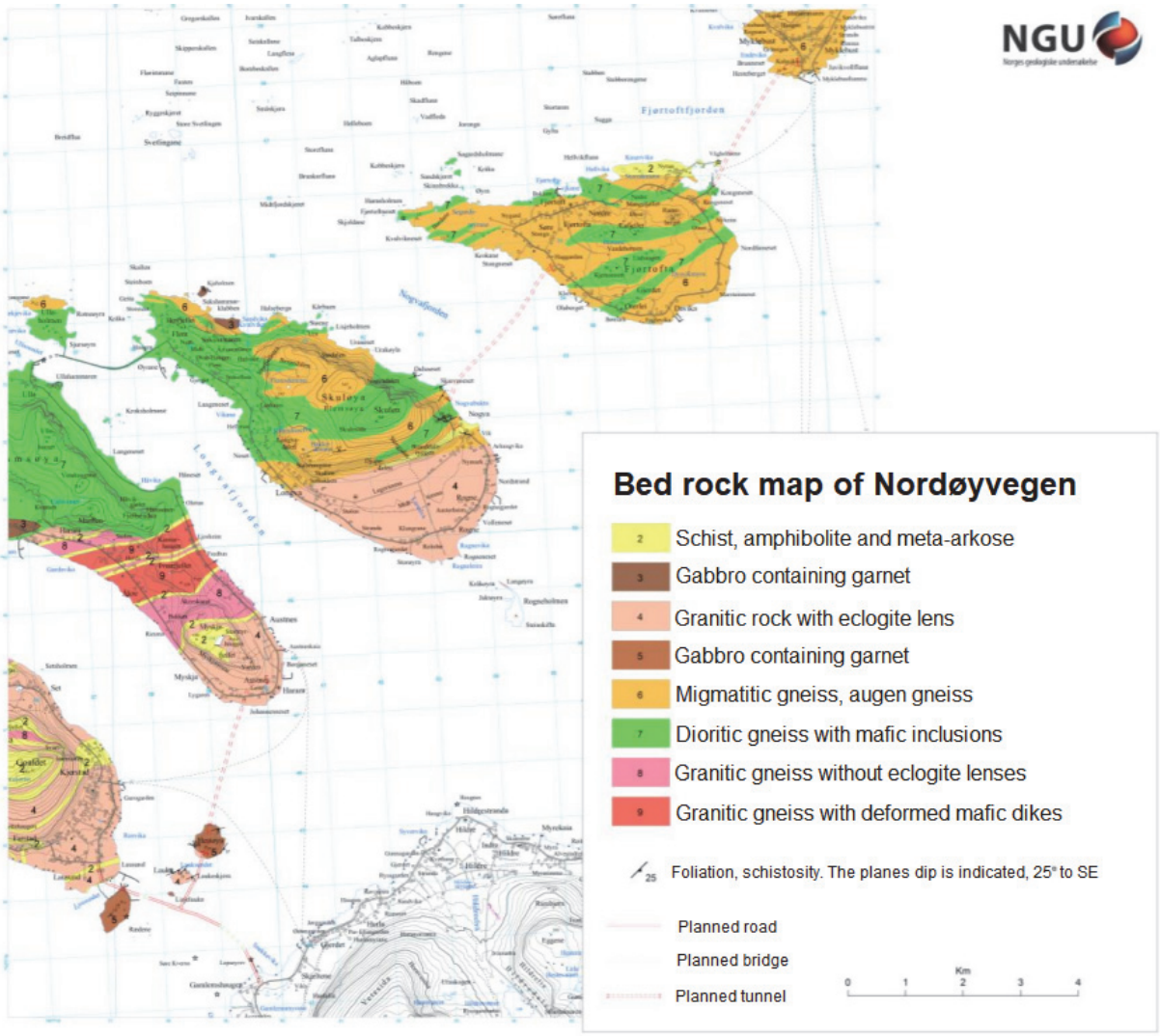


**Figure 16:** Geological map of Nordøyvegen. Translated from Ganerød & Lutro (2011).

The investigations found some lineaments in the geology. They appeared from the magnetic investigations. These were interpreted as faults and weakness zones. All the interpreted faults and weakness zones in the area are gathered in figure 17. The figure shows that

the Fjørtoft tunnel and the Nogva tunnel crosses some of these zones (Dehls et al. 2011). The name weakness zone tell that the rock mass quality is lower around them. This also goes for faults. The thickness of the sprayed concrete lining is based on the rock mass classification. The lower rock mass quality at the weakness zones means the thickness of the sprayed concrete increases (NGI 2015). Therefore, it is important to know where they are located before the tunnelling start to be prepared. The preparations are used to estimate the costs and quantity of materials needed.

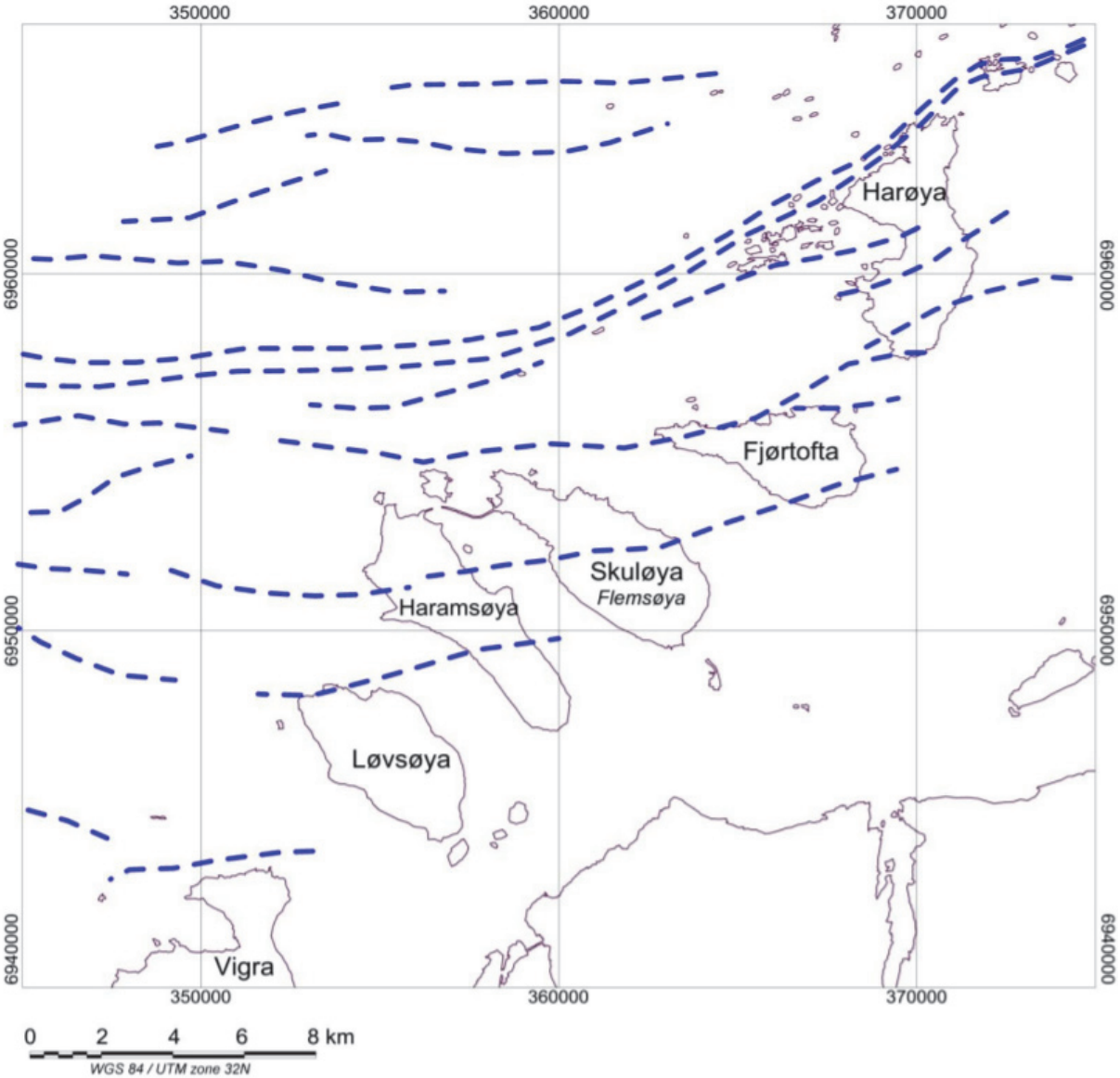


**Figure 17:** Interpreted faults and weakness zones at Nordøyvegen. The blue dashed lines show the interpreted faults and weakness zones. Taken from Dehls et al. (2011).

## 3.2 Sampling

### 3.2.1 Sampling Equipment and Procedure

The sampling was done with handheld coring equipment. This was chosen for its efficiency and that it is easy to use. All the sampling was done by Entreprenørservice. They have a lot of experience with this kind of work. Therefore, it was no need for comprehensive training to operate the equipment.

There are different types of coring equipment with different lengths and diameters. The coring could be done with diameters up to 122 mm. The length had to be long enough to penetrate the whole sprayed concrete lining. Therefore, it was decided to use a length of 15 cm. Cores taken from sprayed concrete should have a diameter that is minimum 50 mm, preferably 60 mm. The length to diameter ratio (L/d) should be in the area 1.0 to 2.0. A compressive strength test should consist of at least 3 cores to be considered as valid. Cores with strength that deviates with more than 20% from the average of the cores that makes up the test should be dropped. Therefore, it is recommended to have 4 or 5 cores per test (NB 2011). Here it was decided to follow the recommendations, therefore was the diameter set to 60 mm and 5 cores were taken out at each site.

The samples could also have been cut out in cubes or prisms. Vassenden (2019) compared sampling with cores and cutting out cubes or prisms. She summarised this in figure 18. The figure shows that cutting prisms is time consuming, expensive and there is need for comprehensive training before use. Therefore, it was decided that coring was most practical for a master's thesis.

| | Cutting cubes or prisms | Core drilling |
|---|---|---|
| Time consume | ÷ | + |
| Cost | ÷ | + |
| Availability of equipment | ÷ | + |
| A high number of cutter grooves in one sample | + | ÷ |
| Weight of big samples | ÷ | ÷ |
| Sampling depth | ÷ / + | + |
| Need for comprehensive training before use | ÷ | + |
| Risk of damaging the sample when loosening | ÷ | + |
| Risk of damaged cutters if the samples are big | ÷ | ÷ |
| Information value for each sample | + | ÷ |

**Figure 18:** Advantages and disadvantages for cutting and coring. Taken from Vassenden (2019).

All the sprayed concrete core samples were taken out according to NS-EN 12504-1 (NS 2019*c*).

### 3.2.2 Sampling at Nordøyvegen

The sprayed concrete cores were taken out from two tunnels, Fjørtofta and Longva, at Nordøyvegen. 5 core samples were taken out at 3 locations in each tunnel. This makes it a total number of 30 sprayed concrete cores for the testing. All the cores were taken out by Entreprenørservice. There were travel restrictions with the COVID-19 situation. These restrictions stopped me from participating in the coring process.

The equipment used for the coring was a Shibuya TS-92 boring machine. That is light and compact machine. It is easy to carry (Shibuya 2020). The machine is fastened to the tunnel wall during the coring. This is to keep the machine stable during the coring to get nice and straight cores. Figure 19 shows the boring machine used to get the cores from the two tunnels.

**Figure 19:** Boring machine, Shibuya TS-92, used to get the sprayed concrete samples.

## 3.3 Mix Design

The core samples were taken from two different tunnels at the project. The tunnels got the concrete from two different batching plants. Both batching plants were Unicon mobile batching plants. The mix design in both plants were the same. Table 9 presents the mix design for the sprayed concrete. The fibre content in the mix design has two values. This is for the different energy absorption classes, E700 and E1000, used for the sprayed concrete

in the tunnelling. The durability class in both tunnels was M40 and the strength class was B35 (Hetlebakke 2020).

**Table 9:** Mix design from the batching plants (Hetlebakke 2020). The fibre content have two values. This is for the different energy absorption capacities need for sprayed concrete given in table 1, E700 and E1000.

| Constituent | Amount per $m^3$ |
|---|---|
| Cement cem II | 539.6 kg |
| Silica fume | 22.5 kg |
| Sand 0-8 mm | 1515.4 kg |
| Steel fibre | 17/28 kg |
| SP | 4.98 kg |
| Air | 2.5 kg |
| Total water | 214.5 kg |
| V/(C+S) <0.37 | |

## 3.4 Description of Laboratory Used for Testing

The lab tests were conducted at the Rock Mechanics Laboratory and the Engineering Geology Laboratory at the department of Geoscience and Petroleum at NTNU. The Rock Mechanics lab has specialised equipment to measure the uniaxial compressive strength of rock and concrete. The machine used for the compressive strength tests is GCTS RTR-4000. It got a max loading capacity of 4000 kN. The dimensions the core samples can have is a diameter of 35-100 mm and a length less than 250 mm. All the tests are controlled by an automated computer (Vistnes, Li & Larsen 2020). The Engineering geology lab have equipment made to crush down rock to smaller particles for drillability measurements (Vistnes, Nilsen & Dahl 2020). The jaw crusher in this lab was used to crush sprayed concrete cores to separate the fibres. Table 10 shows the period the different test was performed in the labs and which tunnel the test material came from.

**Table 10:** Period the tests were performed, type of tests and where the test material came from.

| Date | Test preformed | Tunnel |
|---|---|---|
| 05-09.06.2020 | Dye penetrant | Fjørtofta |
| 11.06.2020 | UCS | Fjørtofta |
| 12-15.06.2020 | Fibre content | Fjørtofta |
| 19.06.2020 | Dye penetrant | Longva |
| 24.06.2020 | UCS | Longva |
| 25.06.2020 | Fibre content | Longva |

## 3.5 Crack Visualisation

### 3.5.1 Background

Today most literature that quantify shrinkage cracks in concrete do it by measuring visual cracks on selected locations. There are also imaging methods used to map cracks. They demand a good lighting for the image quality (Ruiz-Ripoli et al. 2013). These are macro cracks. The quantification of micro cracks is done in a different way. The concrete must be prepared into thin sections that can be looked at through microscope. There are two methods to look at micro shrinkage cracking. They are Fluorescence Light Microscopy and Environmental Scanning Electron Microscopy. Both methods show good results. The down side with the methods are that they are time consuming and only show the cracks on a little part of the concrete (Bisschop & van Mier 1999). In this thesis another method is going to be tried out to map crack on sprayed concrete cores. The method is dye penetrant mapping. This is a method that have been used to map cracks on rock cores with good results.

Vassenden (2019) wrote a doctoral thesis on rock breaking under rolling tunnel boring machine (TBM) disc cutters. She used dye penetrant to visualise cracks in rock cores in the thesis. This was a fast and easy method to visualise cracks in rock. An example of crack visualisation with dye penetrant is showed in figure 20. These cracks were induced from blasting.

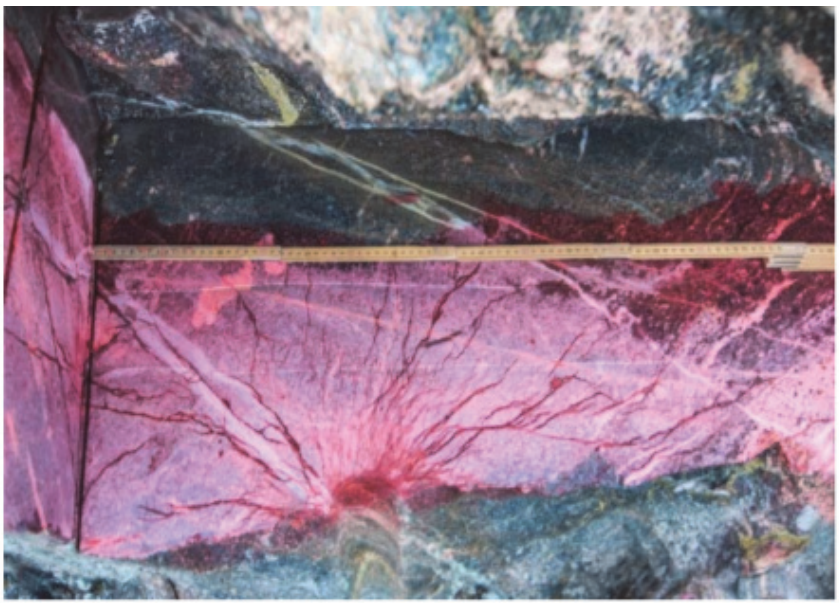

**Figure 20:** Visualisation of cracks induced from blasting. Taken from Vassenden (2019).

My supervisor Eivind Grøv, who also supervised Solveig Vassenden during her doctoral thesis, and I decided in a meeting to test dye penetrant on sprayed concrete. It would be interesting to see if this method could work to visualise shrinkage cracks in sprayed concrete cores from tunnel linings.

### 3.5.2 Dye Penetrant Inspection

Dye penetrant inspection is a low-cost method to locate cracks and defects on the surface of non-porous materials. Examples of this is metals, plastic, and ceramics. The method is used to find cast errors, welding flaws or abrasion on the surface. The dye penetrant makes it possible to visualise cracks, surface porosity and leakages. Figure 21 shows how cracks can be detected with dye penetrant (Gianfrancesco 2017).

Figure 21 shows a crack that cannot be seen with the naked eye. Before the test specimen have been cleaned, the cracks may be filled with dust and dirt that may hinder the penetrant of infiltrating the crack. Therefore, the test specimens must be cleaned before the dye penetrant is applied. The dye penetrant is sprayed over the whole surface of the test specimen. Then the fluid infiltrates all the cracks and pores on the surface of the test specimen. After a little while, the penetrant is cleaned off the surface. A developer is sprayed onto the clean surface. The developer is a white substance that draws the penetrant up from the cracks. This makes the cracks visible as red lines on the surface.

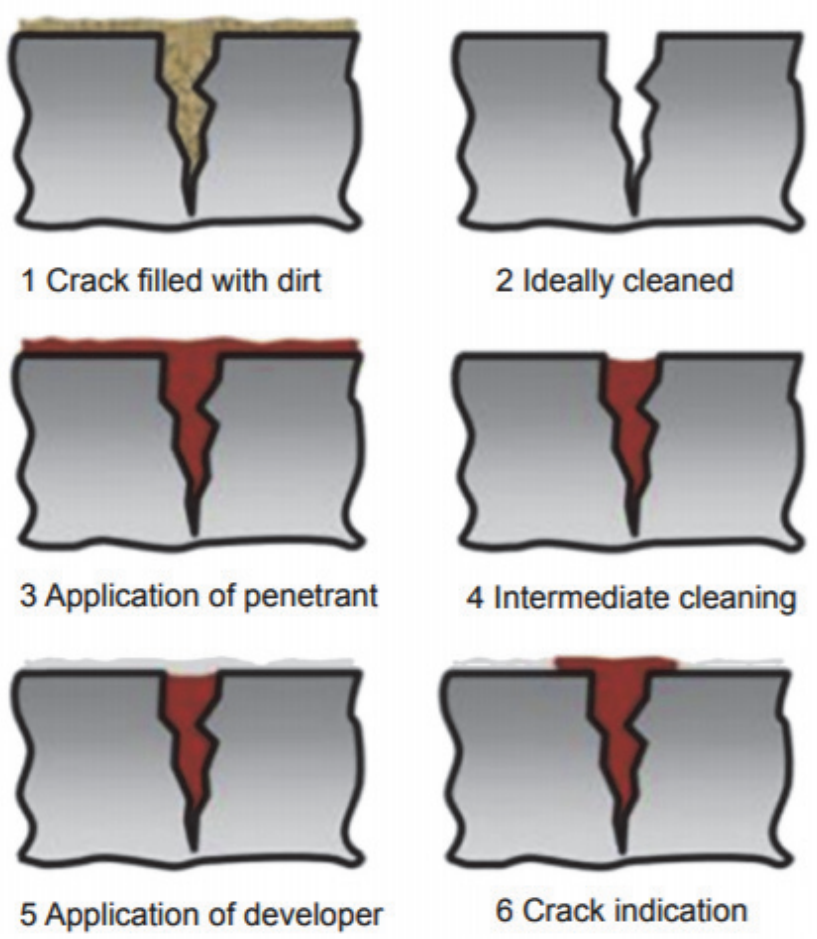


**Figure 21:** Procedure for crack visualisation with dye penetrant. Found in Gianfrancesco (2017).

Vassenden (2019) used this method to visualise cracks in cores from tunnel faces during tunnelling with a TBM. The method made surface cracks as small as 10-20 micrometres visible. The cracks appeared as bright red lines on the surface of the test specimens. This was because of the developer that made the surface white and gave a good contrast to the red dye in the cracks.

### 3.5.3 Products Used for Dye Penetrant Testing

The dye penetrant testing was done with these products from Magnaflux:

- BYCOTEST RP20 - Water-washable Visible Penetrant
- BYCOTEST D30A - Solvent-based Developer
- BYCOTEST C10 - Solvent Cleaner/Remover

The products were applied to the cores by spray cans.

### 3.5.4 Dye Penetrant Application Procedure

The procedure on how to use the different products are described in the product data sheets for the products used from Magnaflux. These instructions were followed in the investigations on the cores from the tunnel to get the best results. The procedure is described in the following paragraphs.

It is important that the cores are cleaned properly before the penetrant is applied. This is to remove contamination. Contaminants in the cracks hiders the penetrant to enter the cracks. The cleaning can be done in two ways with the BYCOTEST C10 cleaner. The cleaner can be sprayed directly onto the surface of the cores, and then be wiped off with a clean cloth. The other way to use the cleaner is to soak a clean cloth with it, and then wipe the core clean. Then the cores are dried before the penetrant is applied (Magnaflux 2019*b*).

The penetrant is applied by spraying the whole core completely with BYCOTEST RP20 red dye penetrant. After the spray have been applied, it must be allowed to penetrate the cracks. A minimum penetration time is 2 to 5 minutes. In most situations 10 minutes is adequate (Magnaflux 2019*c*). Vassenden (2019) saw that 15 minutes of penetration time was needed for the rock cracks to absorb the penetrant. Therefore, 15 minutes was used as penetration time in this study. She also stated that it was important that the penetrant did not dry out. The penetrant was applied every 5 minutes to keep the cores wet.

After the penetrant has been on the core for 15 minutes, the penetrant on the surface must be cleaned off. The cleaning is done with the BYCOTEST C10 cleaner. The cleaner is applied on a lint-free cloth. The surface is wiped clean with the cloth. It is important that the cleaner is not sprayed directly onto the core samples as this impair sensitivity (Magnaflux 2019*a*).

The final part of the penetrant testing is the application of a developer. Before the developer is applied, it is important to ensure that the surface of the cores is clean, free of excess penetrant and dry. Then the developer, BYCOTEST D30A, is sprayed onto the cores in thin layers which just wet the surface. The developer causes excessive bleeding and the running of indicators if too much is applied. Too little developer leads to slow development and possible loss in overall sensitivity (Magnaflux 2019*b*).

After the penetrant inspection, the developer should be removed. This can be done by wiping the cores with a cloth or with water and detergent wash.

### 3.5.5 Quantification of Cracks

The cracks that appeared in the dye penetrant testing had to be quantified. All the cracks on each core were counted. The length, width (where it was possible) and angle from the surface were measured on each crack on every core. The angles were measured with the smallest angle (0-90°) from the horizontal surface, parallel to the surface on the top of the cores after they had been prepared for UCS testing. Measurements were done with ruler and protractor.

## 3.6 Uniaxial Compressive Strength

The procedure for determining the uniaxial compressive strength (UCS) for the concrete cores is described after NS-EN 12390-3 (NS 2019*a*). The compressive strength is determined by dividing the maximum load by the cross-section area of the sample. The testing was done according to NS-EN 12390-3.

The cores must be prepared before the compressive strength testing. The samples should not have any significant defects. Defects may affect the quality of the test results. The ends of the core samples should be flattened. The length (L) of the cores should be measured at three locations separated by 120 degrees around the perimeter. The diameter (d) should be measured at three places separated by 60 degrees at both ends. The average diameter is calculated from the six measurements and expressed to the nearest 1 mm.

L/d should be between 1.9 and 2.1. Longer cores should be shortened to the desired length. A correction factor for the compressive strength should be used if the L/d is less than 2. The correction factor can be calculated with equation viii. The L/d must be between 1,0 and 2,0 after cutting and flattening of the ends for sprayed concrete (NB 2011).

NS-EN 12390-1 gives the required shape and dimensions for the specimens. The tolerance for the flatness of the load bearing surface is 0.0006d mm for cylinders. d is the diameter of the cylinder. The perpendicularity of the sides have a tolerance of 0.007d mm. The height (2d) have a tolerance of 5% (NS 2012).

The surfaces of the core and the bearing faces of the compressiv strength machine should be wiped clean before the test. The cores are placed in the lower bearing block in the machine. The loading of the samples is applied continuously until the sample fails and a well-defined fracture pattern is developed. The maximum load is recorded. The type of failure pattern according to figures 22 and 23 is noted. The failure pattern is used to see if the test is satisfactory or not. Every sample is photographed before and after the loading.

The machine used for the compressive strength test should fulfil the specifications in NS-EN 12390-4. The standard gives the specifications for testing machines to ensure the quality of the results (NS 2020).

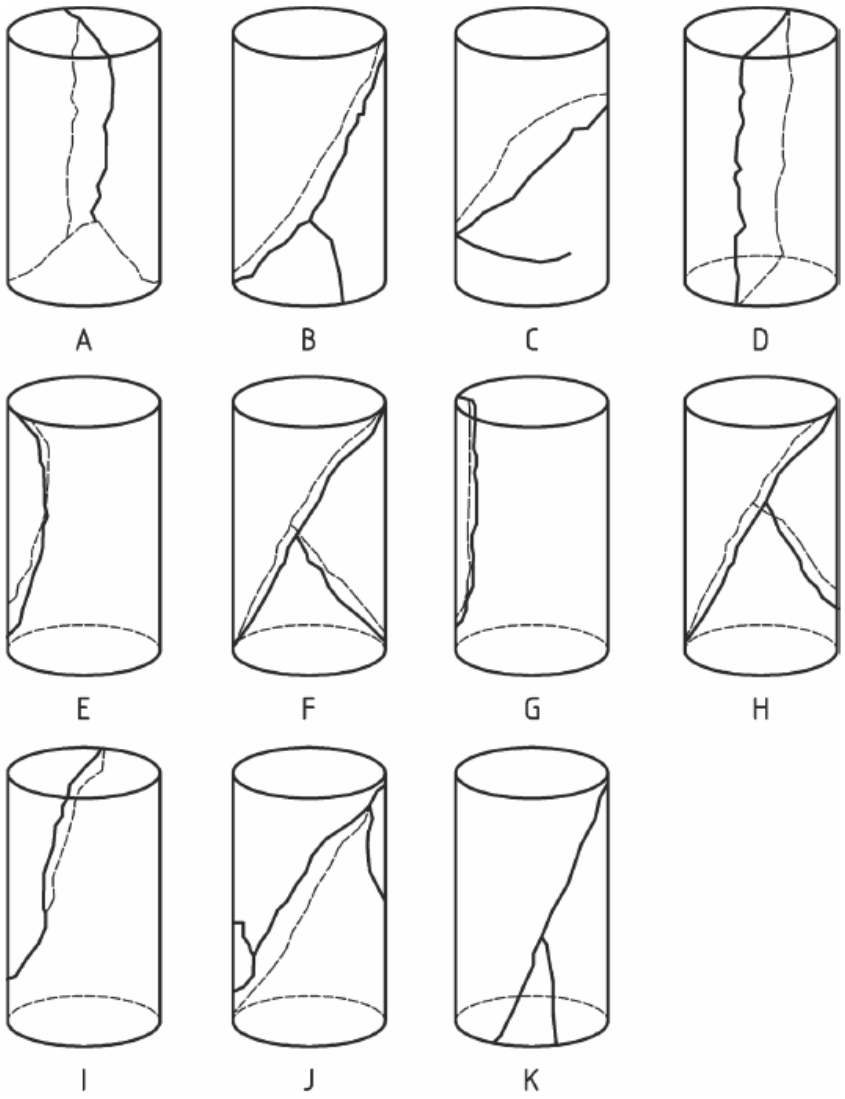


**Figure 22:** Examples of unsatisfactory failure of cylinder specimens. Found in NS-EN 12390-3 (NS 2019*a*).

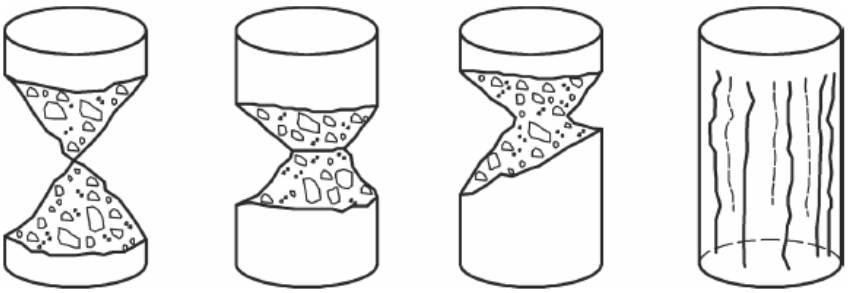

**Figure 23:** Examples of satisfactory failure of cylinder specimens. Found in NS-EN 12390-3 (NS 2019*a*).

The equation for calculating the compressive strength of a cylinder ($f_{c,cyl}$) is given in equation vii.

$$f_{c,cyl} = \chi_{c,cyl} * \frac{F}{A_c}. \tag{vii}$$

Where F is the maximum force (N) from the press machine on the sample. $A_c$ is the pressed area ($mm^2$) of the sample and $\chi_{c,cyl}$ is the correction factor. The correction factor is necessary to be able to compare the strength characteristics of cylinder test samples with a L/d less than 2. Equation viii shows how to calculate the correction factor (Mynarcik 2015).

$$\chi_{c,cyl} = 0.80 + \sqrt{\frac{\frac{L}{d} - 0.933}{26.667}}. \tag{viii}$$

Where L is the length of the core sample and d is the diameter.

Concrete is often tested by cube strength. Therefore, it is important to be able to compare strength measured for cubes with cylinders and vice versa. Table 11 under taken from NS-EN 206 shows how to compare strength for cubes and cylinders with normal and heavy concrete. The characteristic strength is given for cylinders with a diameter of 150 mm and height 300 mm and the cubes with length 150 mm. Both are tested at 28 days (NS 2017).

The data in table 11 can be used for a regression. The regression can be used to make an equation to transform cube strength to cylinder strength. Equation ix is the regression line from the plotted data in the table. The plot is shown in figure 85 in appendix D. These formulas were used to transform cylinder strength into cube strength.

$$\begin{aligned} f_{ck,cyl} &= 0.86 f_{ck,cube} - 1.89 \\ f_{ck,cube} &= 1.16 f_{ck,cyl} + 2.75 \end{aligned} \tag{ix}$$

A test series should consist of at least 3 cores for the test to be valid. The test results are given as the average value of the series (3 or more cores). Cores that deviates with with

more than ± 20% from the average strength in the series gets rejected. Therefore, it is recommended to have 4-5 cores in each series (NB 2011).

**Table 11:** Compressive strength classes for normal-weight and heavy-weight concrete. Taken and modified from NS-EN 206 (NS 2017).

| **Compressive strength class** | **Minimum characteristic cylinder strength** $f_{ck,cyl}$ $(N/mm^2)$ | **Minimum characteristic cube strength** $f_{ck,cube}$ $(N/mm^2)$ |
|---|---|---|
| C8/10 | 8 | 10 |
| C12/15 | 12 | 15 |
| C16/20 | 16 | 20 |
| C20/25 | 20 | 25 |
| C25/30 | 25 | 30 |
| C30/37 | 30 | 37 |
| C35/45 | 35 | 45 |
| C40/50 | 40 | 50 |
| C45/55 | 45 | 55 |
| C50/60 | 50 | 60 |
| C55/67 | 55 | 67 |
| C60/75 | 60 | 75 |
| C70/85 | 70 | 85 |
| C80/95 | 80 | 95 |
| C90/105 | 90 | 105 |
| C100/115 | 100 | 115 |

## 3.7 Measurement of Density

The density of the concrete cores were measured in compliance with NS-EN 12390-7 (NS 2019*b*).

The volume of the specimens can be determined in three ways. The first and most precise is submerging the sample in water and read the displacement of the water. The second method is by measurements of the specimen with rulers and callipers. The last one is using checked, designated dimension. Here the second method was used, as it was described in the section on UCS.

The mass of the specimen is decided from weighing specimen. It is important to note if the specimen was weighed as it was received, water saturated or oven dried. Here the core specimens were weighted as they were received. The weight is measured with a maximum error of 1 g.

The density ($kg/m^3$) is then calculated with equation x.

$$D = \frac{m}{V} * 1000. \tag{x}$$

Where m is the mass (g) and V is the volume ($cm^3$) of the specimen.

## 3.8 Measurement of In-Situ Fibre Content

The fibre content measurements were done according to NS-EN 14488-7 (NS 2006). The measurement should be done on cores drilled perpendicular to the concrete surface.

Three or more cores must be cut from the in-situ material. The diameter of the cores shall be between 50 and 100 mm. The length should be between 75 and 150 mm. The core length should be equal to the layer thickness if the layer thickness is thinner than 75 mm.

The volume of the cores is determined by measurements or by submerging them in water. The measurements are used to calculate the volume. The volume is read directly from the displacement of the water if the cores are submerged.

The cores must be crushed in a compression testing machine or other suitable devices. This must be done in a way that all the fibres can be separated from the concrete. A magnet can be used to collect magnetic fibres. All the collected fibres shall be cleaned thoroughly and then weighed. The mass is given to the closest 0.1 g.

The cores were first crushed in the compression testing machine. They were crushed further down with a jaw crusher. The fibres were picked up with a magnet in between each round in the jaw crusher. The material was also sieved. The sieving made it easier to detect the fibres. Figure 24 shows all the steps in the process. The photo to the far right is all the fibres collected from one core.

**Figure 24:** Method for crushing and separating the fibres from the cores.

The fibre content of the sprayed concrete was calculated with equation xi.

$$C_f = \frac{m_f}{V_d} * 1000. \tag{xi}$$

Where $C_f$ is the fibre content (kg/m$^3$), $m_f$ is the mass (g) of the fibre extracted from the sample and $V_d$ is the volume (cm$^3$) of the sample.

The drawbacks of this method are that the samples must be crushed. This can be done together with UCS. The results are affected by the human factor. The quality of the separation and cleaning of the fibres depends on the expertise of the technician (Silva et al. 2015).

## 3.9 Rock Mass Classification

### 3.9.1 Background

The most common system for rock mass classification in Norway is the Q-system (NFF 2008). Therefore, the Q-system is the only system explained. This system was used in the tunnels the core samples were collected from.

Q-system is a classification system of rock masses for the stability of tunnels and caverns. The classification is based on 6 parameters. Based on the 6 parameters can the Q-value be calculated with equation xii. Each of the parameters are explained under, as they are given in the handbook for using the Q-system from NGI (2015).

$$Q = \frac{RQD}{J_n} * \frac{J_r}{J_a} * \frac{J_w}{SRF} \tag{xii}$$

Rock Quality Designation (RQD) is a simple classification system. The value varies between 0-100, but in the Q-system all values under 10 is set as 10. A value of 0 gives a Q-value of 0. This is not wanted. The RQD values are found from the number of joints per cubic meter in the rock mass. Figure 48 in appendix B shows the classification table for RQD.

Joint set number ($J_n$) is describing the joint geometry. All joints within a joint set are nearly parallel and have a distinct spacing between the joints. The joints that do not occur systematically are called random joints. Fewer joints give a lower $J_n$ value. The values can vary between 0.5-20. The classification table for $J_n$ is given in figure 49 in appendix B.

Joint roughness number ($J_r$) tells about the surface of the joints. It can be given a value between 0.5-4. The values are estimated with figure 50 in appendix B. Rough surfaces give higher values and smoother surfaces gives low values.

Joint alteration number ($J_a$) tells about the surface alteration of the joints. Higher values are given for highly altered joints. The values are in between 0.75-20. The detailed table for calculating $J_a$ is given in figure 51 in appendix B.

The next parameter is the joint water reduction factor ($J_w$). This factor tells about the water inflow to the tunnel or cavern. The values can be given between 1-0.05. Higher value means less water. The water affects stability as it lowers friction on the joint planes. Figure 52 in appendix B shows details for determining the value for $J_w$.

The last parameter is stress reduction factor (SRF). This factor describes the relation of stress and rock strength around tunnels and caverns. Figure 53 in appendix B is divided in four separate situations that affects the stress distribution. The situations are weakness zones, competent rock, squeezing rock and swelling rock. They all affect the underground opening different. This can be seen in the values given for SRF in the different situations. The values of SRF can vary between 0.5-400.

### 3.9.2 Classification in the Tunnels

The rock mass in the tunnels were mapped according to the Q-system. This was done before the rock mass got covered by sprayed concrete. The mapping was conducted by engineers from the main contractor. The Q-values from the test locations was given from the owner, Møre and Romsdal county (Gjørva 2020). They are shown in the results.

## 3.10 Analysis of Test Results

The test data was plotted in several diagrams after all the testing had been conducted. The diagrams were bar charts and scatter plots. The scatter plots plotted the results from two tests together. Trendlines were added to the scatter plots. A $R^2$-value was added to the plots to show how well the trendlines fits to the data.

$R^2$ is a statistical measure. This value shows how well the fitted regression line fits to the data. The definition of $R^2$ is $R^2$ = Explained variation / Total variation. The values of $R^2$ is always in between 0 and 100%. A regression line with $R^2$ = 0% indicates that the model does not explain any of the variability of the data around its mean. At 100% the regression line explains all the variability of the data. Higher values mean the models fits better to the data (Frost 2013).

It is important to check if the regression model is unbiased when using $R^2$ values. This can be done with residual plots. Residual plots are typically used to find problems with regression. Residual values are how much a regression line misses a data point. The residual values should be equally and randomly spaced around the horizontal axis in residual plots. The data is biased if the residual plots are not randomly or equally spaced around the horizontal axis. Biased data is not fit for regression (Glen 2015). Residuals were plotted for all trendlines made from the data. The residual plots are shown in appendix D.

# 4 Results

Here in this section, all the results from the laboratory testing are presented. Starting with the dye penetrant testing, then the results from the other tests. The other tests were UCS, measurement of the density and the in-situ fibre content. After all the test results have been presented, the data is analysed. The analysis investigates if the cracks or the rock mass affects or is affected by the other factors.

## 4.1 Crack Measurements

The results from the dye penetrant crack mapping is presented in table 12 and 13. Table 12 shows the cracks discovered on the sprayed concrete cores from Longva, and table 13 shows what was found on the cores from Fjørtofta. The tables show the measured length and angle of the cracks. The angles were measured from the horizontal planes (normal to the length axis of the cores). The length of the cracks was measured in proportion to the length axis. The measurement of the width had to be dropped as the cracks were not distinct enough. Only three cores were tested from each location in Longva. The penetrant spray was emptied and since so few cracks appeared during the testing, it was decided not to buy a new one for the last cores.

Tables 12 and 13 shows that quite few cracks appeared during the dye penetrant testing. On the cores from Longva there was more cores without any cracks than with cracks. 12 of the cores did not show any cracks. That was 50% of the tested cores.

**Table 12:** The crack measurements from the dye penetrant testing on the sprayed concrete core samples from Longva.

| **Sample nr.** | | **Crack nr.** | | |
|---|---|---|---|---|
| | | 1 | 2 | 3 |
| **Profile nr. 8876** | 1 | L: 23 mm<br>A: 60 deg | - | - |
| | 2 | - | - | - |
| | 3 | L:15 mm<br>A: 55 deg | - | - |
| **Profile nr. 8910** | 1 | L: 33 mm<br>A: 55 deg | - | - |
| | 2 | - | - | - |
| | 3 | - | - | - |
| **Profile nr. 23910** | 1 | - | - | - |
| | 2 | - | - | - |
| | 3 | - | - | |

**Table 13:** The crack measurements from the dye penetrant testing on the sprayed concrete core samples from Fjørtofta.

| **Sample nr.** | | **Crack nr.** | | |
|---|---|---|---|---|
| | | 1 | 2 | 3 |
| **Profile nr. 32450** | 1 | L: 60 mm<br>A: 0 deg | L: 42 mm<br>A: 20 deg | - |
| | 2 | L: 60 mm<br>A: 0 deg | - | - |
| | 3 | L: 60 mm<br>A: 0 deg | L: 26 mm<br>A: 0 deg | L: 36 mm<br>A: 20 deg |
| | 4 | L: 60 mm<br>A: 0 deg | L: 64 mm<br>A: 20 mm | L: 62 mm<br>A: 5 deg |
| | 5 | L: 60 mm<br>A: 0 deg | L: 60 mm<br>A: 0 deg | - |
| **Profile nr. 32500** | 1 | - | - | - |
| | 2 | - | - | - |
| | 3 | - | - | - |
| | 4 | - | - | - |
| | 5 | L: 37 mm<br>A: 10 deg | - | - |
| **Profile nr. 32560** | 1 | L: 40 mm | - | - |
| | 2 | - | - | - |
| | 3 | - | - | - |
| | 4 | L: 50 mm<br>A: 0 deg | L: 43 mm<br>A: 25 deg | - |
| | 5 | L: 64 mm<br>A: 20 deg | - | - |

The first crack measured on all the cores from profile number 32450 in table 13 is not shrinkage cracks. It is a boundary between two sprayed concrete layers. This boundary can be seen on the sprayed concrete cores before the tests started. The dark line on the cores from profile number 32450 in figure 99 in appendix D is the boundary between the two sprayed concrete layers. Since sprayed concrete does not stick perfectly to the substrate, it is natural that there is a crack between the two layers. The dye penetrant test highlighted this boundary.

Figure 25 shows one of the cores during the dye penetrant testing. This is an interesting core as the left end of the core is rock. Here the difference between dye penetrant testing on sprayed concrete and rock can be compared. The core also has a boundary between two sprayed concrete layers. The boundary got a darker red colour than the rest of the core.

In the rock, which is the left end of the core, it is possible to see a small crack and some larger cracks. The concrete did not show any cracks as distinct as the ones on the rock.

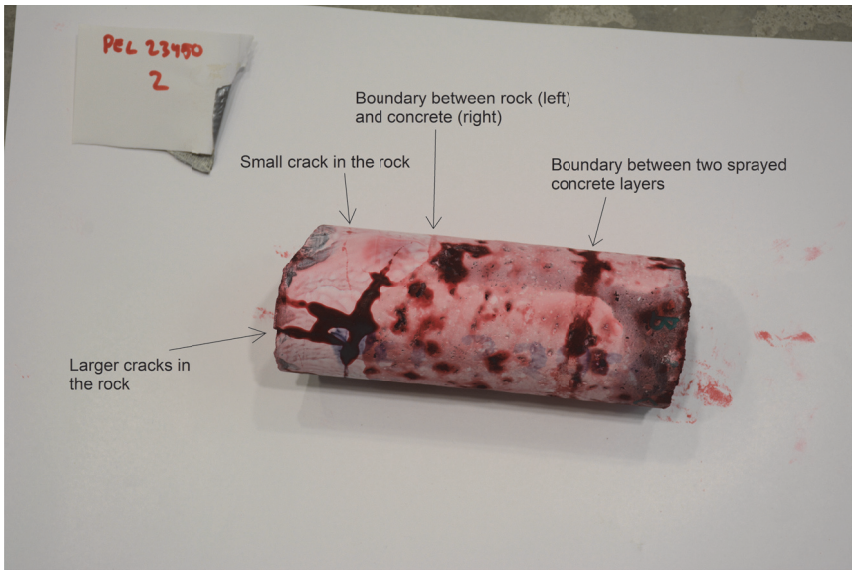


**Figure 25:** Dye penetrant crack mapping on sprayed concrete core nr. 2 from profile number 32450 with explanation to what is seen on the core.

Core number 1 from profile number 23917 had the most distinct crack in the concrete of all the cores. This was the only crack in the sprayed concrete similar to the one in the rock in figure 25. The crack can be seen in figure 26. This was one of the last cores to be tested.


**Figure 26:** Dye penetrant crack mapping on sprayed concrete core nr. 1 from profile number 23917 with an arrow showing the crack on the core.

The same boundary as in figure 25 between the two sprayed concrete layers can be seen in figure 27. The photo shows a potential crack in the sprayed concrete. This is mapped as the third crack in table 13 for core number 3 at profile number 32450. Figure 27 is displayed to illustrate what a crack in the sprayed concrete might look like. The photos of the rest of the cores are in appendix C. All the cores in appendix C are divided into four quadrants. Each photo shows a quadrant of the cores.

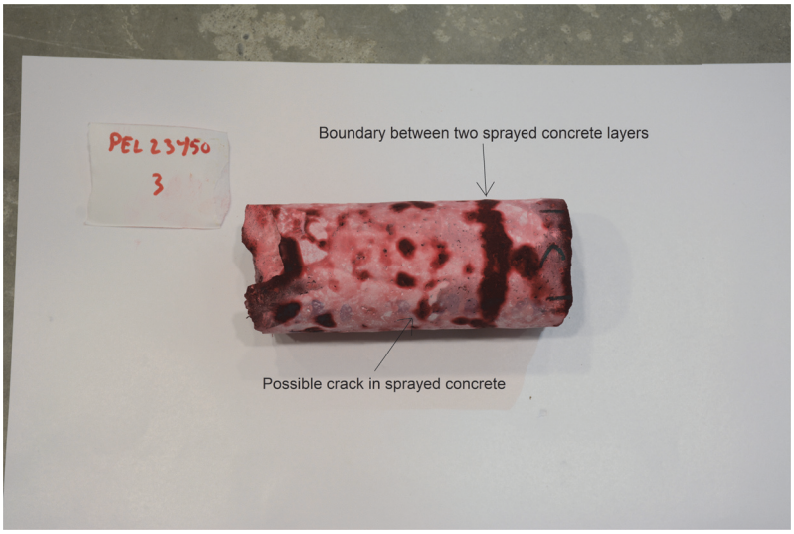


**Figure 27:** Dye penetrant crack mapping on sprayed concrete core nr. 3 from profile number 32450 with explanation to what is seen on the core.

The penetration of the dye in the cores became visible during the preparation for UCS testing. The ends of the cores had to be flattened in the preparation for UCS testing. This showed how deep the dye had penetrated the cores. Figure 28 shows how deep the penetration was on core number 3 from profile number 32560. The dye penetrated around half a centimetre around the whole sprayed concrete core. Similar depths were seen in the other cores as well.

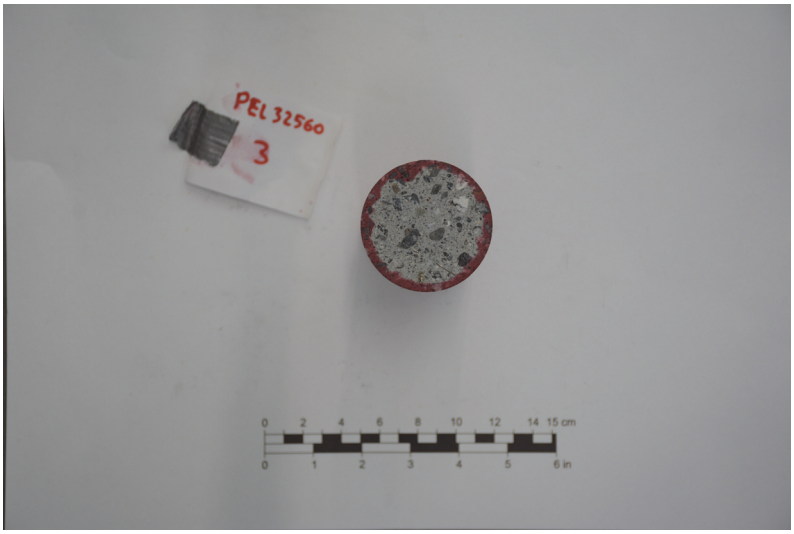


**Figure 28:** Penetration depth of dye on sprayed concrete core 3 from profile 32560.

The data from the crack testing showed one interesting trend. This trend is presented in figure 29. Here the number of cracks is plotted against the age of the sprayed concrete core. The linear regression of the data shows that the number of cracks increase with the age of the cores. A $R^2$ at 48% indicates that there is some connection between the age and number of cracks.

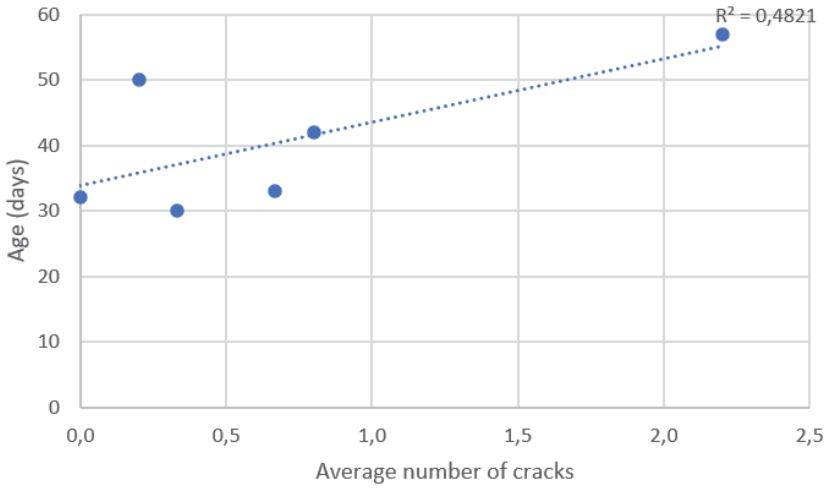


**Figure 29:** Plot of the amount of cracks against the age of the cores at testing with a trendline. The $R^2$ is 48%, which indicates a connection between the age and the amount of cracks.

## 4.2 Uniaxial Compressive Strength

The results from the UCS testing is summarised in figure 30. There the average UCS values after length correction for each location is shown. The orange line is the strength class, B35, for the sprayed concrete. Profile number 32500 is included in the figure. It is important to know that this value is based on two cores. Two cores are not enough to get a valid estimate for the sprayed concrete strength at a location. The minimum is three cores for a valid estimate of the strength.

The testing shows the sprayed concrete has a much higher strength than the strength class. All the locations, except profile number 32450, has a strength higher than the strength class. The strength is varying from 15-30 MPa higher than the strength class. At profile number 32450, the strength was measured to 33.4 MPa. This is slightly under the strength class B35. The strength class says the sprayed concrete should at least achieve a strength of 35 MPa.

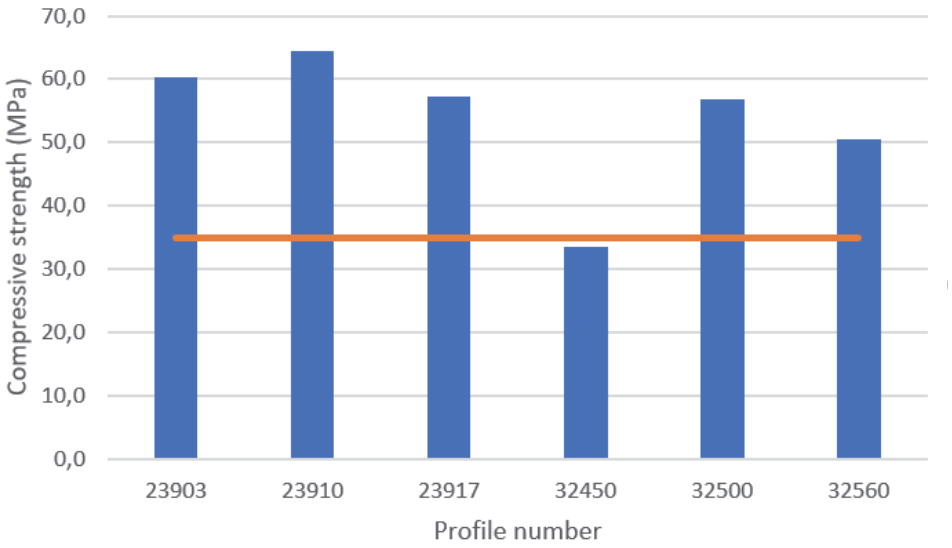


**Figure 30:** The average UCS values for each location after L/d correction. The orange line shows the strength class, B35, of the sprayed concrete.

Figures 31 to 36 displays the fractures from all the UCS testing. In figure 34 of the cores from profile number 32450, it can be seen that all the cores failed along the boundary between the two sprayed concrete layers. There the strength of the boundary was tested and not the intact sprayed concrete strength. From location 32500 there was only two cores that were long enough from UCS testing. These are shown in figure 35. Figure 36 shows the cores from location 32560 after UCS testing. The only cores with a L/d = 2 from Fjørtofta were cores 1-4 from location 32560. The correction factor had to be used on all the other cores for comparison with the cores that had L/d = 2. On the cores from Longva, the correction factor only had to be used on 5 of the 15 sprayed concrete cores. The red colour of the cores comes from the dye penetrant testing.

The crack patterns of the cores looks like the unsatisfactory patterns in figure 22. None of them look like the satisfactory ones in figure 23. Even though the crack patterns are not according to the standard, the results are going to be used in the analysis. All the cores achieved strengths far greater than what was needed, except those from profile number 32450.


**Figure 31:** All cores from profile 23903 after compressive strength testing, with failure patterns.

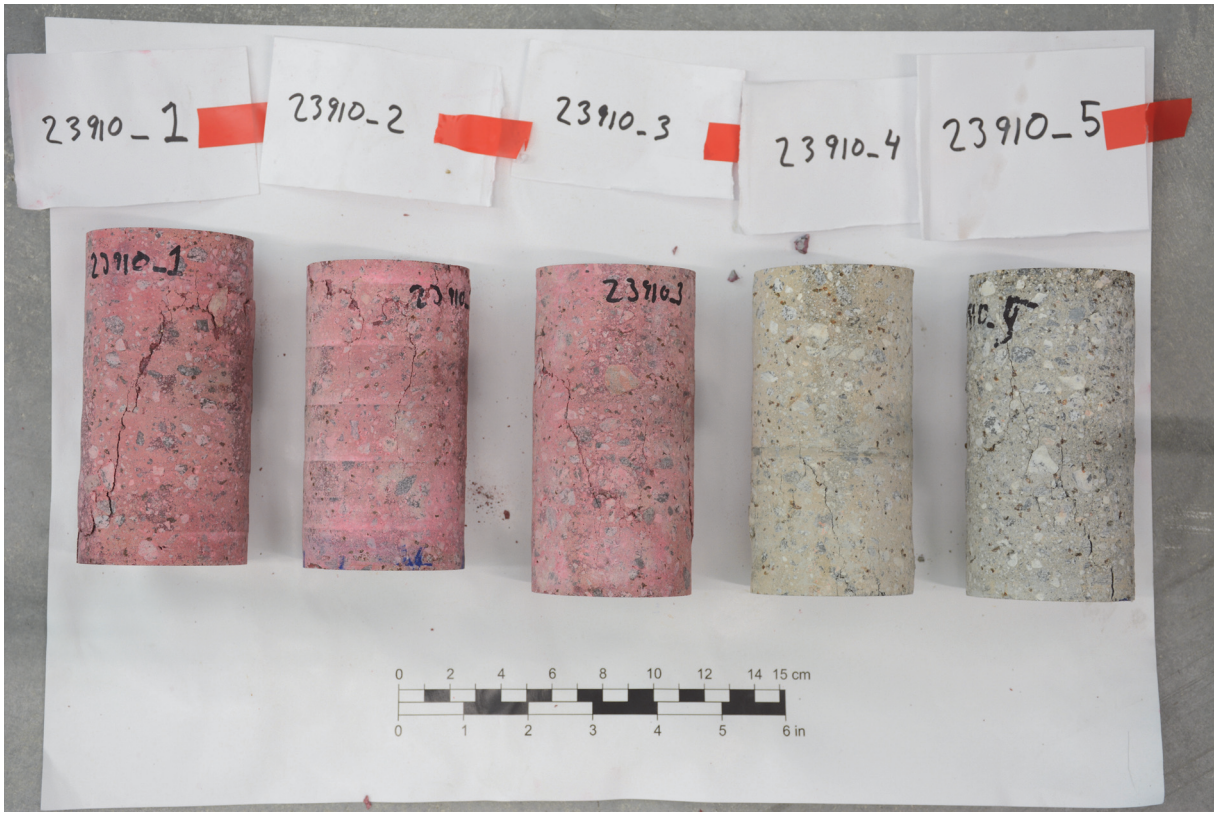


**Figure 32:** All cores from profile 23910 after compressive strength testing, with failure patterns.


**Figure 33:** All cores from profile 23917 after compressive strength testing, with failure patterns.


**Figure 34:** All cores from profile 32450 after compressive strength testing, with failure pattern along the boundary between two sprayed concrete layers.


**Figure 35:** Two cores from profile 32500 after compressive strength testing, with failure patterns.

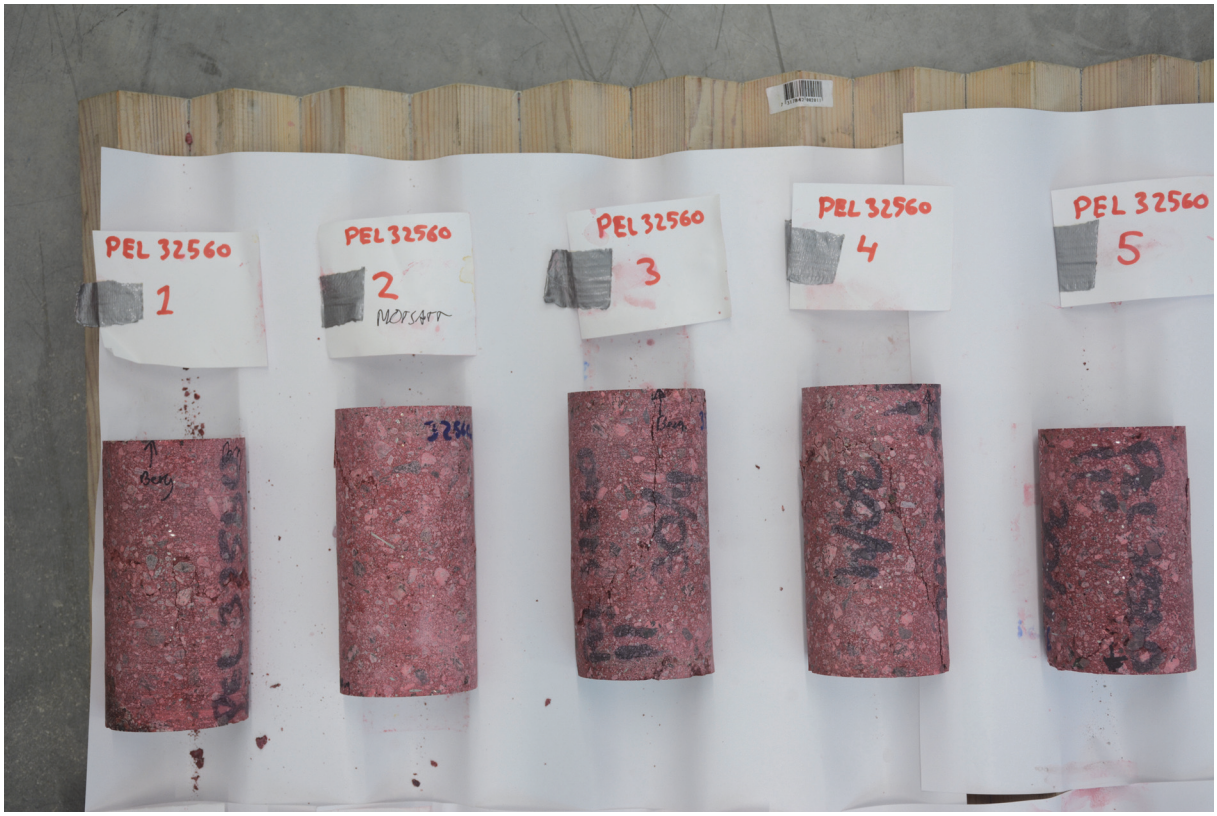


**Figure 36:** All cores from profile 32560 after compressive strength testing, with failure patterns.

## 4.3 Density

The density measurements are summarised in figure 37. There the average density measurements for each location is shown. The orange line represents the density of the mix design for E1000 sprayed concrete from table 9. That value comes from adding all the constituents in the mix design. The density of the mix design was 2327 kg/m$^3$. All the locations have a lower density than the initial mix design. The densities from the locations vary from 8-135 kg/m$^3$ lower than the mix design. The highest density was measured at profile number 23903 with a value of 2308 kg/m$^3$ and the lowest at profile number 32450 with a value of 2181 kg/m$^3$.

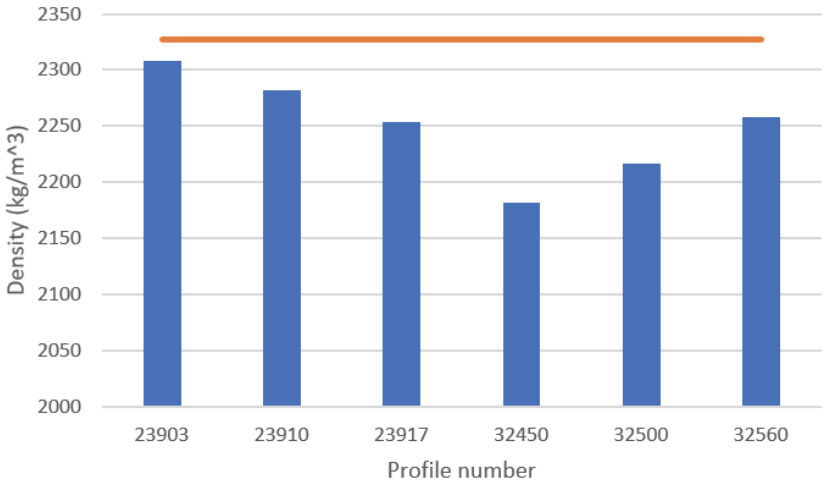


**Figure 37:** The average density values for each location. The orange line shows the density of the initial mix design of E1000 sprayed concrete from table 9, 2327 kg/m$^3$.

## 4.4 Fibre Content

The fibre content was different for some of the tunnel sections. There were different energy absorption capacities used at the different locations. Four locations used E700 and two used E1000 sprayed concrete. Table 14 shows where E700 and E1000 was used in the tunnels. The table informs of the fibre content in the mix design for the different energy absorption classes.

**Table 14:** Energy absorption classes used at each profile number with fibre content of the mix design.

| Profile number | Energy absorption capacity | Fibre content (kg/m$^3$) |
|---|---|---|
| 23903 | E700 | 17 |
| 23910 | E1000 | 28 |
| 23917 | E700 | 17 |
| 32450 | E700 | 17 |
| 32500 | E700 | 17 |
| 32560 | E1000 | 28 |

The measurements of the in-situ fibre content is gathered in figure 38. The average fibre content for each location is shown. The grey and orange lines represent the fibre content in the mix design. The fibre content of the mix design was 17 and 28 kg/m$^3$ for the E700 and E1000 sprayed concretes. All the locations have a lower fibre content than the mix design. Location 32500 have the lowest fibre content, 12 kg/m$^3$, and 23910 the highest, 27.5 kg/m$^3$. The deviation from the mix design varied at the locations. Location 32560 had the largest deviation, 5.7 kg/m$^3$, and location 23903 had the lowest deviation, 0.1 kg/m$^3$.

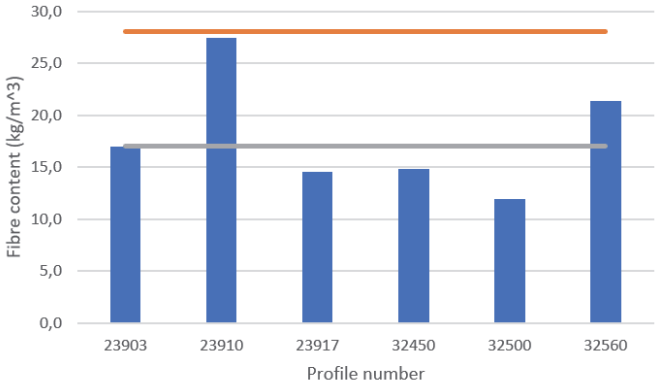


**Figure 38:** The average fibre content for each location. The grey line shows the E700 fibre content in the mix design, 17 kg/m$^3$, and the orange line shows the E1000 fibre content, 28 kg/m$^3$.

Figure 39 shows the average fibre content plotted against the average length of the cores from each location. The figure indicates that the longer cores have a higher fibre content. It would have been better to compare the fibre content to the thickness of the sprayed concrete layers. The cores are cut down to L/d = 2 if the sprayed concrete layer is thicker than 120 mm. This gives an overweight of plots around 120 mm. The residual plot for the trendline showed that the data might be bias as the variation increases with the longer cores. Therefore, too much should not be read from the regression.

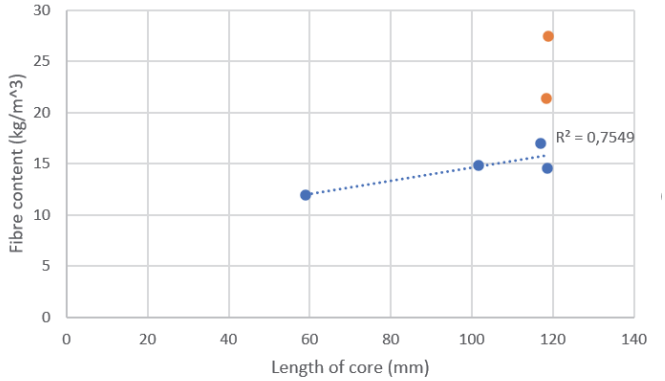


**Figure 39:** Plot of fibre content against the length of the cores with a trendline for E700. The blue dots are the cores with E700 and the orange is E1000 sprayed concrete.

## 4.5 Rock Mass Quality

All the rock mass classification given from the Nordøyvegen project is summarised in table 15. The table shows the values for each parameter in the Q-system as they were mapped by the main contractor at the project. The Q-values were calculated with equation xii. At Fjørtofta, all the locations have $Q > 10$, this gives support category I. Support category I indicates that the rock mass quality is good at all the locations. $J_w$ and SRF is set to 1. This means the tunnel is dry and the stresses in the tunnel is favourable according to the mapping schemes in appendix B. At Longva, the rock mass quality was lower. This means the rock mass was less massive and had more cracks. This is shown with the lower RQD values and higher $J_n$ values. At profile number 23903, there was a weakness zone, which gave a higher alteration of the cracks in the rock mass, and this resulted in support category III. The explanation of the support categories are shown in table 1.

**Table 15:** Rock mass classification and rock type for all the locations in Longva and Fjørtofta (Gjørva 2020).

| **Profile number** | **23903** | **23910** | **23917** | **32450** | **32500** | **32560** |
|---|---|---|---|---|---|---|
| RQD | 60 | 75 | 80 | 75 | 80 | 90 |
| $J_n$ | 6 | 9 | 9 | 4 | 3 | 3 |
| $J_r$ | 1.5 | 1.5 | 2 | 2 | 2 | 2 |
| $J_a$ | 4 | 2 | 2 | 3 | 2 | 3 |
| $J_w$ | 1 | 1 | 1 | 1 | 1 | 1 |
| SRF | 1 | 1 | 1 | 1 | 1 | 1 |
| **Q** | **3.75** | **6.3** | **8.9** | **13** | **27** | **20** |
| Support category | III | II | II | I | I | I |
| Rock type | Gneiss* | Gneiss | Gneiss | Gneiss | Gneiss** | Gneiss |
| * Weakness zone with crushed and altered rock from right abutment and down into the wall.<br>** Comment on good rock. | | | | | | |

Table 16 summarises the test results from all the tests. Here the mean values and standard deviation for each location is show for the measured test data. The age of the cores at the time of testing is also shown in the table. The data from the table has been used for the analysis. The analysis is presented in the next sections.

**Table 16:** Summary of the test results with mean values and standard deviation for each location. The age of the cores at the testing and Q-values are included at the bottom.

| Profile number | 23903 | 23910 | 23917 | 32450 | 32500 | 32560 |
|---|---|---|---|---|---|---|
| Number of cracks | 0.7 ± 0.6 | - | 0.3 ± 0.6 | 2.2 ± 0.8 | 0.2 ± 0.4 | 1.0 ± 0.8 |
| UCS (MPa) | 60.2 ± 2.5 | 64.4 ± 4.1 | 57.3 ± 1.3 | 33.4 ± 4.0 | 56.7 ± 1.0 | 50.5 ± 1.8 |
| Density (kg/m$^3$) | 2308 ± 12 | 2282 ± 9 | 2253 ± 13 | 2181 ± 21 | 2216 ± 17 | 2258 ± 8 |
| Fibre content (kg/m$^3$) | 16.9 ± 2.8 | 27.5 ± 1.8 | 14.6 ± 1.2 | 14.8 ± 3.4 | 12.0 ± 2.0 | 21.3 ± 1.5 |
| Age (days) | 33 | 32 | 30 | 57 | 50 | 42 |
| Q-value | 3.75 | 6.3 | 8.9 | 13 | 27 | 20 |

## 4.6 Analysis of Crack Number with the Other Test Results

Here the average number of cracks per core is compared to the other tested factors. This is to see which of the factors that might be affected by or affects the cracking. This is based on the dye penetrant testing. It is assumed that the dye penetrant testing showed all the macro shrinkage cracks in the sprayed concrete cores. The assumption is important. The data from the dye penetrant testing can be used as a basis to see how the cracking affects the other test results with this assumption.

The average number of cracks per core is compared to the strength of the sprayed concrete cores in figure 40. Each plotted dot represents one of the locations the cores were taken from. The plots indicate that the strength gets lower with an increasing number of cracks. The cores from profile number 32450 is excluded from the trendline. Those cores tested the strength of the boundary between two layers and not the intact strength of the sprayed concrete. The plot indicates that the strength decreases with an increasing number of cracks. This also reflected by the $R^2$ value, at 48%.

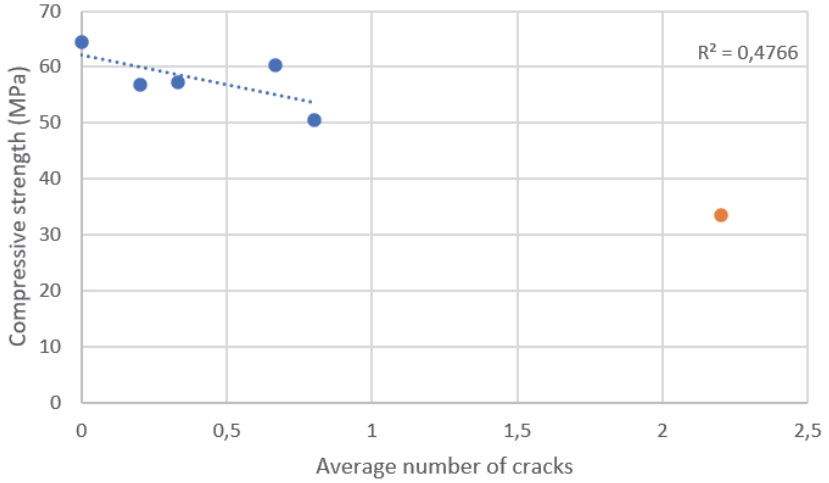


**Figure 40:** Average number of cracks plotted against the average UCS value for each location.

Figure 41 presents the average number of cracks per core compared to density measured at each location. Each plotted dot represents one location the cores were taken from. The cores with two sprayed concrete layers are excluded from the regression of this plot. The density of those cores was affected by the boundary. The trendline shows an increasing density with more cracks. The $R^2$ value is 8%. This means the density and number of cracks are independent values based on this data. The trendline should not be emphasised based on the $R^2$.

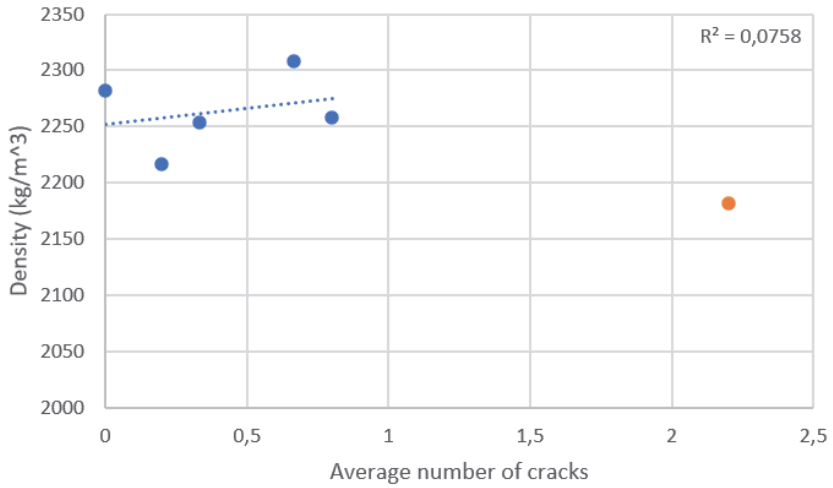


**Figure 41:** Average number of cracks plotted against the average density for each location.

The next factor to be compared to the average number of cracks per core is the in-situ fibre content. This is shown in figure 42. Here the fibre content is plotted against the number of cracks per core. Each dot represents a location. The figure shows that the fibre content on the location with the most cracks is similar to the fibre content at the locations with the least cracks. Based on this data, the number of cracks is independent from fibre content. The $R^2$ at 9% confirms this.

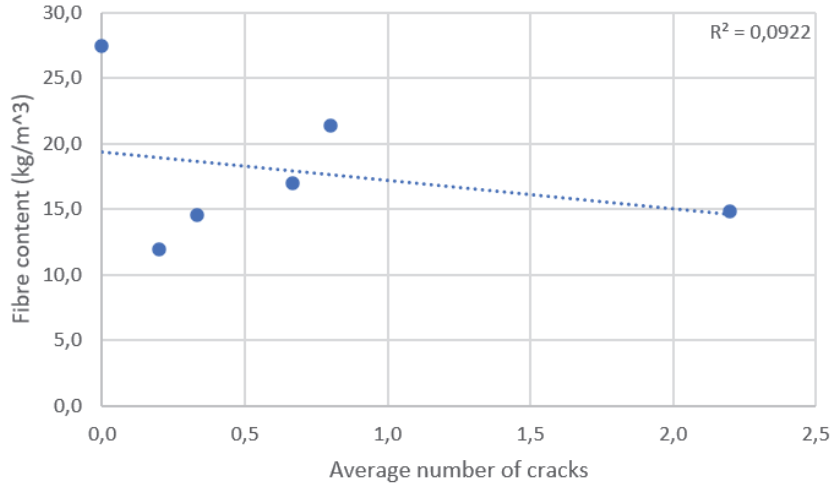


**Figure 42:** Average number of cracks plotted against the average fibre content for each location.

The last factor to be compared to the average number of cracks per core is the Q-values for each location. This is shown in figure 43. Here the Q-values are plotted against the number of cracks per core. Each of the dots represents a location the cores were taken from. The plots show a random spread of the number of cracks compared to the Q-value. The trendline has a $R^2$ at 0%. This means the number of cracks and rock mass quality is independent based on this data.

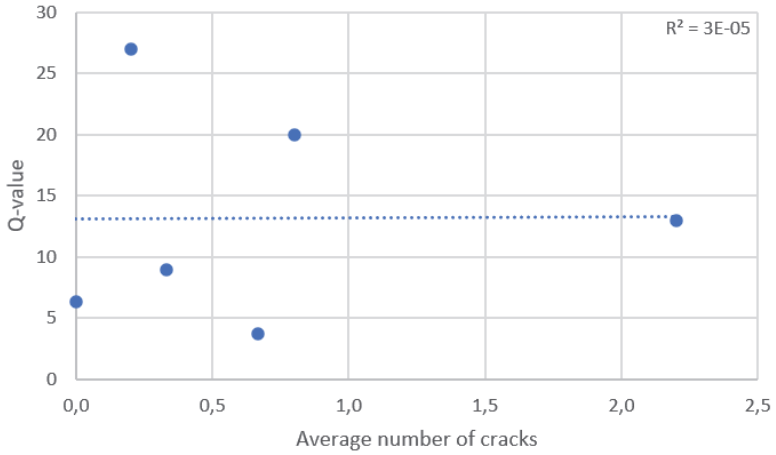


**Figure 43:** Average number of cracks plotted against the Q-value for each location.

## 4.7 Analysis of the Effect the Rock Mass Quality has on the Other Test Results

The rock mass quality is compared to the other test results in this section. This is to see if the substrate material affects the different factors or if they are independent. First one to be plotted against the rock mass quality is the average UCS values for the different locations. Figure 44 shows these values plotted against each other. Each dot represents the Q-value and UCS value from one location. The UCS values decreases with higher Q-values in the plot. This indicates that the strength of the sprayed concrete depends on the quality of the substrate. Substrates of lower quality gives better quality of sprayed concrete in terms of strength. The UCS value of the location with two sprayed concrete layers is dropped in the linear regression.

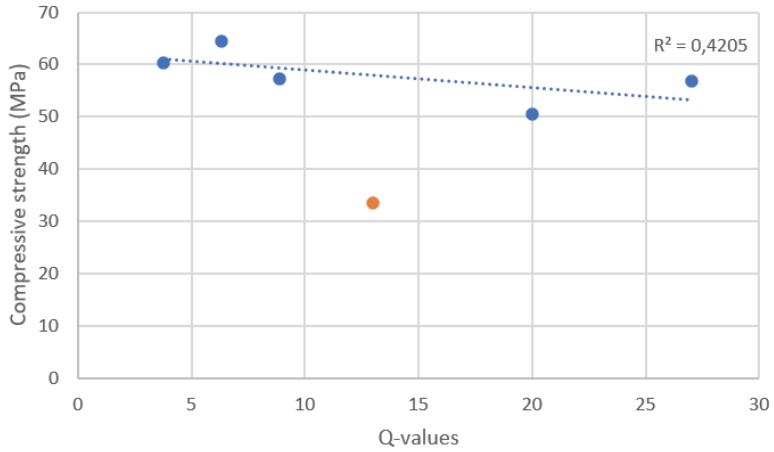


**Figure 44:** Average UCS value plotted against the Q-value for each location.

The next factor to be compared to the rock mass quality is the density measurements. Figure 45 shows the average density measurement plotted against the Q-values for the locations. The lowest density is measured at the location with the highest Q-value, and the highest is at the location with the lowest Q-value. The location with two sprayed concrete layers is not part of the regression. The boundary affected the density measurements. The linear regression shows that the density depends on the Q-values. The density decreases with better rock mass quality. $R^2$ at 77% shows that the regression fits very well to the data.

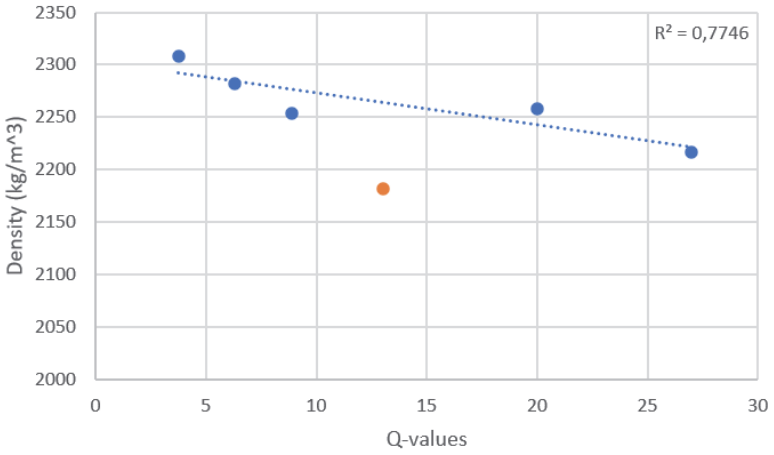


**Figure 45:** Average density plotted against the Q-value for each location.

The density for the E700 and E1000 sprayed concrete is slightly different. Since the amount of fibres is different per cubic metre. The difference is 11 kg/m$^3$. This means the data in figure 45 can be plotted in a different way. It can be plotted with the deviation from the mix design density against the Q-value. Figure 46 demonstrates how the data looks. The deviation increases with an increasing Q-value when this is done. The $R^2$ also increases when the data is plotted in this way.

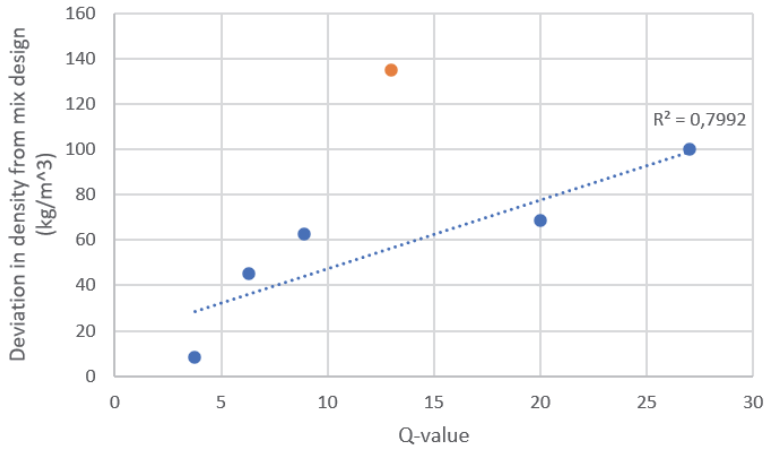


**Figure 46:** Deviation of the density from the mix design plotted against the Q-value for each location.

The last one is the fibre content plotted against the rock mass quality. This is shown in figure 47. Each dot represents one of the profile numbers. The fibre content is lowest at the locations with the highest Q-values. The highest fibre content is at the locations with the lowest Q-value. The regression of the E700 sprayed concrete, blue line, shows a strong connection between the fibre content and Q-values with $R^2 = 92\%$. $R^2$ for the orange line should be ignored. A line fits perfectly when there are only two data points. The line shows the same trend. That the fibre content decreases as the rock mass quality improves.

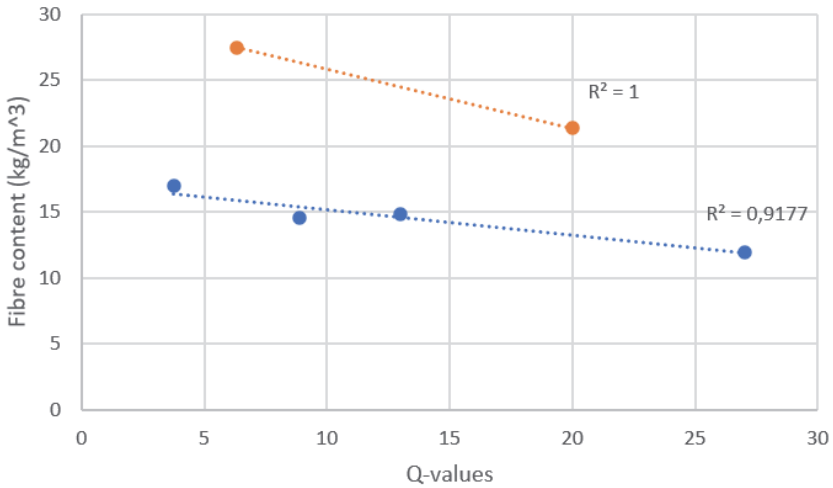


**Figure 47:** Average fibre content plotted against the Q-value for each location. Blue line is E700 and the orange line is E1000 sprayed concrete.

# 5 Discussion

Here in this section, the findings in the literature review and the results from the testing is discussed. The results are connected to the theory. It comes with some suggestions to things that could have been done differently. All the tests are discussed individually first, and then the analysis of the test results are discussed.

## 5.1 Literature Review

The findings of the literature review are discussed in this section. The first interesting fact was how similar the mechanisms of the different shrinkage types appeared in the literature. Plastic shrinkage and drying shrinkage are basically the same. They just happen at different stages. The driving forces in both are evaporation and drying. The difference is when it happens. Plastic shrinkage happens in the plastic phase, before the concrete hardens. Drying shrinkage happens in the hardened concrete. Since they have the same driving forces, it is hard to separate them. It is also a question of separating the different phases. Concrete hardens gradually. The gradual hardening makes the separation of the phases difficult. It could be easier to combine them. Since the same mechanisms work in both shrinkage types.

Autogenous shrinkage is very similar to drying shrinkage and plastic shrinkage. The capillary tension is responsible for the shrinkage in all of them. The difference is what causes the negative capillary pressure. Drying and evaporation causes it in plastic- and drying shrinkage, and self-desiccation is the reason in autogenous shrinkage. All are a result of lower humidity in the concrete. Since the mechanisms are similar it could be hard to separate them.

Autogenous-, plastic- and drying shrinkage depends on the humidity in the concrete. The lower the humidity is the more negative capillary tension in the concrete. This is reflected in the shrinkage mitigating measures. Most of the mitigation measures involve solutions to increase the humidity inside the concrete. The humidity is increased by lowering the evaporation, adding water on the surface or inside the concrete through internal curing. The exception is mitigation with additives. This affects the surface tension of the capillary water directly. SUPERCON aims to increase the durability of sprayed concrete. The durability could be increased by controlling the humidity in the sprayed concrete. Therefore, it would be important to develop methods to control the humidity.

Shrinkage in sprayed concrete can be divided into two major types. The major types are chemical shrinkage and shrinkage due to loss of hydration. Thermal shrinkage is not a major factor. This type of shrinkage has the biggest effect on massive concrete structures. In these massive structures, the temperature difference is large between the centre of the concrete and the environment. This is not the case in sprayed concrete. Sprayed concrete

is very thin. The temperature difference is small during the hardening in thin sections. The major shrinkage types in sprayed concrete can be decreased by adding water to keep it moist. This is easier said than done. Sprayed concrete has a large and rough surface area. The large surface area makes it hard to treat.

The shrinkage mitigation measures mentioned here could be a way to increase the durability of sprayed concrete. The increased durability comes from lowering the shrinkage. There is a lot of uncertainty with the mitigation measures for sprayed concrete. Most of the measures mentioned here are developed for normal cast concrete. Therefore, it is uncertain they would work on sprayed concrete. Sprayed concrete differs from normal cast concrete. It differs with the high accelerator usage, the pneumatic spraying and large surface area compared to thickness. The difference might be so significant that they cannot be compared. The mitigation measures should be developed specifically for sprayed concrete. Specific measures would decrease the shrinkage in sprayed concrete. Most of the literature on shrinkage mitigation in the literature review were on cast concrete. It was little literature based on sprayed concrete.

The amount of cracking in sprayed concrete depends on two things. They are the amount of shrinkage and the restraint. The sprayed concrete would shrink freely without any restraints. Removing the restraints would also take away the tension forces. Normally, there are restraints in sprayed concrete. The restraints build tension within the sprayed concrete. They also stop the concrete from shrinking freely. The amount of shrinkage affects how the tensions builds. Large amounts of shrinkage would increase the tension. Little shrinkage makes smaller tension forces. Lagerblad et al. (2010) showed that there is more shrinkage in sprayed concrete compared to normal cast concrete. They also demonstrated that there are more restraints in sprayed concrete. The extra restraints come from the stiffening from the high accelerator usage. From this it can be assumed that sprayed concrete is more exposed to cracking.

## 5.2 Dye Penetrant

The dye penetrant testing on the concrete cores did not show good results. No cracks or very few cracks appeared in the tests. There is a lot of uncertainty with the mapped cracks. The mapped crack in figure 27 is an example of this uncertainty. This could just as well be multiple pores in a line. There are multiple reasons why this did not work so well. This is discussed in this section.

Sprayed concrete is much more porous than rock. The porosity affected the results. This is one of the reasons the results differ from Vassenden (2019). The dye penetrant dried up quickly when it was applied on the sprayed concrete cores. It seemed like the liquid penetrated all the pores of the sprayed concrete, not just the cracks. This made the liquid vanish fast from the surface. Figure 28 give a strong indication of this. There the dye has

penetrated around half a centimetre all around the sprayed concrete core. The application of the developer pulled the liquid from all the pores. This made the whole surface red. The red colour made it hard to see any cracks.

The developer may have affected the results. The method section mentioned that the developer could cause excessive bleeding and running of the indicators (Magnaflux 2019*b*). This happens when too much developer is applied. This might have happened in the testing. Figures 25 to 27 can demonstrate this. Figure 26 has a light red to pink colour. The cores in the other two figures has a much darker colour. The darker colour could be excessive bleeding and running of the indicator. This comes from excessive usage of the developer. The core in figure 26 was one of the last to be tested. On this core the only distinct crack appeared in all the testing. This reveals that the developer usage was adjusted in the later tests. The high developer usage on the cores from Fjørtofta makes the results on those cores even more uncertain.

The dye penetrant liquid could have been the problem. One spray can was used for all the tests. The spray can was therefore tested on a marble core. This was to check if the can was the problem. The test made cracks appear on the marble core. The lab technicians did not take photos of this test. Figure 25 shows how the dye penetrant works on rock. That core was partly rock. The cracks in the rock became clear red lines. The marble core also stayed moist much longer after the spraying. The penetration was much slower on the marble core. The test on the marble core indicated that the dye penetrant liquid was not the problem. The reason, the sprayed concrete cores showed little cracks had to come from something else.

Self-healing might be a reason that the dye penetrant testing showed so few cracks. The cement content was very high in the sprayed concrete used in the tunnels, where the cores were taken from. The mix design in table 9 shows this. In sprayed concrete with high cement content parts of the cement could be non-hydrated. The non-hydrated cement gets exposed when the concrete cracks. The cracks make the cement exposed to moisture. This starts the hydration of the exposed cement. The hydration of the cement might seal the cracks shut (Alhalabi et al. 2017). It is possible that this happened to the cores. Then the tests would show less cracks. The tests could also show no cracks, if all the cracks got sealed from self-healing.

Creep effects in the early ages of the sprayed concrete might have reduced the restrained shrinkage cracking in the sprayed concrete. Creep can reduce the stresses in the sprayed concrete up 50% (Tao & Weizu 2005). This might be a large enough reduction in the stresses for restrained shrinkage cracks to develop. The stress reduction could also reduce the size of the cracks. The reduction of crack sizes would make it harder for the liquid to penetrate them. This might be a reason, the testing did not show good results.

The shrinkage cracks on the cores might be too fine for the penetrant liquid to penetrate them. It is easier for the liquid to penetrate the pores if the cracks are finer than the pores. The cracks would then be dry. The application of the developer would pull the liquid out of the pores. Since the cracks were dry, they would not appear. The photos of the cores after the dye penetrant testing shows this. The cores had a lot of circular concentrations of dye. The circular concentrations indicate pores rather than cracks. From this it could be interesting to use the method to map pores. Unfortunately, the method does not reveal all pores. A lot of surface pores can be seen in the photos without larger concentrations of dye around them.

The measurement of the cracking was done on the surface of sprayed concrete cores on a macroscopic level. Normally, this should also be measured on a microscopic level. This would give a better picture of the cracking of the concrete. On a macroscopic level thing can seem to be intact. The cores can still have a lot of cracks. There is a lot of uncertainty with the measurements done here. These measurements only show the largest shrinkage cracks. Therefore, there might be a lot of microscopic shrinkage cracks. These cracks might affect the strength of the concrete cores. This has not been considered. The results from the dye penetrant was not good. Therefore, the testing should have been done on thin sections as well. This was not possible due to the COVID-19 situation. The situation delayed the dye penetrant mapping. The delay was so long that there was not enough time to get access to another lab.

The dye penetrant testing did not show as good results as hoped. The results are quite uncertain. The uncertainty of the shrinkage mapping makes effect of the cracks on the other factors even more uncertain. The tests showed that the boundary between the sprayed concrete layers had a big effect on the results. This effect was greater than the cracks. The UCS values and density measurements in the results are lower on the sprayed concrete cores from the location with two sprayed concrete layers.

The dye penetrant testing was done on quite old cores (30-57 days). The testing happened so late, that it is not possible to differentiate the different types of shrinkage cracks. Thermal-, plastic- and autogenous shrinkage cracks starts to develop in the early stages. Drying shrinkage cracking happens later. The testing should be done on different stages to separate the different types. Also, the tests do not say anything on how the cracks was developed. They could come from shrinkage, loads or borders between different layers. The test only says if there are cracks or not. This means that the cracks mapped here might not be shrinkage cracks at all. They could come from loads from the rock mass.

Figure 29 indicates that the number of cracks increase with the age of the sprayed concrete cores. The increase could come from the drying. Sayahi et al. (2014) wrote that drying may expand plastic shrinkage cracks. The cracking may be similar in all the cores. The older cores have been subjected to more drying. The drying could have increased the crack width on the older cores. The expanded cracks might be the reason more cracks

appeared on the older cores. The cracks in the younger cores might be too small for the dye penetrant to be able to reveal them.

## 5.3 Uniaxial Compressive Strength

There were some interesting results from the other tests, even though the dye penetrant testing did not work as planned. The strength testing on the cores from Fjørtofta was not the best. At profile number 32450 the failure of the test specimens happened along the boundary of the two sprayed concrete layers. On these cores, it was the strength along the boundary that was tested. The test did not determine the strength of the intact sprayed concrete. The sprayed concrete cores from profile number 32500 were too short for the UCS testing. Only two of the cores were long enough, L/d $> 1$, after the preparation of the cores. Two cores are not enough to get a valid strength measurement of the sprayed concrete at a location according to NS-EN 12390-3 (NS 2019*a*).

The UCS testing had some interesting results. Figure 30 shows that most of the test locations had a strength far higher than the strength class. The strongest cores had a strength of almost 30 MPa higher than what is required. There are different reasons to why this happened.

The most likely reason to why the sprayed concrete achieved so high strengths is because of the durability class. The durability class requires a much lower w/c than the strength class. The lower w/c in the durability class increases the strength. Another reason to these results, may be that water is loss with the rebounded particles. This makes the efficient w/c lower. The age of the sprayed concrete cores might be a reason for the high strengths. The cores should be tested at 28 days according to the standard. All the cores here got tested at an older age than that. The ages of the cores can be seen in table 16. This has given the sprayed concrete more time for the late hardening of the cement. The late hardening might have increased the strength. This is unlikely if we look at figure 12. That figure shows that the strength gain after 28 days is minimal, when the concrete is not continuously moist.

The failure patterns on the cores did not look like the satisfactory ones in the standard. The satisfactory failures are shown in figure 23. The fibres in the sprayed concrete cores have changed the way the sprayed concrete fails. The addition of fibres has increased the flexural strength of the sprayed concrete. The increased flexural strength makes the concrete endure larger deformations before it fails (Henager 2003). Therefore, the UCS tests were deemed satisfactory, as the fibres affected the failure patterns. The unsatisfactory UCS tests were on the cores from profile number 32450. There the cores failed along the boundary between two sprayed concrete layers, and not in the solid sprayed concrete. Those test results were excluded in the analysis. Since they gave the strength of the boundary and not the strength of the sprayed concrete.

Melbye et al. (2001) wrote that the thickness of the sprayed concrete should be applied in numerous thinner layers rather than in one pass. The results of the UCS testing demonstrates something else. The strength is highest in the cores with one thick layer. The sprayed concrete cores with two sprayed concrete layers were the only ones not to achieve the strength class in figure 30. Boundaries between layers are weaknesses in the sprayed concrete. This indicates higher strength is achieved with fever layers. The indication is based on observations from only one location. Therefore, this should be tested at multiple locations before any conclusions can be drawn.

## 5.4 Density

The density testing shows that the sprayed concrete cores have a lower density than the initial mix design. The cores have a density varying between 8-135 kg/m$^3$ lower than the mix design. The most likely reason for the lower density is worse compaction than the initial mix design. The compaction is affected by the factors given in figure 2. The nozzle angle may have influenced the results. The angle should be normal to the surface during the spraying, at smaller angles the rebound increases and the compaction gets lower. The density might also be influenced by the accelerator usage. The accelerator usage may have led to flash setting in the sprayed concrete. The flash setting prevents complete compaction and increases the rebound loss (Melbye et al. 2001).

The two sprayed concrete layers at profile number 32450 affected the density. The surface of the first sprayed concrete layer was most likely very rough. The roughness made it hard for the next layer to fill all the irregularities in the surface. The surface irregularities may have increased the amount of air voids at the boundary. Air has a low density. All the extra air voids in the boundary lowers the total density of the test samples from this location. This makes the density at this location lower than the other locations. Even though the mix design is the same for all the test sites.

The density measurements might have been affected by the dye penetrant testing. The cores were weighted after they had been prepared for the UCS testing. This was done after the dye penetrant testing. Figures 31 to 36 shows the cores after the UCS testing. Most of the cores have a red colour in those figures. The red colour indicates that there is still dye left in the cores. This might have increased the weight. The increased weight from the dye might have resulted in higher density measurements.

## 5.5 Fibre

The measurement of the fibre content in the sprayed concrete cores had some interesting results. All the cores had a lower fibre content than the mix design. This is presented in figure 38. The figure also shows a big variation in the fibre content between the locations.

The big variation in fibre content between the different location could be from rebound. The studies of Banthia et al. (1992) showed that rebound of steel fibres is higher than the other constituents in dry mix sprayed concrete. It seems like this is the case for wet mix sprayed concrete as well. Since all the locations had a fibre content lower than the initial mix design.

Figure 39 showed that the fibre content increased with the length of the samples. The tendency could be explained with Newton's third law of motion. If an object exerts a force on another object, then other object must exert a force of equal magnitude in the opposite direction back on the first object. The particles in the sprayed concrete hits the rock surface more directly in the thinner layers, and the force exerted from the tunnel wall on the fibres is large. The increased thickness of the sprayed concrete muffles the incoming fibres from the spraying. This absorbs energy from the fibres and the impact force is lowered. A lower impact force results in a lower force exerted from the rock wall on the fibres. The lower force exerted on the fibres results in lower rebound. The fibre content increases, when the rebound of the fibres is lower. It would have been interesting to see, if the fibre content is highest were the thickness is greatest. The length of the sprayed concrete cores stops at L = 2d. Therefore, it is not possible to say anything about the thickness from this data. The data only demonstrates that the fibre content increases in longer cores. The residual plot also showed that the data might be biased. This means that there should not be put too much emphasis on the data. More data is needed to see if the fibre content increases with thicker layers, since this data is not good enough.

The fibre content measurements highly depend on the human factor. How well the fibres get separated depends on the technician (Silva et al. 2015). Let us say that half a gram of the fibres is not detected or lost in all the fibre content measurements. This has a bigger effect on the measured fibre content in the smaller cores than in the longer cores. In the smallest core, half a gram of fibres is a difference on 3 $kg/m^3$ in fibre content, while in a core with L/d = 2 the difference is only 1.5 $kg/m^3$ in fibre content. It is important to be aware that the smaller cores are more sensitive when measuring the fibre content. The differences in the fibre content could be smaller if the same amount of fibres is lost in all the measurements of the fibre content.

## 5.6 Analysis of Crack Number with the Other Test Results

Here in this subsection, the comparison of the results from the crack mapping to the other test results are discussed. It is important to be aware that there is a lot of uncertainty in the results from the dye penetrant mapping. In this section, the discussion builds on the assumption that the results from the crack mapping shows all the macro cracks in the cores. The focus is on what the comparison shows, and not the uncertainty of the crack mapping. The uncertainty has already been discussed in the subsection on dye penetrant.

The comparison of the crack number with UCS was interesting. Figure 40 showed an interesting tendency. The tendency was that the UCS gets lower with an increasing number of cracks in the sprayed concrete. This is what could be expected. Cracks weakens the integrity of the sprayed concrete. A crack would be a weaker part that could induce the failure in the core under high loads. There is some uncertainty to the trendline. The $R^2$ number demonstrates this. The number gives an indication. Since it is under 50%, it shows that the trend is very uncertain, and more data is needed to come with a reliable conclusion.

The next comparison was not as interesting. This was the comparison of number of cracks to the density. Figure 41 shows very little dependency between the density and the number of cracks. This could because of the size of the cracks. The cracks may be so small that they are such a small part of the total volume, that they do not affect the total density. Larger cracks like a boundary between two sprayed concrete layers has a bigger effect on the density. These cracks have a large enough volume for it to lower the density measurements. The measurements from profile number 32450 indicates this.

The relationship between the number of cracks and the fibre content were one of the more interesting tests in advance. There is a lot of research showing that fibres have an effect on cracking in concrete and sprayed concrete. The results here were disappointing. The plot in figure 42 shows no tendency. Based on this data the fibre content does not affect the number of cracks. It was expected that the cores with the lowest fibre content would have had the highest number of cracks. The fibre content could be high enough in all the cores to prevent cracking. This has created restraints inside the concrete. The restraints reduced the cracking (Qiao et al. 2010). The fibres could also have reduced the size of the cracks. Making the cracks too small for the dye penetrant to detect them.

The last comparison with the crack number was with the rock mass quality, Q-values. Here there was no tendency. The $R^2$ value showed that the two factors are independent based on the data collected here. This can be connected to what Ozturk & Tannant (2011) studied. They saw that the adhesion depended more on the chemical reaction between the rock grains and the liner material. The chemical reaction was more important for the adhesion strength than the mechanical interlocking. Since the rock type at all the test locations were gneiss, the chemical reaction between the liner and the rock should be the same. Therefore, the adhesion should be the same at all locations. The adhesion decides the restraint, and when the restraint is the same for all locations the rock mass should not affect the cracking differently.

## 5.7 Analysis of the Effect the Rock Mass Quality has on the Other Test Results

Here in this section, the results from the comparison of the rock mass qualities and the other test results are discussed. Some interesting results appeared from this comparison in the results section.

Figure 44 shows a nice tendency. The tendency shows the strength of the sprayed concrete depends on the quality of the rock mass in the substrate. The trendline shows that the UCS decreases as the rock mass improves. This is very interesting. It is likely that this is connected to the rebound. The same tendency can be seen in the density and fibre content measurements. It makes sense that the strength gets lower when the density and fibre content is lowered. A lower density means increased air content and probably a higher porosity. The increased air content can explain why the strength gets lower. The strength of concrete decreases by 4-6% for every 1% the air content increases (Zhang et al. 2018).

The comparison of the fibre content and the density to the rock mass quality had the highest $R^2$ value for the linear regressions. This means that the regression explains the variability most precisely for these relations. These factors show the highest dependency. The relations can be explained with rebound. The higher the Q-value is the more solid and massive is the rock surface. Lower Q-values means the rock surface is more cracked and weaker. A more solid and hard surface would cause more rebound. Hard surfaces absorb less impact energy than a weaker and more cracked surface would do. Surfaces that absorbs less energy gives the particles more energy to rebound. This causes more particles to bounce off the surface. The increased rebound results in lower densities. Figure 46 strengthens this assumption.

In the last comparison between the fibre content and the rock mass, the same tendency as for the density can be seen. The fibre content gets lower with the higher Q-values. This can be explained in the same way as for the density.

# 6 Conclusions

This master's thesis tested a new method to map shrinkage cracks on sprayed concrete cores. The new method was dye penetrant. It was used to map the surface cracking on cores. The shrinkage crack mapping was used to see if the cracking had an effect on the UCS and density. The effect of the fibre content and rock mass on the amount of cracking was also checked.

The literature review showed that sprayed concrete differs from normal cast concrete in many ways. It also differs when it comes to shrinkage. Sprayed concrete is stiff when it hits the rock surface because of the accelerator. The accelerator affects how it shrinks and the porosity. Chemical shrinkage is more dominant in sprayed concrete. It also makes it more porous. The higher porosity makes the sprayed concrete more prone to drying. The high cement content increases the shrinkage even more. The large shrinkage combined with the restraints from the rock surface makes sprayed concrete prone to cracking.

It can be concluded, that using dye penetrant to map shrinkage cracks on sprayed concrete cores was unsuccessful. The method is unsuitable for shrinkage crack mapping on sprayed concrete cores. This is due to the porosity of sprayed concrete. This was seen in figure 28. The dye penetrant has penetrated all around the sprayed concrete core in the figure. The penetration should only have been in the cracks. The method works well on less porous surfaces. This became clear on the cores with rock parts. On the rock, the cracks became clear red lines, which it should, with the method.

The effect of the shrinkage cracks on the other tests could not be investigated properly. Since the dye penetrant testing was unsuccessful. Anyway, the other tests had interesting results. The tests showed that the sprayed concrete had much higher strength than the strength class. The density and fibre content in the cores were lower than the initial mix design at all locations.

The tests indicated that the strength of the sprayed concrete is affected by the rock mass quality. Higher rock mass qualities gave weaker sprayed concrete. This was due to rebound. The rebound on more solid rock masses is increased. The increased rebound lowers the density and fibre content in the sprayed concrete. This results in lower strength.

This master's thesis is written in cooperation with the research project SUPERCON. The goal of the thesis was to contribute to the durability goal of SUPERCON. The contribution would be through increased knowledge on shrinkage cracking. The hope was to be able to map shrinkage cracks with dye penetrant on the surface of sprayed concrete cores. The results from the mapping would have been used to see how the cracks affected the strength and density, and how the fibre content effected the cracking. This was not possible with the results of the dye penetrant testing. The method did not work as intended. Therefore, the contribution to increased knowledge on shrinkage cracking was not achieved.

# 7 Further Work

The goal of this master's thesis was to see how cracks affected the mechanical strength of sprayed concrete and to see how the fibre content affected the number of cracks in the sprayed concrete. Due to the COVID-19 pandemic, there was only conducted limited tests. There is other factors and measures that should be tested to develop an impermeable sprayed concrete tunnel lining. This is something the SUPERCON research project aim. Here in this section I come with some suggestions to topics it could be interesting to look at to build up knowledge on cracks and crack mitigation. These suggestions might help to develop an impermeable sprayed concrete tunnel lining.

The method used to map shrinkage cracks in this master's thesis did not work very well. It could be interesting to test different methods to map shrinkage cracks. This could be used to figure out the best and most efficient method for this purpose. The results from testing different methods could be used to standardise shrinkage crack mapping in-situ.

The w/c together with the cement content and degree of hydration is the most important factors when it comes to the type and amount of shrinkage in concrete. The cement content is higher in sprayed concrete compared to normal cast concrete. This means that the sprayed concrete experience more shrinkage. The shrinkage could be decreased by finding ways to lower the cement content. The cement content could be reduced with replacement materials. The replacement materials develop strength slower. This is a problem for the early strength gain. The early strength gain is not a problem if another impermeable layer of sprayed concrete is added outside the load bearing lining. Replacement materials could be used in this lining. The impermeable lining would not carry any weight. The early strength gain is not important when the lining does not carry weight. This would give the lining time hydrate and develop.

The thesis mentions some mitigation measures in the theory. The original plan was to test some of them in this thesis. The pandemic made it difficult to do any kinds of tests. Therefore, the mitigating measures mentioned earlier could be tested in later research to see if they work on sprayed concrete. It would have been interesting to see if self-healing or SAP works in sprayed concrete. The abilities of self-healing and SAP could possibly self-seal the shrinkage cracks that develop during the hardening. The different mitigation could be tested to see their effect. The effects could be compared to figure out which on is the most efficient. The different measures should also be tested together to see if this improves or worsens their abilities to mitigate cracks.

Spayed concrete is a thin concrete with a very large surface. This makes the concrete vulnerable to evaporation. It should therefore be developed new curing methods to keep the moisture inside the sprayed concrete, to avoid plastic and drying shrinkage. Since the surface is so large. It is difficult to find an efficient and cost-effective way to protect it from

evaporation compared to normal cast concrete. If a new curing method for sprayed concrete were developed the shrinkage could be reduced greatly. The reduction of shrinkage reduces the cracking. This could decrease the permeability and make less fluids flow through the concrete. All in all, this could make the concrete more durable.

Looking at figure 2. One question comes to mind. Is it possible to make impermeable sprayed concrete with the spraying technique we have today? On the right side of that figure, there is a grading of the sprayed concrete quality. According to that grading, the sprayed concrete never gets better than good with the spaying technique we have today. The goal should be to move this to excellent. This could be done by improving the technology. The improved technology could possibly improve the compaction, lower the permeability, and reduce the cracks.

The geology is an important part of how sprayed concrete preforms. The adhesion between the rock surface and the sprayed concrete affects the restraint and therefore the cracking. It would be interesting to see if the mix design could be optimised for different geologies. The optimisation would be to reduce cracking. Then it would be important to figure out which geological factors the mix design should consider. This could optimise the interaction between sprayed concrete and the rock surface.

# References

Ålesund muncipality (2020): *Karantenereglar*, Ålesund kommune. `https://alesund.kommune.no/helse-og-omsorg/korona/karantenereglar/`.

ACI (2007): *Estimating Evaporation Rates to Prevent Plastic Shrinkage Cracking*, Concrete International.

ACI (2010): *Report on Chemical Admixtures for Concrete*, Farmington Hills, MI.

Alhalabi, S., Alhalabi, Z. O. & Dopudja, D. (2017): *Self-Healing Concrete: Definition, Mechanism and Application in Different Types of Structures*, Meždunarodnyj naučno-issledovatel'skij žurnal (International Research Journal).

Altoubat, S. A. & Lange, D. A. (2001): *Creep, Shrinkage and Cracking of Restrained Concrete at Early Age*, ACI Materials Journal.

Andersen, P. J. & Johansen, V. (1993): *A Guide to Determining the Optimal Gradation of Concrete Aggregates*, Strategic Highway Research Program.

Ansell, A. (2010): *Investigation of Shrinkage Cracking in Shotcrete on Tunnel Drains*, Tunnelling and Underground Space Tachnology.

Atrushi, D. S. (2003): *Tensile and Compressive Creep of Early Age Concrete: Testing and Modelling*, NTNU.

Aïtcin, P. C. (2016): *Science and Technology of Concrete Admixtures*, Woodhead Publishing, p.27-51.

Bakhsh, K. N. (2010): *Evaluation of Bond Strength between Overlay and Substrate in Concrete Repairs*, Royal Institute of Technology (KTH).

Bamforth, P. B. (2007): *Early-Age Thermal Crack Control in Concrete*, CIRIA.

Banthia, N., Trottier, J.-F. & Beaupré, D. (1994): *Steel-Fiber-Reinforced Wet-Mix Shotcrete: Comparisons with Cast Concrete*, Journal of Materials in Civil Engineering.

Banthia, N., Trottier, J.-F., Wood, D. & Beaupre, D. (1992): *Steel Fibre Reinforced Dry-Mix Shotcrete: Effect of Fibre Geometry on Fibre Rebound and Mechanical Properties*, Fibre Reinforced Cement and Concrete: Proceedings of the Fourth RILEM International Symposium, Taylor & Francis Group.

Bažant, Z. P. (1985): *Fracture Mechanics of Concrete: Structural Application and Numerical Calculation*, Martinus Nijhoff Publishers.

Bentz, D. P. & Peltz, M. A. (2008): *Reducing Thermal and Autogenous Shrinkage Contributions to Early-Age Cracking*, ACI Materials Journal.

Bernard, S. (2010): *Shotcreting in Australia*, Concrete Institute of Australia.

Bertoncini, A., Dugat, J., Frouin, L., Jaquier, J.-L. & Prat, E. (1999): *Process for Spraying Concrete or Mortar*, United States Patent (Patent number: 5,895,688).

Beshr, H., Almusallam, A. A. & Maslehuddin, M. (2002): *Effect of Coarse Aggregate Quality on the Mechanical Properties of High Strength Concrete*, Construction and Building Materials.

Bisschop, J. & van Mier, J. G. M. (1999): *Quantification of Shrinkage Micro-Cracking in Young Mortar with Fluorescence Light Microscopy and ESEM*, Heron.

Bissonnette, B., Pigeon, M. & Vaysburd, A. M. (2007): *Tensile Creep of Concrete: Study of Its Sensitivity to Basic Parameters*, ACI Material Journal.

Boghossian, E. & Wegner, L. D. (2008): *Use of Flax Fibres to Reduce Plastic Shrinkage Cracking in Concrete*, Cement & Concrete Composites.

Branch, J., Hannant, D. J. & Mulheron, M. (2002): *Factors Affecting the Plastic Shrinkage Cracking of High-Strength Concrete*, Magazine of Concrete Research.

Bryne, L. E., Ansell, A. & Holmgren, J. (2014*a*): *Investigation of Restrained Shrinkage Cracking in Partially Fixed Shotcrete Linings*, Tunnelling and Underground Space Technology.

Bryne, L. E., Ansell, A. & Holmgren, J. (2014*b*): *Laboratory Testing of Early Age Bond Strength of Shotcrete on Hard Rock*, Tunnelling and Underground Space Technology.

CEMEX (2013): *The Effects of Water Additions to Concrete: What's a little water going to hurt?*, CEMEX USA.

Claisse, P. A. (2016): *Civil Engineering Materials; Chapter 18 - Cements and cement replacement materials*, Butterworth-Heinemann.

Combrinck, R. & Boshoff, W. P. (2013): *Typical Plastic Shrinkage Cracking Behaviour of Concrete*, Magazine of Concrete Research.

Dehls, J. F., Olesen, O. & Rønning, J. S. (2011): *Magnetisk og batymetrisk kartlegging ved vegprosjektet Fv. 659 Nordøyvegen, Møre og Romsdal*, Geological Survey of Norway (NGU).

Dias, W. P. S. (2003): *Influence of Mix and Environment on Plastic Shrinkage Cracking*, Magazine of Concrete Research.

Duan, L., Zhang, Y. & Lai, J. (2019): *Influence of Ground Temperature on Shotcrete-to-Rock Adhesion in Tunnels*, Advances in Materials Science and Engineering.

EFNARC (2019): *EFNARC Nozzleman Certification Scheme - EFNARC C2 Training and Certification Plan*, European Federation of National Associations Representing producers and applicators of specialist building products for Concrete.

Elakneswaran, Y., Noguchi, N., Matumoto, K., Morinaga, Y., Chabayashi, T., Kato, H. & Nawa, T. (2019): *Characteristics of Ferrite-Rich Portland Cement: Comparison With Ordinary Portland Cement*, Frontiers in Materials.

Essili, M. (2017): *Control of Early Age Shrinkage Cracking in Reinforced Concrete Bridge Decks*, The University of Akron.

Frost, J. (2013): *Regression Analysis: How Do I Interpret R-squared and Assess the Goodness-of-Fit?*, Data Science Central.

Fujiwara, T. (2008): *Effect of Aggregate on Drying Shrinkage of Concrete*, Journal of Advanced Concrete Technology.

Ganerød, G. V. & Lutro, O. (2011): *Berggrunnsgeologisk og strukturgeologisk kartlegging i forbindelse med prosjektet Fv. 659 Nordøyvegen, Møre og Romsdal*, Geological Survey of Norway (NGU).

Ghodke, P. & Mote, S. (2018): *The Self-Healing Concrete - A Review*, International Journal of Advances in Engineering and Technology.

Gianfrancesco, A. D. (2017): *Materials for Ultra-Supercritical and Advanced Ultra-Supercritical Power Plants*, Woodhead Publishing, p.233.

Gjørva, M. B. (2020): *Re: Bergmassekartlegging til master*, Message to Bjarte Grindheim, 23.06.2020. E-mail.

Glen, S. (2015): *Residual Plot: Definition and Examples*, Statistics How To.

Goodwin, F. (2006): *Significance of Tests and Properties of Concrete & Concrete-Making Materials: Chapter 21 - Volume Change*, ASTM International.

Grassl, P., Wong, H. S. & Buenfeld, N. R. (2009): *Influence of Aggregate Size and Volume Fraction on Shrinkage Induced Micro-Cracking of Concrete and Mortar*, Cement and Concrete Research.

Grindheim, B. (2019): *Faktorar som påverkar haldbarheita til sprøytebetong, Fordjupingsprosjekt*, NTNU.

Grøv, E. (2019): *SUPERCON*, Sintef. `https://www.sintef.no/projectweb/supercon/`.

Hansen, R. K. T. (2017): *Effekt av å bruke retarderende stoff (R-stoff) i herdingsprosessen i store betongkonstruksjoner i kaldt klima*, UiT - Norges Arktiske Universitet.

Hasholt, M. T., Jensen, O. M., Kovler, K. & Zhutovsky, S. (2012): *Can Superabsorbent Polymers Mitigate Autogenous Shrinkage of Internally Cured Concrete without Compromising the Strength?*, Construction and Building Materials.

Hemphill, G. B. (2012): *Practical Tunnel Construction*, Wiley.

Henager, C. H. (2003): *Steel Fibrous Shotcrete: A Summary of the State-of-the-Art*, Shotcrete.

Henkensiefken, R., Nantung, T. & Weiss, J. (2009): *Internal Curing - From the Laboratory to Implementation*, LWC Bridges Workshop.

Hetlebakke, J.-E. (2020): *Følgeseddel Terning - Longva Mobil*, Message to Bjarte Grindheim, 03.06.2020. E-mail.

Hewlett, P. & Liska, M. (2019): *Lea's Chemistry of Cement and Concrete*, Butterworth-Heinemann.

Huang, Y. (2017): *Activated Carbon Fiber and Textiles: Chapter 7 - Electrical and Thermal Properties of Activated Carbon Fibers*, Woodhead Publishing.

Höfler, J. & Schlumpf, J. (2004): *Shotcrete in Tunnel Construction*, Putzmeister AG.

In, C.-W., Holland, R. B., Kim, J.-Y., Kurtis, K. E., Kahn, L. F. & Jacobs, L. J. (2013): *Monitoring and Evaluation of Self-Healing in Concrete using Diffuse Ultrasound*, NTD&E International.

Jacobsen, S., Maage, M., Smeplass, S., Kjellsen, K. O., Sellevold, E. J., Lindgård, J., Cepuritis, R., Myrdal, R., Bjøntegaard, Ø. & Geiker, M. (2015): *Concrete Technology*, NTNU.

Jolin, M., Burns, D., Bissonnette, B., Gagnon, F. & Bolduc, L.-S. (2009): *Understanding the Pumpability of Concrete*, Shotcrete for Underground Support - Engineering Conferences International.

Khan, I., Castel, A. & Gilbert, R. I. (2017): *Tensile Creep and Early-Age Concrete Cracking due to Restrained Shrinkage*, Construction and Building Materials.

Khitab, A. (2015): *Shotcrete: Methods and Compositions*, Mirpur University of Science and Technology.

Knoppik-Wróbel, A. & Klemczak, B. (2015): *Analysis of Early-Age Thermal-Shrinkage Stresses in Reinforced Concrete Walls*, Silesian University of Technology Faculty of Civil Engineering.

Kozul, R. & Darwin, D. (1997): *Effects of Aggregate Type, Size, and Content on Concrete Strength and Fracture Energy*, Structural Engineering and Engineering Materials.

Kumar, R., Rai, R. & Srivastava, A. K. (2015): *Effect of Air Entraining Agent on Properties of Concrete*, Journal of Civil Engineering and Environmental Technology.

Lagerblad, B., Fjällberg, L. & Vogt, C. (2010): *Shrinkage and Durability of Shotcrete*, Tyler & Francis Group.

Lagerblad, B., Holmgren, J., Fjällberg, L. & Vogt, C. (2006): *Hydratation och krympning hos sprutbetong*, Swedish Rock Engineering Research.

Laning, A. (1992): *Synthetic Fibers: Primarily used to Reduce Shrinkage Cracking, Polypropylene, Nylon, and Polyester Fibers offer other Benefits as well*, Concrete Construction.

Lea, F. M. & Mason, T. O. (2019): *Cement*, Britannica Encyclopædia.

Leung, C. K. Y. (2001): *Concrete as a Building Material*, Encylopedia of Materials: Science and Technology (Second Edition), Pergamon.

Li, V. C. & Yang, E.-H. (2007): *Self Healing in Concrete Materials*, Springer Series in Material Science.

Liwu, M. & Min, D. (2006): *Thermal Behaviour of Cement Matrix with High-Volume Mineral Admixtures at Early Hydration Age*, Cement and Concrete Research.

Lundgren, M., Helsing, E., Babaahmadi, A. & Mueller, U. (2018): *State-of-the-Art Report on: Material Type, Requirements and Durability Aspects of Sprayed Concrete in Tunnels*, RISE Reasearch Institutes of Sweeden.

Magnaflux (2019*a*): *Product Data Sheet - C10*, Magnaflux.

Magnaflux (2019*b*): *Product Data Sheet - D30A, D30plus*, Magnaflux.

Magnaflux (2019*c*): *Product Data Sheet - RP20*, Magnaflux.

Malmgren, L., Nordlund, E. & Rolund, S. (2005): *Adhesion Strength and Shrinkage of Shotcrete*, Tunneling and Underground Space Technology.

Melbye, T., Dimmock, R. & Grashol, K. F. (2001): *Sprayed Concrete for Rock Support*, MBT International Underground Construction Group.

Mignon, A., Snoeck, D., Dubruel, P., Vlierberghe, S. V. & Belie, N. D. (2017): *Crack Mitigation in Concrete: Superabsorbent Polymers as Key to Success?*, Materials.

Mihashi, H. & de B. Leite, J. P. (2004): *State-of-the-Art Report on Control of Cracking in Early Age Concrete*, Journal of Advanced Concrete Technology.

Mohod, M. V. (2012): *Performance of Steel Fiber Reinforced Concrete*, International Journal of Engineering and Science.

Mynarcik, P. (2015): *Core Sampling for Fiber Concrete Constructions - Context between Quantity of Core Samples and Evaluation of Fiber Concrete Characteristics*, Procedia Engineering.

Naaman, A. E., Wongtanakitcharoen, T. & Hauser, G. (2005): *Influence of Different Fibres on Plastic Shrinkage Cracking of Concrete*, ACI Materials Journal.

Naik, T. R., moon Chun, Y. & Kraus, R. N. (2006): *Reducing Shrinkage Cracking of Structural Concrete Through the Use of Admixtures*, Wisconsin Research Program.

NB (2011): *Sprøytebetong til bergsikring*, Norsk Betongforening.

Neville, A. M. & Brooks, J. J. (2010): *Concrete Technology Second Edition*, Longman Group UK Limited.

Newmann, J. & Choo, B. S. (2003): *Advanced Concrete Technology*, Butterworth-Heinemann.

NFF (2008): *Håndbok nr.05 - Tung bergsikring i undergrunnsanlegg*, Norsk forening for fjellsprengningsteknikk.

NGI (2015): *Handbook Using the Q-system - Rock Mass Classification and Support Design*, Norwegian Geotechnical Institute.

Nguyen, T. T., Picandet, V., Carre, P., Lecompte, T., Amziane, S. & Baley, C. (2011): *Effect of Compaction on Mechanical and Thermal Properties of Hemp Concrete*, European Journal of Environmental and Civil Engineering.

Nilsen, B. (2016): *Ingeniørgeologi-berg grunnkurskompendium*, NTNU.

Nmai, C. K., Vojtko, D., Schaef, S., Attiogbe, E. K. & Bury, M. A. (2014): *Crack-Reducing Admixture*, ACI Concrete International.

NPRA (2020*a*): *Fv. 659 Nordøyvegen*, The Norwegian Public Roads Administration. `https://www.vegvesen.no/Fylkesveg/fv659nordoyvegen`.

NPRA (2020*b*): *Vegtunneler - Håndbok N500*, Norwegian Public Roads Administration.

NS (2006): *NS-EN 14488-7:2006 Testing Sprayed Concrete. Part 7: Fibre content of fibre reinforced concrete*, Standard Norge.

NS (2012): *NS-EN 12390-1:2012 Testing hardened concrete. Part 1: Shape, dimensions and other requirements for specimens and moulds*, Standard Norge.

NS (2017): *NS-EN 206:2013+A1:2016 Concrete: Specification, performance, production and conformity*, Standard Norge.

NS (2019*a*): *NS-EN 12390-3:2019 Testing hardened concrete. Part 3: Compressive strength of test specimens*, Standard Norge.

NS (2019*b*): *NS-EN 12390-7:2019 Testing hardened concrete. Part 7: Density of hardened concrete*, Standard Norge.

NS (2019*c*): *NS-EN 12504-1:2019 Testing concrete in structures. Part 1: Cored specimens: Taking, examining and testing in compression*, Standard Norge.

NS (2020): *NS-EN 12390-4:2019 Testing hardened concrete. Part 4: Compressive strength. Specification for testing machines*, Standard Norge.

Ozturk, H. & Tannant, D. (2011): *Influence of Rock Properties and Environmental Conditions on Thin Spray-On Liner Adhesive Bond*, International Journal of Rock Mechanics & Mining Sciences.

Pawar, C., Sharma, P. & Titiksh, A. (2016): *Gradation of Aggregates and its Effects on Properties of Concrete*, International Journal of Trend in Research and Development.

Pillar, N. M. P. & Repette, W. L. (2015): *The Effect of Fibers on the Loss of Water by Evaporation and Shrinkage of Concrete*, IBRACON Structures and Materials Journal.

Qiao, P., McLean, D. & Zhuang, J. (2010): *Mitigation Strategies for Early-Age Shrinkage Cracking in Bridge Decks*, Washington State Department of Transportation.

Radlinska, A., Rajabipour, F., Bucher, B., Henkensiefken, R., Sant, G. & Weiss, J. (2008): *Shrinkage Mitigation Strategies in Cementitious Systems: A Closer Look at Differences in Sealed and Unsealed Behavior*, Journal of the Transportation Research Board.

Richardson, D. N. (2005): *Aggregate Gradation Optimization - Literature Search*, Missouri Department of Transportation.

Ruiz-Ripoli, L., Barragán, B. E., Moro, S. & Turmo, J. (2013): *Digital Imaging Methodology for Measuring Early Shrinkage Cracking in Concrete*, Strain.

Ruiz-Ripoll, L., Barragán, B. E., Moro, S. & Turmo, J. (2016): *Evaluation of the Techniques to Mitigate Early Shrinkage Cracking through an Image Analysis Methodology: Techniques to Mitigate Early Shrinkage Cracking*, Strain.

Safiuddin, M., Kaish, A. B. M. A., Woon, C.-O. & Raman, S. N. (2018): *Early-Age Cracking in Concrete: Causes, Consequences, Remedial Measures, and Recommendations*, Applied Sciences.

Sayahi, F. (2019): *Plastic Shrinkage Cracking in Concrete - Mitigation and Modelling*, Luleå University of Technology.

Sayahi, F., Emborg, M. & Hedlund, H. (2014): *Plastic Shrinkage Cracking in Concrete: State of the Art*, Nordic Concrete Research.

Schallom III, R. (2006): *Curing Pneumatically Applied Concrete*, Shotcrete.

Scherer, G. W. (2015): *Drying, Shrinkage, and Cracking of Cementitious Materials*, Transport in Porous Media.

Schindler, A., Byard, B. & Tankasala, A. (2019): *Mitigation of Early-Age Cracking in Concrete Structures*, MATEC Web of Conferences.

Schröfl, C., Mechtcherine, V. & Gorges, M. (2012): *Relation between the Molecular Structure and the Efficiency of Superabsorbent Polymers (SAP) as Concrete Admixtures to Mitigate Autogenous Shrinkage*, Cement and Concrete Research.

Sellevold, E. J. & Bjøntegaard, Ø. (2006): *Coefficient of Thermal Expansion of Cement Paste and Concrete: Mechanisms of Moisture Interaction*, Material and Structures.

Shen, D., Jiang, J., Shen, J., Yao, P. & Jiang, G. (2015): *Influence of Curing Temperature on Autogenous Shrinkage and Cracking Resistance of High-Performance Concrete at an Early Age*, Construction and Building Materials.

Shibuya (2020): *Stand: TS-092(AB42) Motor: R1011/R1012*, Shibuya. `http://www.shibuya-group.co.jp/en/product/stand-ts-092ab42-motor-r1011r1012/`.

Shiotani, T., Bisschop, J. & van Mier, J. G. M. (2003): *Temporal and Spatial Development of Drying Shrinkage Cracking in Cement-based Materials*, Engineering Fracture Mechanics.

Silva, C. L., Galobardes, I., Pukadas, P., Monte, R., Figueiredo, A. D., Cavalaro, S. H. P. & Aguado, A. (2015): *Assessment of Fibre Content and Orientation in Steel Fibre Reinforced Concrete with the Inductive Method. Part 2: Application for the Quality Control of Sprayed Concrete*, International Symposium Non-Destructive Testing in Civil Engineering.

Sirajuddin, M. & Gettu, R. (2018): *Plastic Shrinkage Cracking of Concrete Incorporating Mineral Admixtures and its Mitigation*, Material and Structures.

Sivakumar, A. & Santhanam, M. (2007): *A Quantitive study on the Plastic Shrinkage Cracking in High Strength Hybrid Fibre Reinforced Concrete*, Cement & Concrete Composites.

Sjölander, A. & Ansell, A. (2017): *Numerical Simulations of Restrained Shrinkage Cracking in Glass Fibre Reinforced Shotcrete Slabs*, Advances in Civil Engineering.

Son, M. (2013): *Adhesion Strength at the Shotcrete-Rock Contact in Rock Tunneling*, Rock Mechanics and Rock Engineering.

Steinstø, E. & Hetlebakke, J.-E. (2020): *Nordøyvegen*, Entreprenørservice. `https://www.entreprenorservice.no/nordyvegen`.

Tao, Z. & Weizu, Q. (2005): *Tensile Creep due to Restraining Stresses in High-Strength Concrete at Early Ages*, Cement and Concrete Research.

Tatnall, P. C. (2002): *Shotcrete in Fires: Effects of Fibers on Explosive Spalling*, Shotcrete.

Tatro, S. B. (2006): *Significance of Tests and Properties of Concrete & Concrete-Making Materials: Chapter 22 - Thermal Properties*, ASTM International.

Thue, J. V. (2019): *Betong*, Store norske leksikon.

Topçu, İ. B. & Bilir, T. (2010): *Experimental Investigation of Drying Shrinkage Cracking of Composite Mortars Incorporating Crushed Tile Fine Aggregate*, Materials and Design.

TRB (2006): *Control of Cracking in Concrete: State of the Art*, Transportation Research Circular.

Vassenden, S. (2019): *Rock Breaking Under Rolling TBM Disc Cutters in Hard Rock Conditions - Visualization and Documentation of Cracks*, NTNU.

Vistnes, G., Li, C. C. & Larsen, T. (2020): *Bergmekanisk laboratorium*, NTNU. `https://www.ntnu.no/igp/lab/bergmekanisk`.

Vistnes, G., Nilsen, B. & Dahl, F. (2020): *Ingeniørgeologisk laboratorium*, NTNU. `https://www.ntnu.no/igp/lab/inggeologi`.

Wu, K.-R., Chen, B., Yao, W. & Zhang, D. (2001): *Effect of Coarse Aggregate Type on Mechanical Properties of High-Strength Concrete*, Cement and Concrete Research.

Wu, L., Farzadnia, N., Shi, C., Zhang, Z. & Wang, H. (2017): *Autogenous Shrinkage of High Performance Concrete: A Review*, Construction and Building Materials.

Yoo, S. W., Kwon, S.-J. & Jung, S. H. (2012): *Analysis Technique for Autogenous Shrinkage in High Performance Concrete with Mineral and Chemical Admixtures*, Construction and Building Materials.

Zhang, P., Li, D., Qiao, Y., Zhang, S., Sun, C. & Zhao, T. (2018): *Effect of Air Entrainment on the Mechanical Properties, Chloride Migration, and Microstructure of Ordinary Concrete and Fly Ash Concrete*, Journal of Materials in Civil Engineering.

Zhang, W., Zakaria, M. & Hama, Y. (2013): *Influence of Aggregate Materials Characteristics on the Drying Shrinkage Properties of Mortar and Concrete*, Construction and Building Materials.

Zohuriaan-Mehr, M. J. & Kabiri, K. (2008): *Superabsorbent Polymer Materials: A Review*, Iranian Polymer Journal.

# Appendix

# A Exposure Classes

**Table 17:** Exposure classes in NS-EN 206-1. Modified from Jacobsen et al. (2015).

| Class Designation | Description of environment | Informative examples where exposure classes may occur |
|---|---|---|
| **1 No risk of corrosion or attack** | | |
| X0 | For concrete without reinforcement or embedded metal: All exposures except where there is freeze/thaw, abrasion or chemical attack. For concrete with reinforcement or embedded metal: Very dry. | Concrete inside buildings with very low air humidity |
| **2 Corrosion induced by carbonation** | | |
| Where concrete containing reinforcement or other embedded metal is exposed to air and moisture, the exposure shall be classified as follows: NOTE The moisture condition relates to that in the concrete cover to reinforcement or embedded metal, but in many cases, conditions in the concrete cover can be taken as reflecting that in the surrounding environment. In these cases classification of the surrounding environment may be adequate. This may not be the case if there is a barrier beween the concrete and its environment. | | |
| XC1 | Dry or permanently wet | Concrete inside buildings with low air humidity. Concrete permanently submerged in water. |
| XC2 | Wet, rarely dry | Concrete surfaces subjected to long-term water contact. Foundations |
| XC3 | Moderate humidity | Concrete inside buildings with moderate or high humidity. External concrete sheltered from rain. |
| XC4 | Cyclic wet and dry | Concrete surfaces subjected to water contact, not within exposure class XC2. |

| | | |
|---|---|---|
| **3 Corrosion induced by chlorides other than from sea water** | | |
| Where concrete containing reinforcement or other embedded metal is subjected to contact with water containing chlorides, including de-icing salts, from sources other than from sea water, the exposure shall be classified as follows: | | |
| XD1 | Moderate humidity | Concrete surfaces exposed to airborne chlorides, but not direct spray. |
| XD2 | Wet, rarely dry | Concrete exposed to industrial waters containing chlorides.<br>Swimming pools. |
| XD3 | Cyclic wet and dry | Parts of bridges and road pavements that might be in contact with de-icing salts.<br>Parts of parking structures that might be in contact with de-icing salts (floor slabs, lower parts of walls and columns) |
| **4 Corrosion induced by chlorides from sea water** | | |
| Where concrete containing reinforcement or other embedded metal is subjected to contact with chlorides from sea water or air carrying salt originating from sea water, the exposure shall be classified as follows: | | |
| XS1 | Exposed to airborne salt but not in direct contact with sea water | Surface near to or on the coast |
| XS2 | Permanently submerged | Parts of marine structures |
| XS3 | Tidal, splash and spray zones | Parts of marine structures |
| **5 Freeze/thaw attack** | | |
| Where concrete is exposed to significant attack by freeze/thaw cycles whilst wet, the exposure shall be classified as follows: | | |
| XF1 | Moderate water saturation, without de-icing agent | Vertical concrete surfaces exposed to rain and freezing. |
| XF2 | Moderate water saturation, with de-icing agent | Vertical concrete surfaces of road structures exposed to freezing and airborne de-icing agents. |
| XF3 | High water saturation, without de-icing agent | Horizontal concrete surfaces exposed to freezing in wet condition. |
| XF4 | High water saturation, with de-icing agent or sea water | Road and bridge decks exposed to de-icing agents.<br>Concrete surfaces exposed to direct spray containing de-icing agents and freezing.<br>Splash zone of marine structures exposed to freezing. |

<table>
<tr><td colspan="3">6 Chemical attack</td></tr>
<tr><td colspan="3">Where concrete is exposed to chemical attack from natural soils and ground water as given in table 2, the exposure shall be classified as given below. The classification of seawater depends on the geographical location; therefor the classification valid in the place of use of the concrete applies.<br>NOTE<br>Special study may be needed to establish the relevant exposure condition where there is:<br>1) limits outside of table 2 (NS-EN 206-1);<br>2) other aggressive chemicals;<br>3) chemically polluted ground water;<br>4) high water velocity in combination with the chemicals in table 2 (NS-EN 206-1).</td></tr>
<tr><td>XA1</td><td>Slightly aggressive chemical environment according to table 2 (NS-EN 206-1)</td><td rowspan="3">Concentration given in table 2 (NS-EN 206-1), can not be used for choice of durability class for other situations than exposure in natural soil and ground water. Such situations shall be considered separately.</td></tr>
<tr><td>XA2</td><td>Moderately aggressive chemical environment according to table 2 (NS-EN 206-1)</td></tr>
<tr><td>XA3</td><td>Highly aggressive chemical environment according to table 2 (NS-EN 206-1)</td></tr>
<tr><td colspan="3">7 Chemical attack from agricultural fertilizers</td></tr>
<tr><td colspan="3">Where concrete is exposed to chemical attack from fertilizers in the agricultural industry.</td></tr>
<tr><td>XA4</td><td>Structures in contact with fertilizers from animals (manure)</td><td>The class includes structures like floor decks and slates in cow sheds and containments for maure etc.</td></tr>
<tr><td colspan="3">8 Specially aggressive environment</td></tr>
<tr><td>XSA</td><td>Structures exposed to strong chemical attack, but not covered by the other exposure classes and where special protection is needed. This might result in special composed concrete, membranes or similar.</td><td>The class includes structures in contact with liquids with low pH-values like for instance silos for ensiled grass (agricultural industry) and alum shale.</td></tr>
</table>

# B Rock Mass Classification Tables

| 1 | RQD (Rock Quality Designation) | | RQD |
|---|---|---|---|
| A | Very poor | (> 27 joints per $m^3$ ) | 0-25 |
| B | Poor | (20-27 joints per $m^3$) | 25-50 |
| C | Fair | (13-19 joints per $m^3$ ) | 50-75 |
| D | Good | (8-12 joints per $m^3$ ) | 75-90 |
| E | Excellent | (0-7 joints per $m^3$ ) | 90-100 |

Note: i) Where RQD is reported or measured as ≤ 10 (including 0) the value 10 is used to evaluate the Q-value
ii) RQD-intervals of 5, i.e. 100, 95, 90, etc., are sufficiently accurate

**Figure 48:** RQD-values and joints per $m^3$. Taken from NGI (2015).

| 2 | Joint set number | $J_n$ |
|---|---|---|
| A | Massive, no or few joints | 0.5-1.0 |
| B | One joint set | 2 |
| C | One joint set plus random joints | 3 |
| D | Two joint sets | 4 |
| E | Two joint sets plus random joints | 6 |
| F | Three joint sets | 9 |
| G | Three joint sets plus random joints | 12 |
| H | Four or more joint sets, random heavily jointed "sugar cube", etc | 15 |
| J | Crushed rock, earth like | 20 |

Note: i) For tunnel intersections, use 3 x $J_n$
ii) For portals, use 2 x $J_n$

**Figure 49:** $J_n$-values. Taken from NGI (2015).

| 3 Joint Roughness Number | | $J_r$ |
|---|---|---|
| ***a)*** *Rock-wall contact, and*<br>***b)*** *Rock-wall contact before 10 cm of shear movement* | | |
| A | Discontinuous joints | 4 |
| B | Rough or irregular, undulating | 3 |
| C | Smooth, undulating | 2 |
| D | Slickensided, undulating | 1.5 |
| E | Rough, irregular, planar | 1.5 |
| F | Smooth, planar | 1 |
| G | Slickensided, planar | 0.5 |
| Note: i) Description refers to small scale features and intermediate scale features, in that order | | |
| ***c)*** *No rock-wall contact when sheared* | | |
| H | Zone containing clay minerals thick enough to prevent rock-wall contact when sheared | 1 |
| Note: ii) Add 1 if the mean spacing of the relevant joint set is greater than 3 m (dependent on the size of the underground opening)<br>iii) $J_r$ = 0.5 can be used for planar slickensided joints having lineations, provided the lineations are oriented in the estimated sliding direction | | |

**Figure 50:** $J_r$-values. Taken from NGI (2015).

| 4 | Joint Alteration Number | $\Phi_r$ approx. | $J_a$ |
|---|---|---|---|
| ***a)*** *Rock-wall contact (no mineral fillings, only coatings)* | | | |
| A | Tightly healed, hard, non-softening, impermeable filling, i.e., quartz or epidote. | | 0.75 |
| B | Unaltered joint walls, surface staining only. | 25-35° | 1 |
| C | Slightly altered joint walls. Non-softening mineral coatings; sandy particles, clay-free disintegrated rock, etc. | 25-30° | 2 |
| D | Silty or sandy clay coatings, small clay fraction (non-softening). | 20-25° | 3 |
| E | Softening or low friction clay mineral coatings, i.e., kaolinite or mica. Also chlorite, talc gypsum, graphite, etc., and small quantities of swelling clays. | 8-16° | 4 |
| ***b)*** *Rock-wall contact before 10 cm shear (thin mineral fillings)* | | | |
| F | Sandy particles, clay-free disintegrated rock, etc. | 25-30° | 4 |
| G | Strongly over-consolidated, non-softening, clay mineral fillings (continuous, but <5 mm thickness). | 16-24° | 6 |
| H | Medium or low over-consolidation, softening, clay mineral fillings (continuous, but <5 mm thickness). | 12-16° | 8 |
| J | Swelling-clay fillings, i.e., montmorillonite (continuous, but <5 mm thickness). Value of $J_a$ depends on percent of swelling clay-size particles. | 6-12° | 8-12 |
| ***c)*** *No rock-wall contact when sheared (thick mineral fillings)* | | | |
| K | Zones or bands of disintegrated or crushed rock. Strongly over-consolidated. | 16-24° | 6 |
| L | Zones or bands of clay, disintegrated or crushed rock. Medium or low over-consolidation or softening fillings. | 12-16° | 8 |
| M | Zones or bands of clay, disintegrated or crushed rock. Swelling clay. $J_a$ depends on percent of swelling clay-size particles. | 6-12° | 8-12 |
| N | Thick continuous zones or bands of clay. Strongly over-consolidated. | 12-16° | 10 |
| O | Thick, continuous zones or bands of clay. Medium to low over-consolidation. | 12-16° | 13 |
| P | Thick, continuous zones or bands with clay. Swelling clay. $J_a$ depends on percent of swelling clay-size particles. | 6-12° | 13-20 |

**Figure 51:** $J_a$-values. Taken from NGI (2015).

| 5 | Joint Water Reduction Factor | $J_w$ |
|---|---|---|
| A | Dry excavations or minor inflow ( humid or a few drips) | 1.0 |
| B | Medium inflow, occasional outwash of joint fillings (many drips/"rain") | 0.66 |
| C | Jet inflow or high pressure in competent rock with unfilled joints | 0.5 |
| D | Large inflow or high pressure, considerable outwash of joint fillings | 0.33 |
| E | Exceptionally high inflow or water pressure decaying with time. Causes outwash of material and perhaps cave in | 0.2-0.1 |
| F | Exceptionally high inflow or water pressure continuing without noticeable decay. Causes outwash of material and perhaps cave in | 0.1-0.05 |

Note: i) Factors C to F are crude estimates. Increase $J_w$ if the rock is drained or grouting is carried out

ii) Special problems caused by ice formation are not considered

**Figure 52:** $J_w$-values. Taken from NGI (2015).

| 6 Stress Reduction Factor | | | | SRF |
|---|---|---|---|---|
| ***a)*** *Weak zones intersecting the underground opening, which may cause loosening of rock mass* | | | | |
| A | Multiple occurrences of weak zones within a short section containing clay or chemically disintegrated, very loose surrounding rock (any depth), or long sections with incompetent (weak) rock (any depth). For squeezing, see 6L and 6M | | | 10 |
| B | Multiple shear zones within a short section in competent clay-free rock with loose surrounding rock (any depth) | | | 7.5 |
| C | Single weak zones with or without clay or chemical disintegrated rock (depth ≤ 50m) | | | 5 |
| D | Loose, open joints, heavily jointed or "sugar cube", etc. (any depth) | | | 5 |
| E | Single weak zones with or without clay or chemical disintegrated rock (depth > 50m) | | | 2.5 |
| Note: i) Reduce these values of SRF by 25-50% if the weak zones only influence but do not intersect the underground opening | | | | |
| ***b)*** *Competent, mainly massive rock, stress problems* | | $\sigma_c / \sigma_1$ | $\sigma_\theta / \sigma_c$ | SRF |
| F | Low stress, near surface, open joints | >200 | <0.01 | 2.5 |
| G | Medium stress, favourable stress condition | 200-10 | 0.01-0.3 | 1 |
| H | High stress, very tight structure. Usually favourable to stability. May also be unfavourable to stability dependent on the orientation of stresses compared to jointing/weakness planes* | 10-5 | 0.3-0.4 | 0.5-2<br>2-5* |
| J | Moderate spalling and/or slabbing after > 1 hour in massive rock | 5-3 | 0.5-0.65 | 5-50 |
| K | Spalling or rock burst after a few minutes in massive rock | 3-2 | 0.65-1 | 50-200 |
| L | Heavy rock burst and immediate dynamic deformation in massive rock | <2 | >1 | 200-400 |
| Note: ii) For strongly anisotropic virgin stress field (if measured): when $5 \le \sigma_1 / \sigma_3 \le 10$, reduce $\sigma_c$ to $0.75\,\sigma_c$. When $\sigma_1 / \sigma_3 > 10$, reduce $\sigma_c$ to $0.5\,\sigma_c$, where $\sigma_c$ = unconfined compression strength, $\sigma_1$ and $\sigma_3$ are the major and minor principal stresses, and $\sigma_\theta$ = maximum tangential stress (estimated from elastic theory)<br>iii) When the depth of the crown below the surface is less than the span; suggest SRF increase from 2.5 to 5 for such cases (see F) | | | | |
| ***c)*** *Squeezing rock: plastic deformation in incompetent rock under the influence of high pressure* | | | $\sigma_\theta / \sigma_c$ | SRF |
| M | Mild squeezing rock pressure | | 1-5 | 5-10 |
| N | Heavy squeezing rock pressure | | >5 | 10-20 |
| Note: iv) Determination of squeezing rock conditions must be made according to relevant literature (i.e. Singh et al., 1992 and Bhasin and Grimstad, 1996) | | | | |
| ***d)*** *Swelling rock: chemical swelling activity depending on the presence of water* | | | | SRF |
| O | Mild swelling rock pressure | | | 5-10 |
| P | Heavy swelling rock pressure | | | 10-15 |

**Figure 53:** SRF-values. Taken from NGI (2015).

# C Dye Penetrant Testing

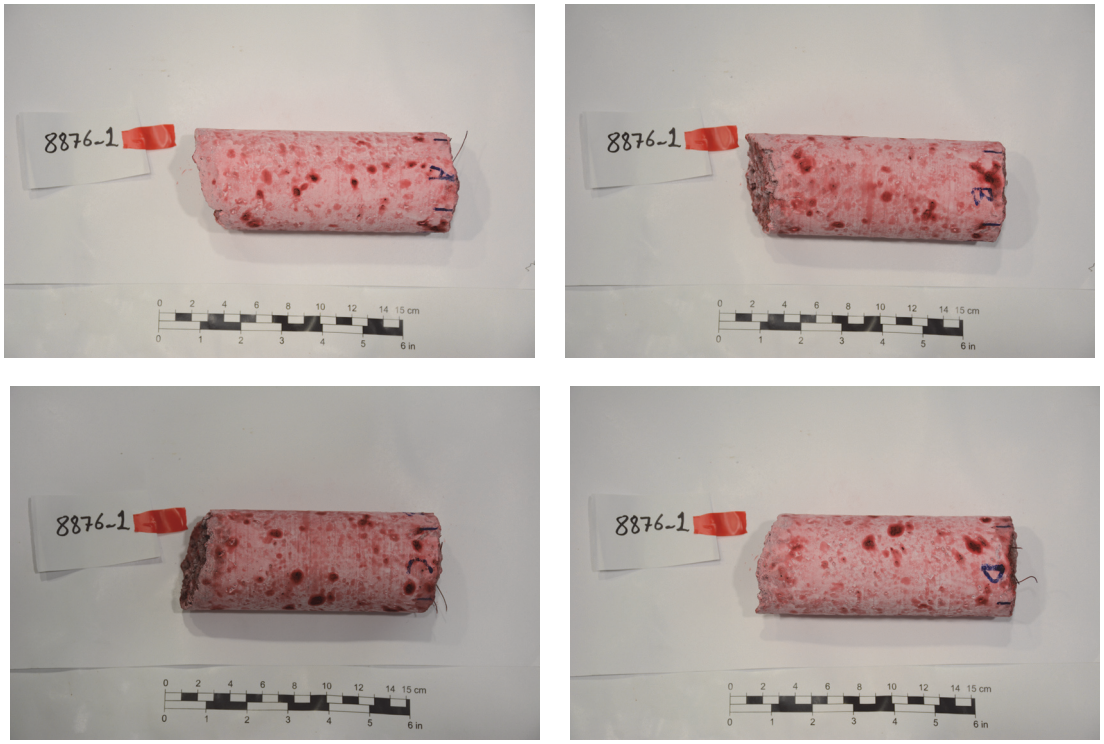


**Figure 54:** Dye penetrant test on sprayed concrete core 1 from profile number 23903.

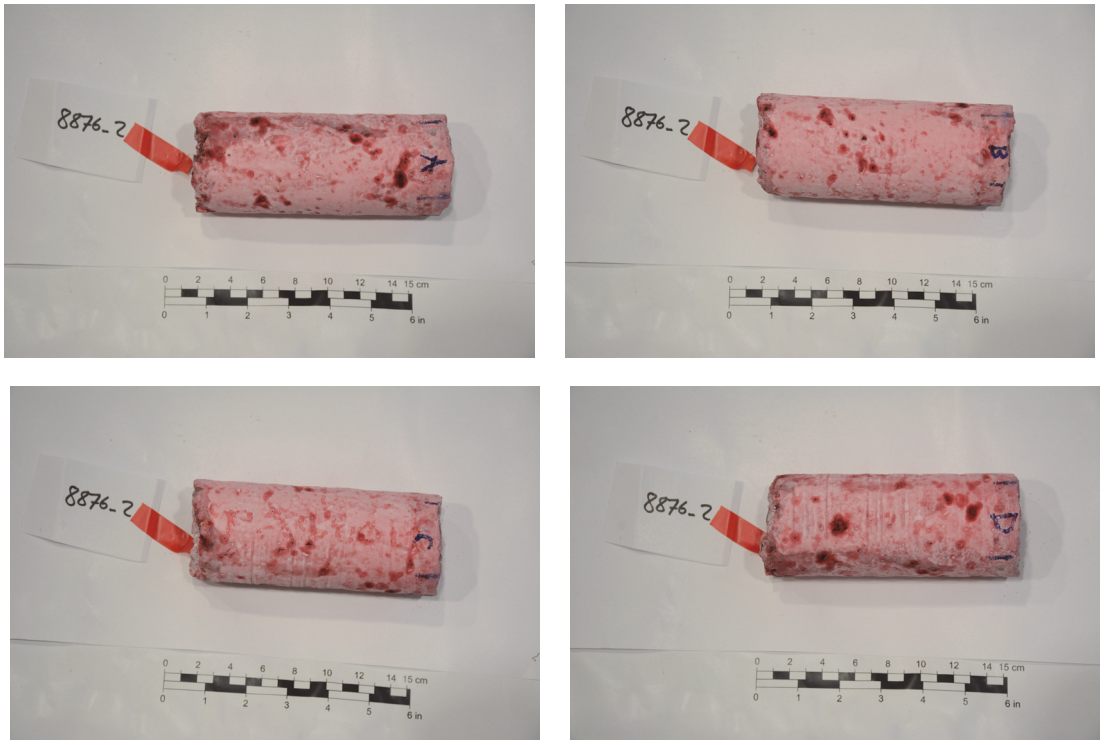


**Figure 55:** Dye penetrant test on sprayed concrete core 2 from profile number 23903.

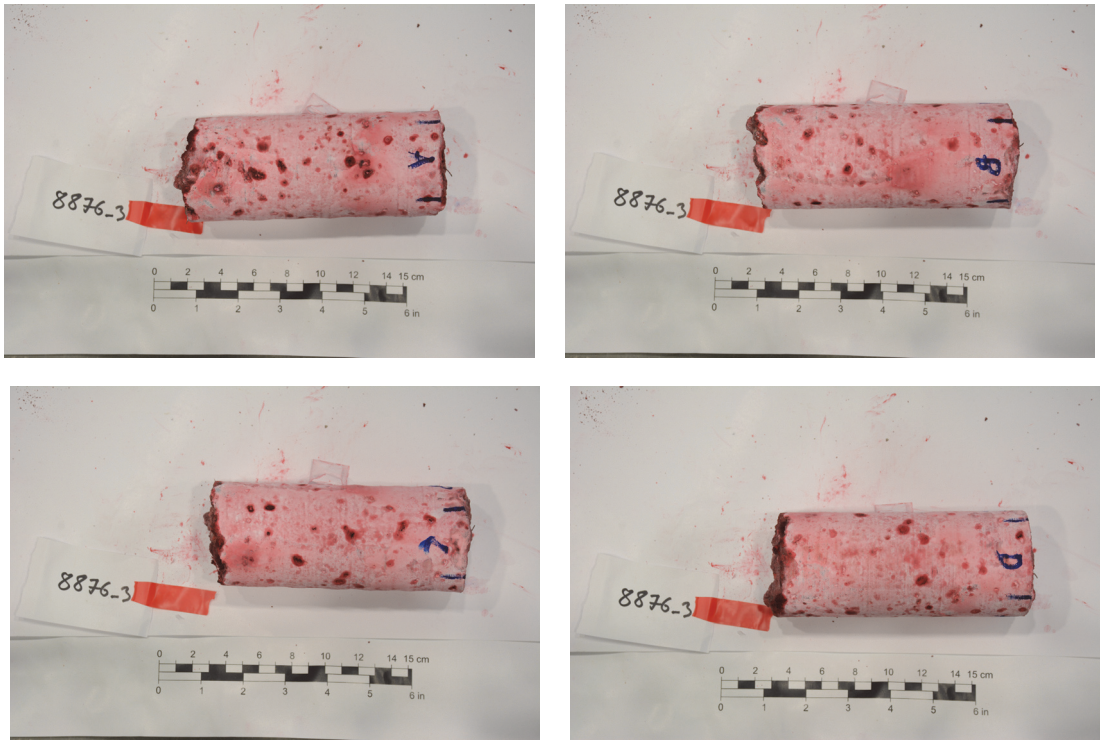


**Figure 56:** Dye penetrant test on sprayed concrete core 3 from profile number 23903.

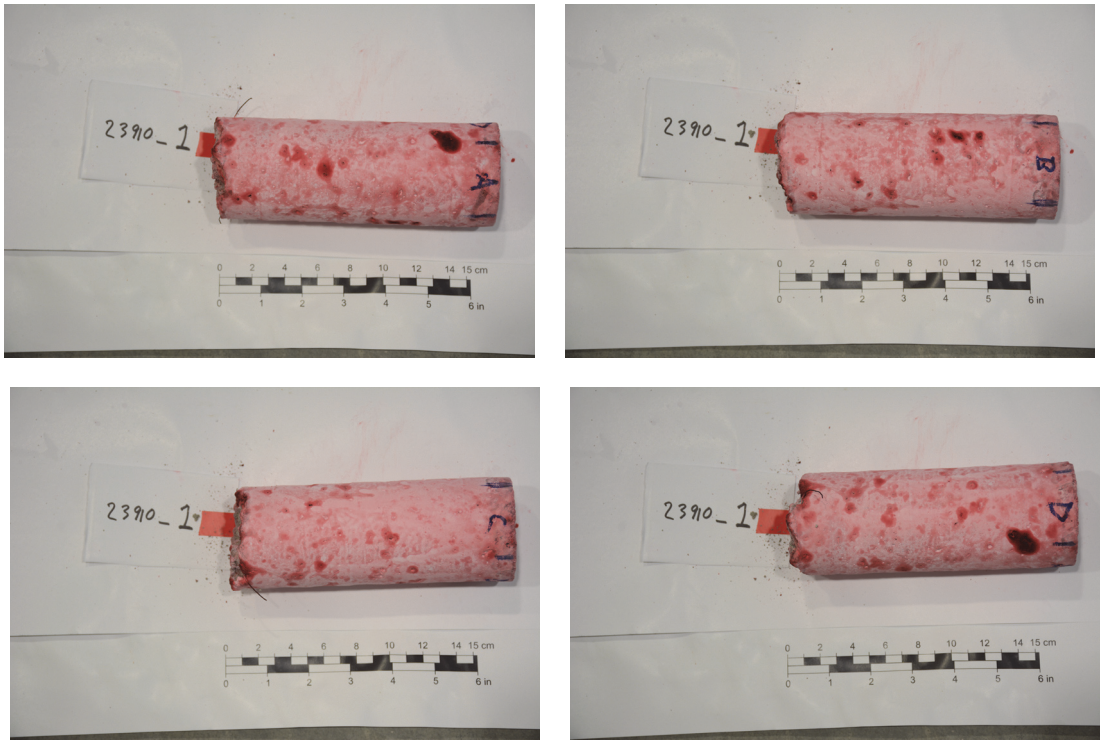


**Figure 57:** Dye penetrant test on sprayed concrete core 1 from profile number 23910.

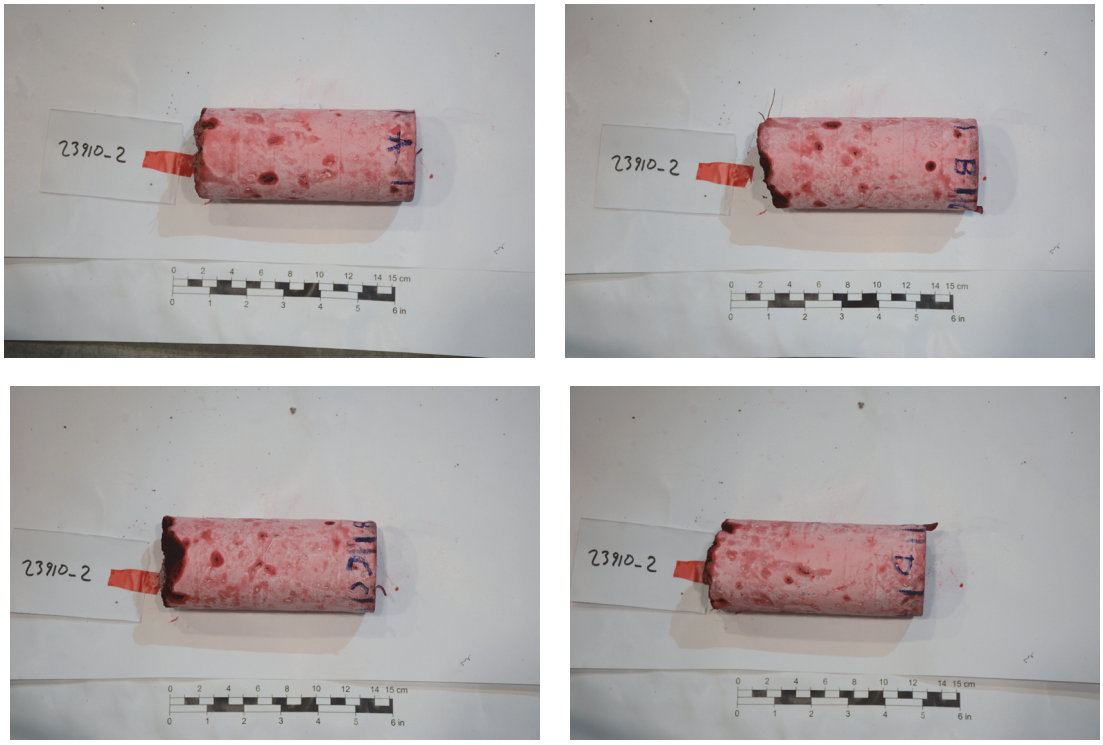


**Figure 58:** Dye penetrant test on sprayed concrete core 2 from profile number 23910.

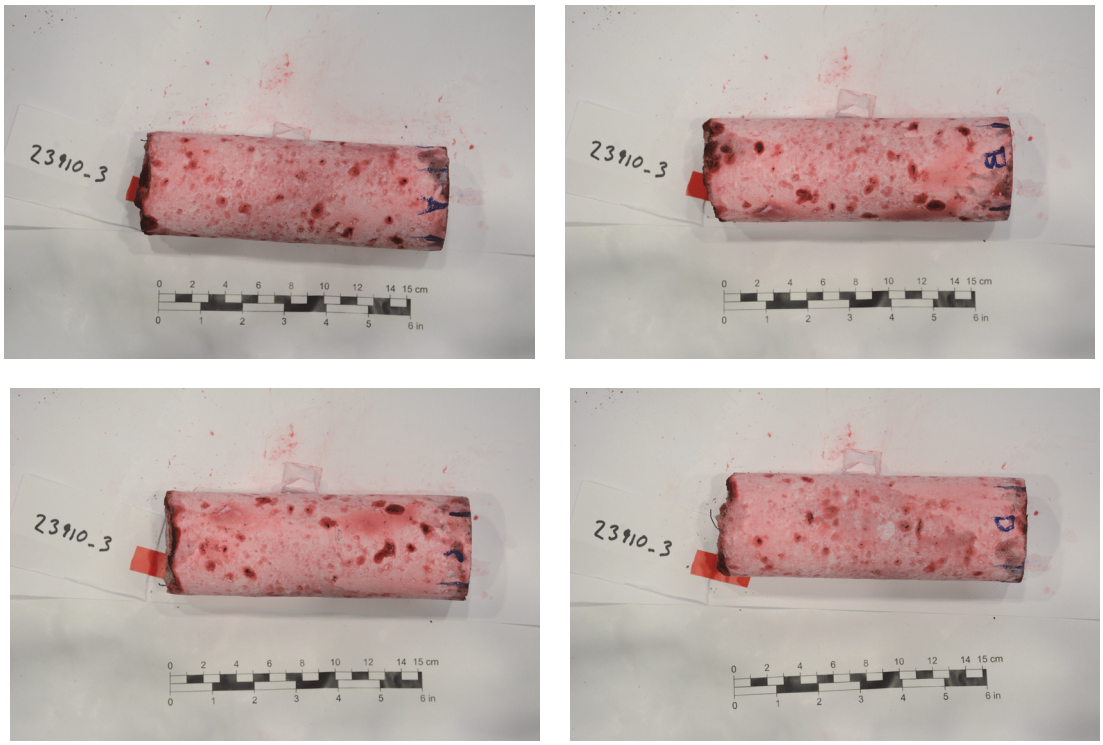


**Figure 59:** Dye penetrant test on sprayed concrete core 3 from profile number 23910.

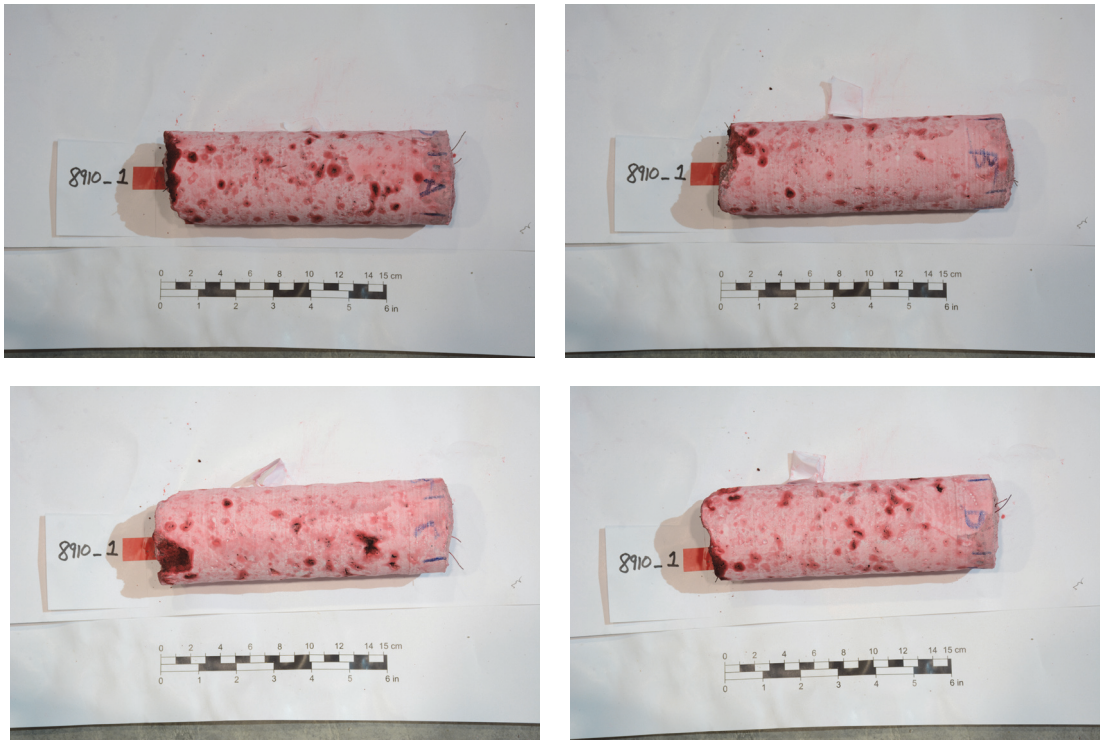


**Figure 60:** Dye penetrant test on sprayed concrete core 1 from profile number 23917.

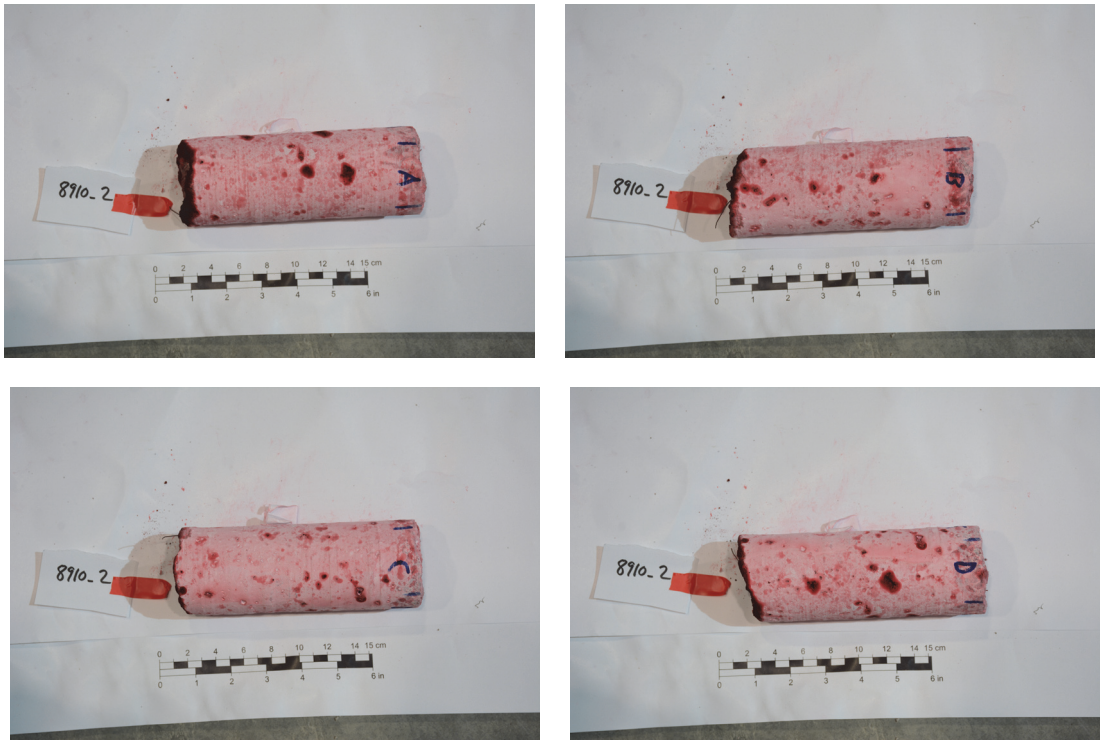


**Figure 61:** Dye penetrant test on sprayed concrete core 2 from profile number 23917.

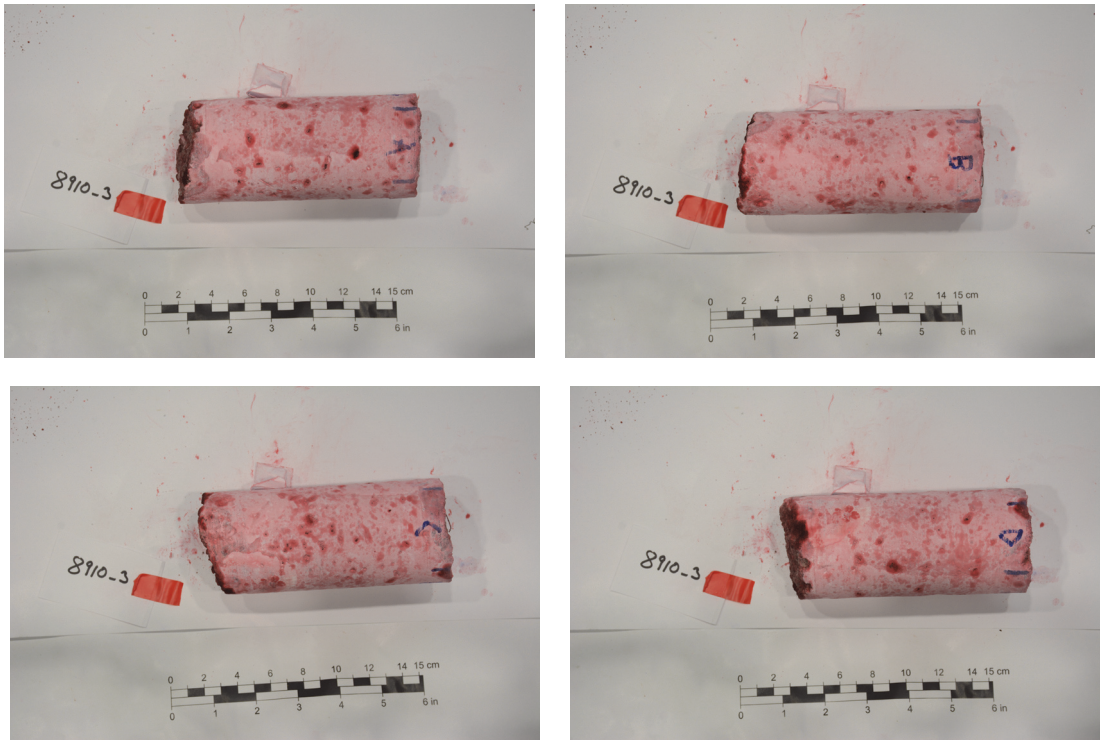


**Figure 62:** Dye penetrant test on sprayed concrete core 3 from profile number 23917.

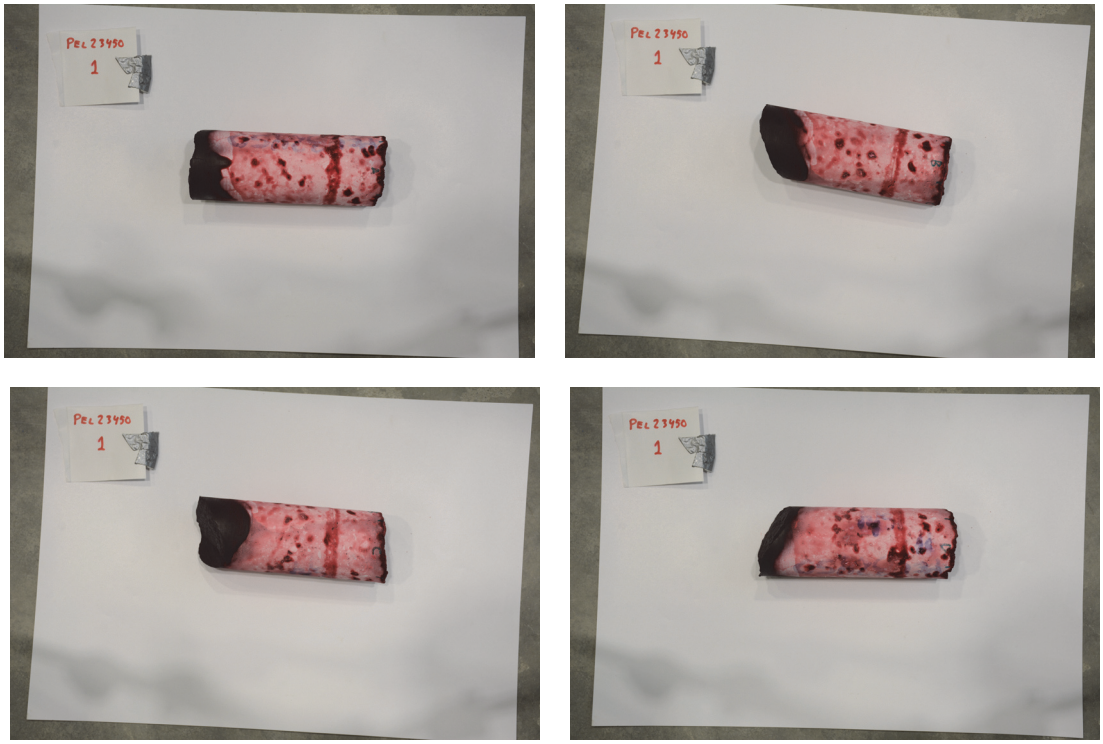


**Figure 63:** Dye penetrant test on sprayed concrete core 1 from profile number 32450.

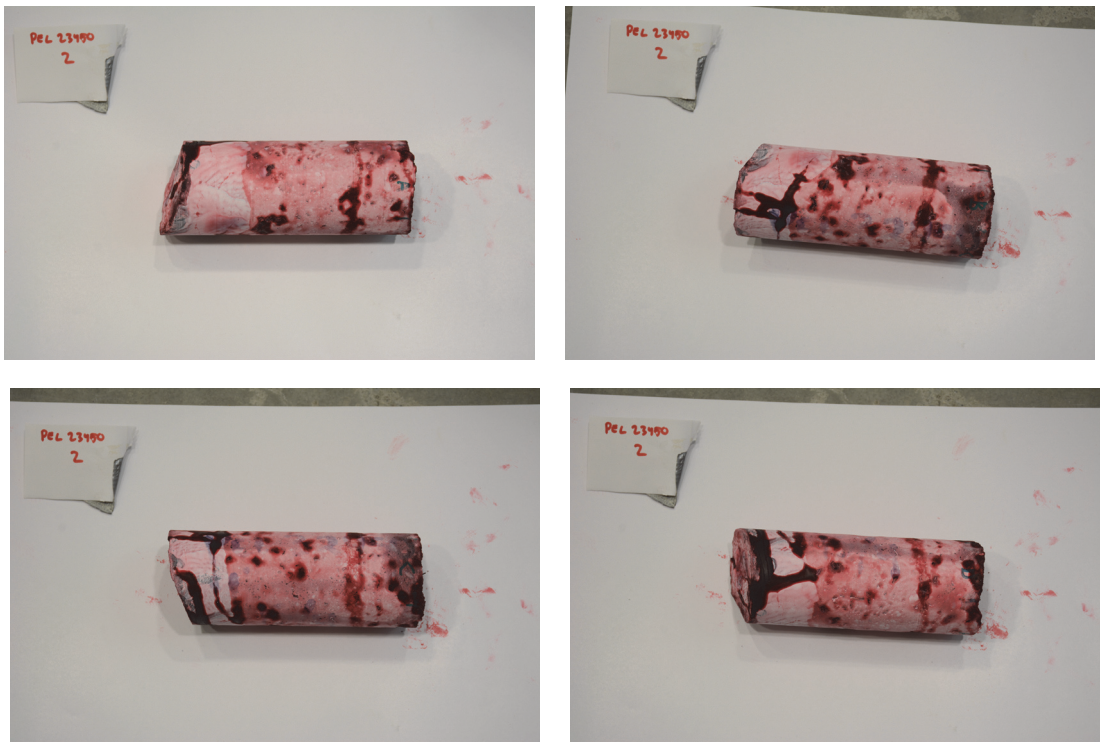


**Figure 64:** Dye penetrant test on sprayed concrete core 2 from profile number 32450.

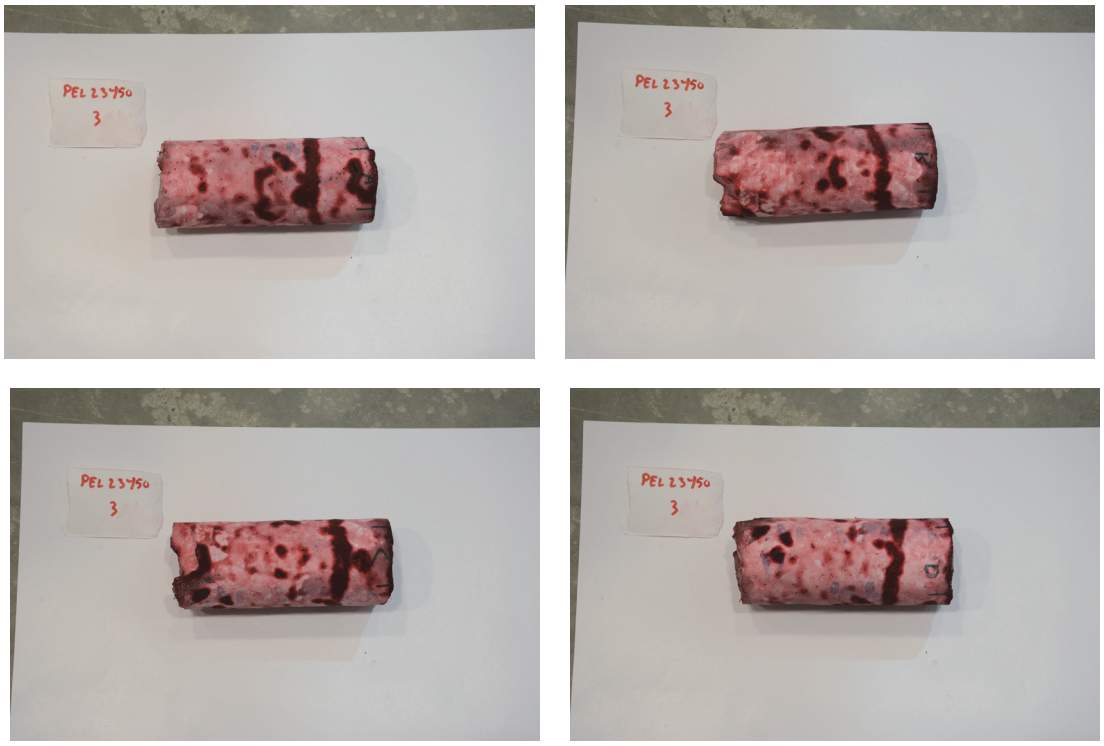


**Figure 65:** Dye penetrant test on sprayed concrete core 3 from profile number 32450.

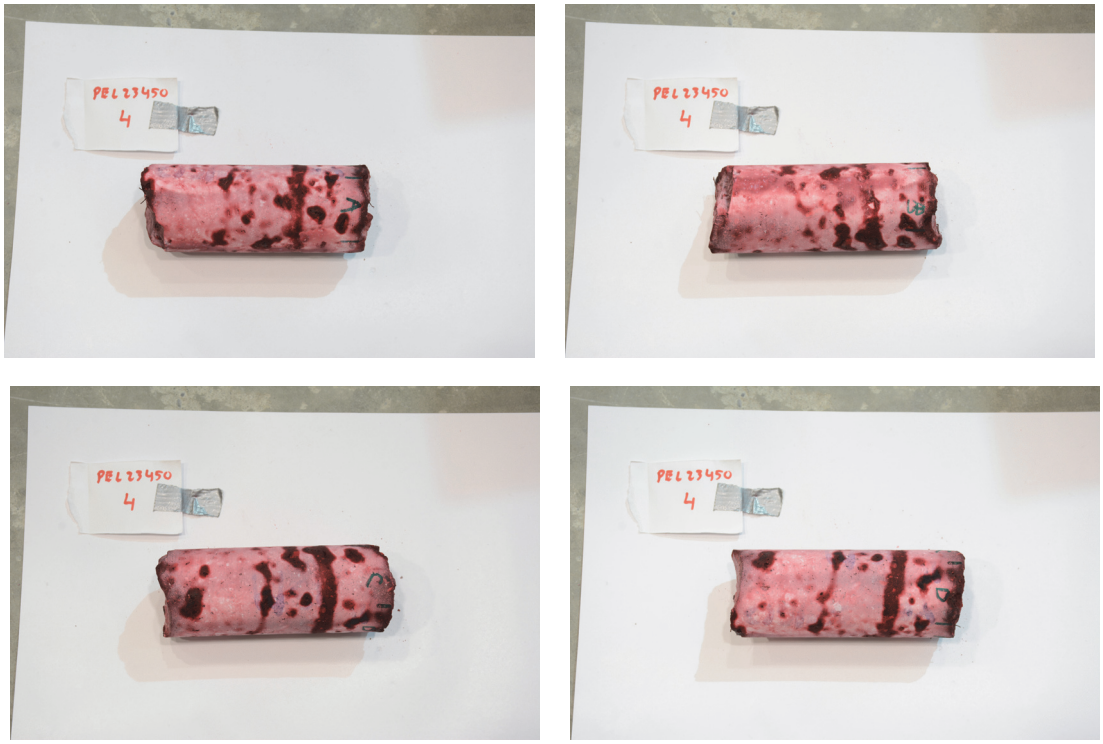


**Figure 66:** Dye penetrant test on sprayed concrete core 4 from profile number 32450.

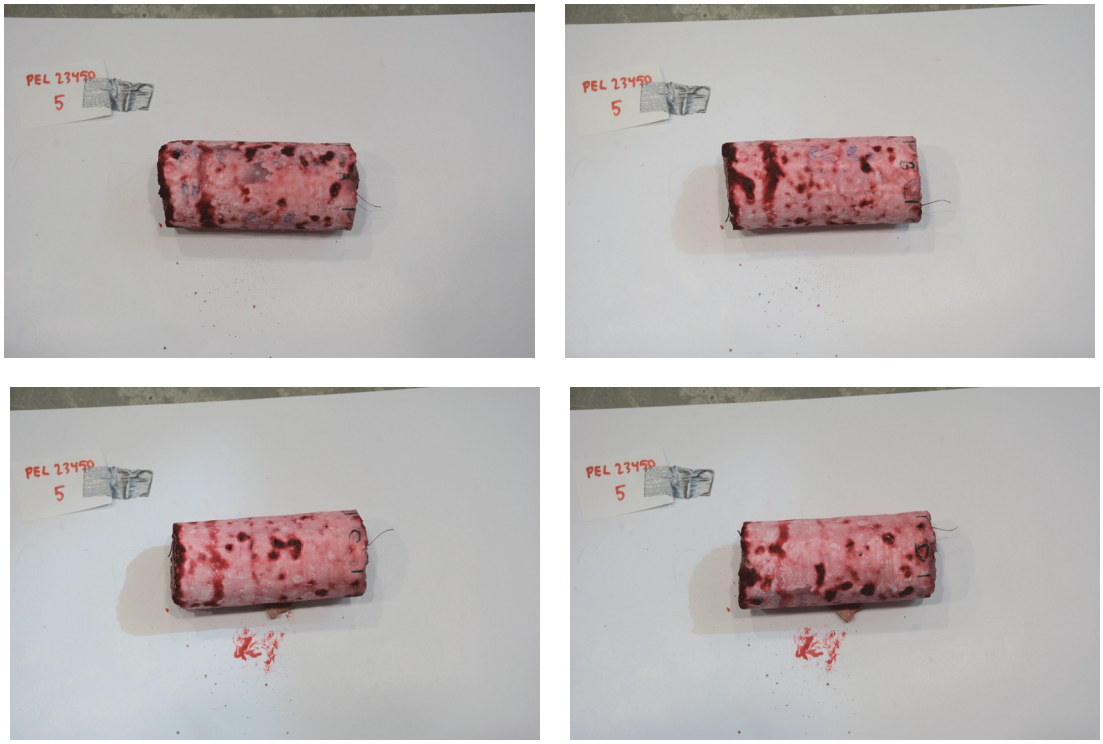


**Figure 67:** Dye penetrant test on sprayed concrete core 5 from profile number 32450.


**Figure 68:** Dye penetrant test on sprayed concrete core 1 from profile number 32500.


**Figure 69:** Dye penetrant test on sprayed concrete core 2 from profile number 32500.


**Figure 70:** Dye penetrant test on sprayed concrete core 3 from profile number 32500.

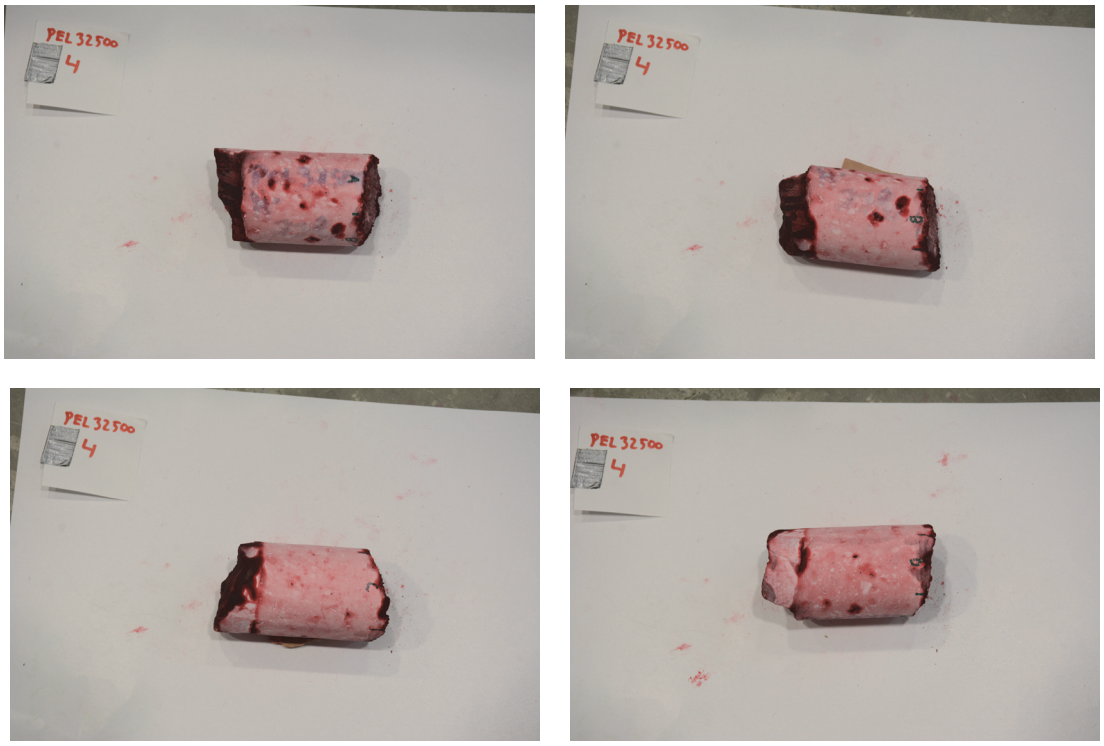


**Figure 71:** Dye penetrant test on sprayed concrete core 4 from profile number 32500.

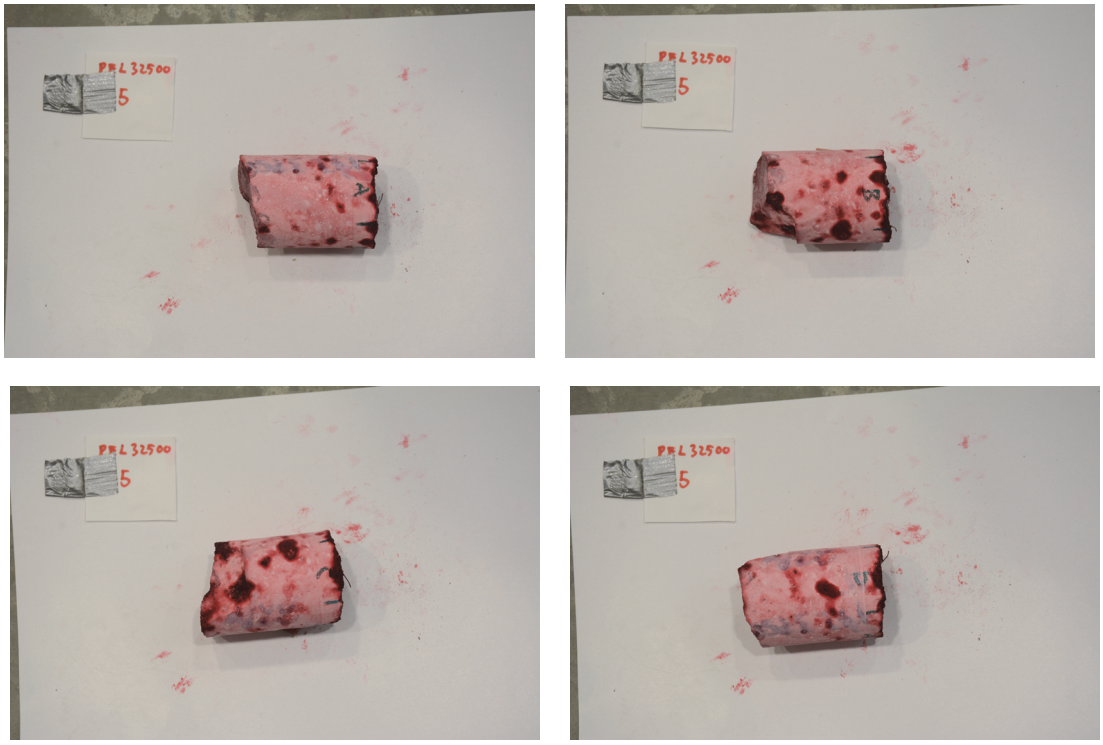


**Figure 72:** Dye penetrant test on sprayed concrete core 5 from profile number 32500.

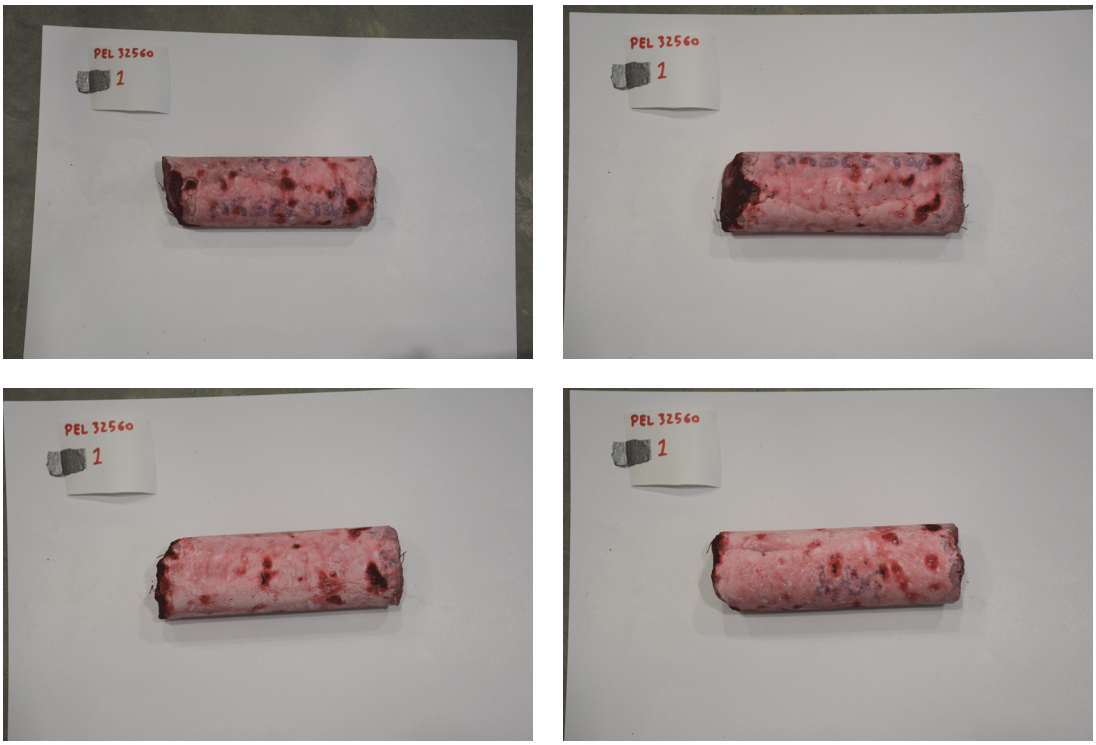


**Figure 73:** Dye penetrant test on sprayed concrete core 1 from profile number 32560.

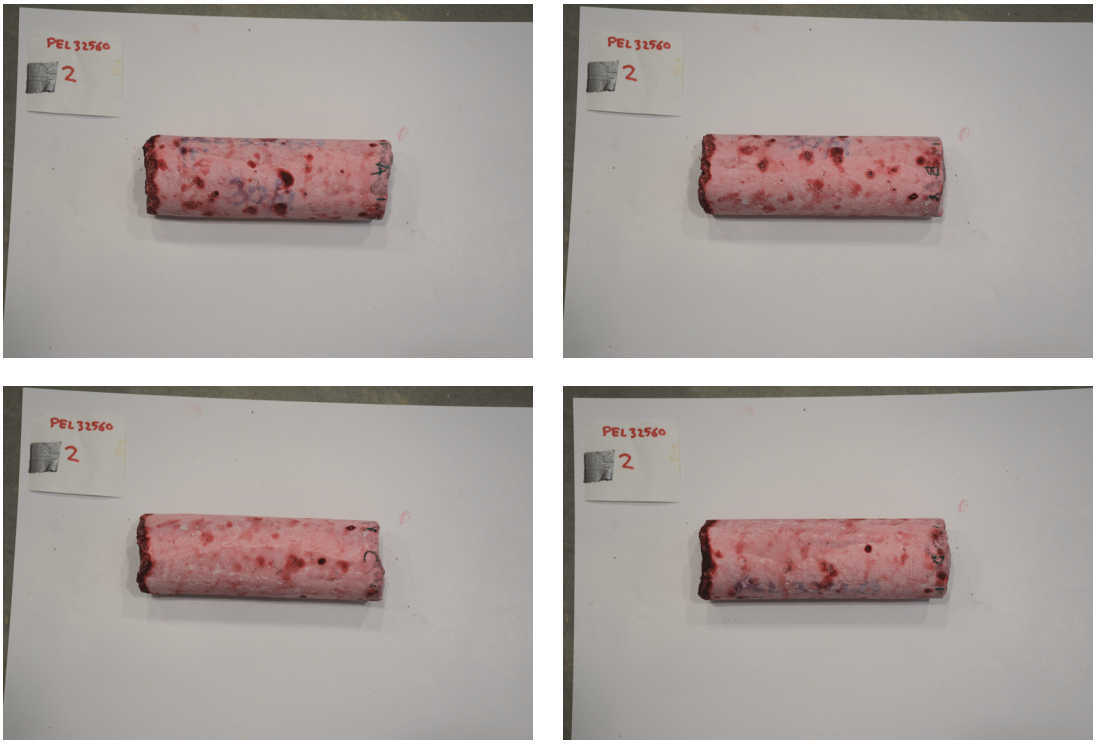


**Figure 74:** Dye penetrant test on sprayed concrete core 2 from profile number 32560.

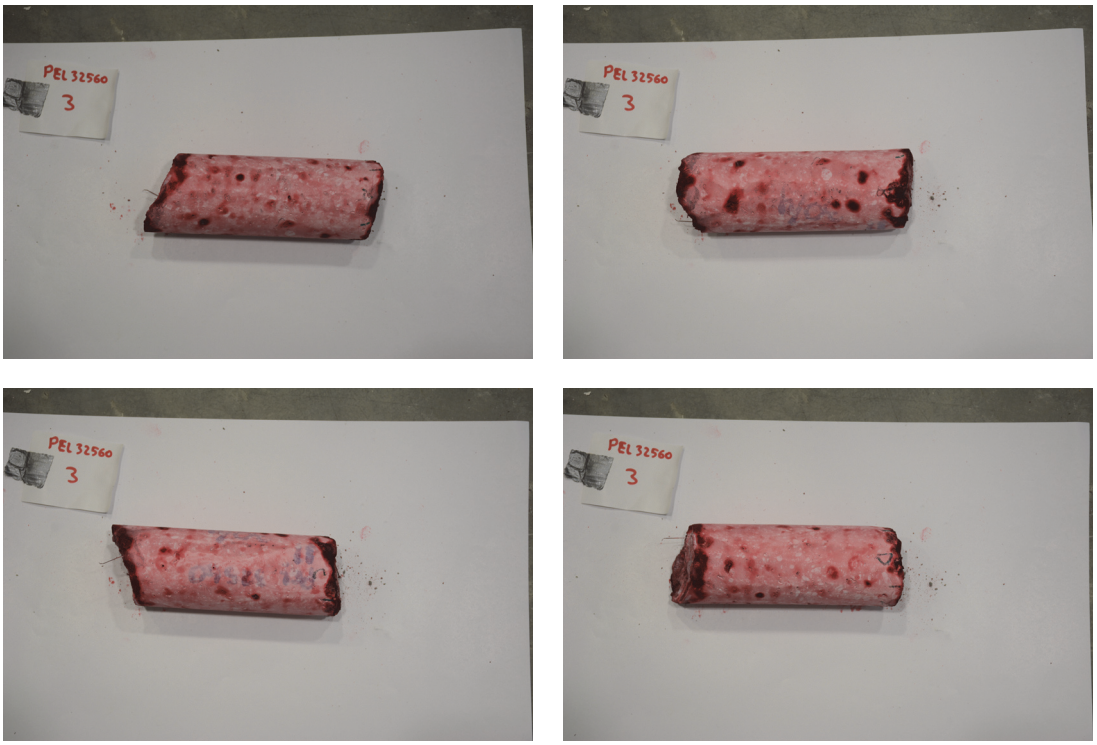


**Figure 75:** Dye penetrant test on sprayed concrete core 3 from profile number 32560.

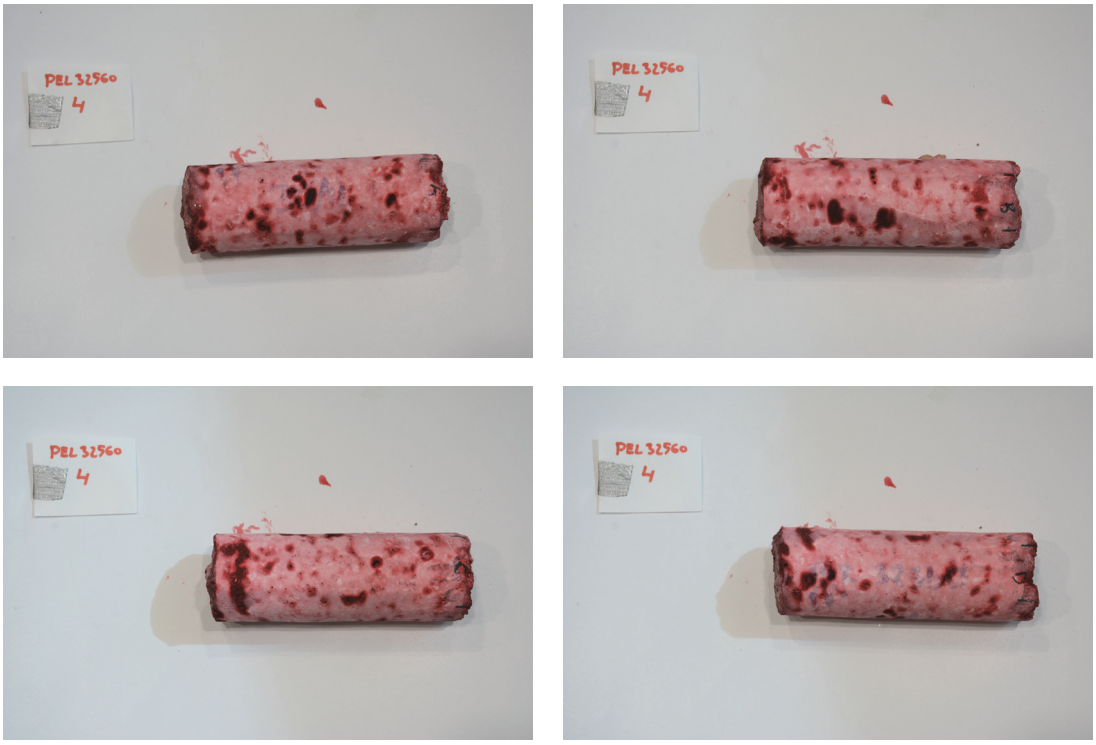


**Figure 76:** Dye penetrant test on sprayed concrete core 4 from profile number 32560.

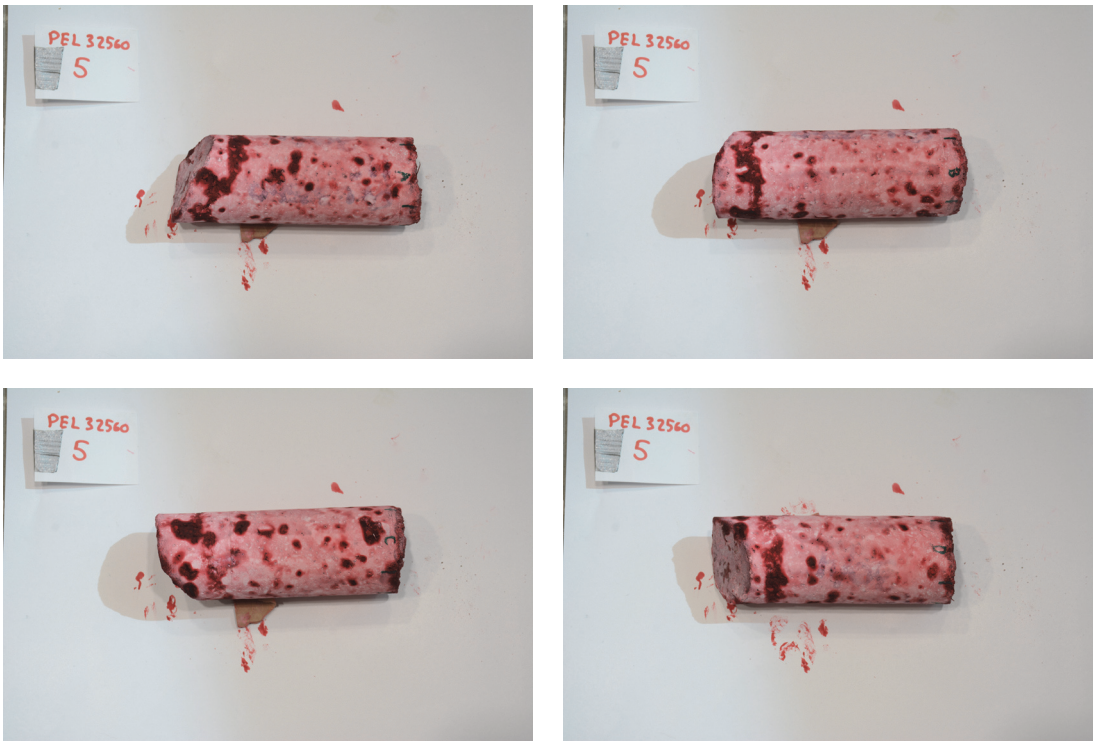


**Figure 77:** Dye penetrant test on sprayed concrete core 5 from profile number 32560.

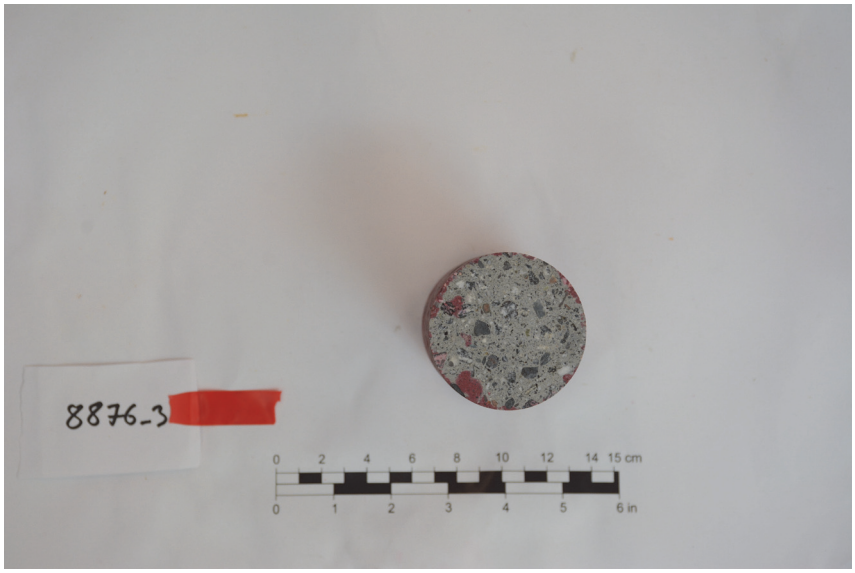


**Figure 78:** Penetration depth of dye on sprayed concrete core 3 from profile 23903.

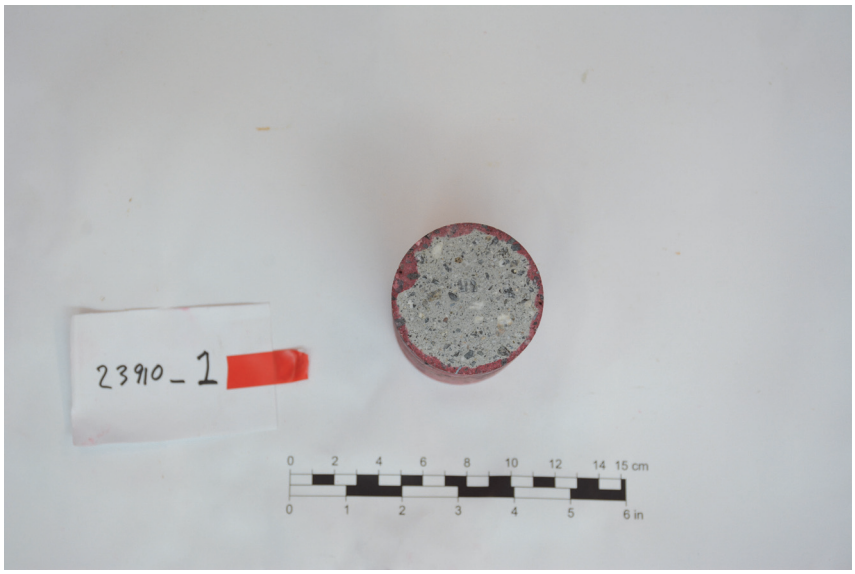


**Figure 79:** Penetration depth of dye on sprayed concrete core 1 from profile 23910.


**Figure 80:** Penetration depth of dye on sprayed concrete core 1 from profile 32500.

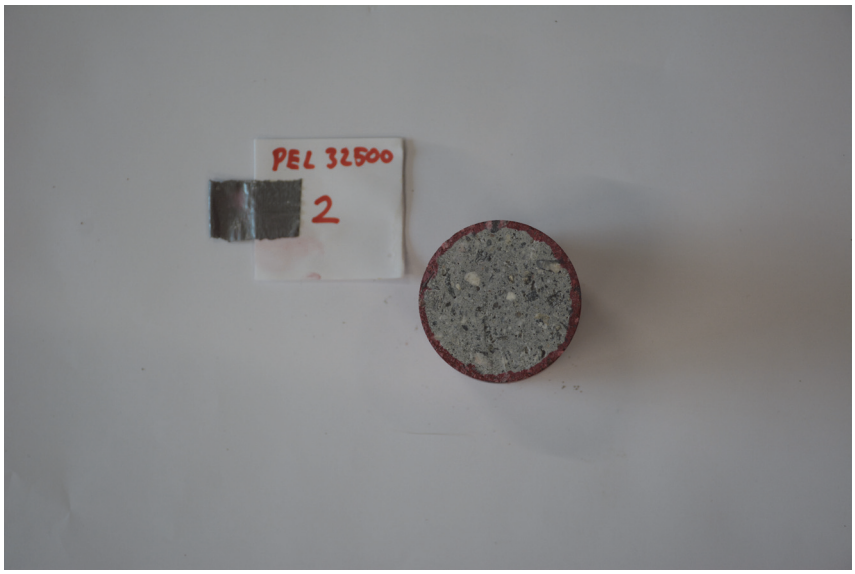


**Figure 81:** Penetration depth of dye on sprayed concrete core 2 from profile 32500.

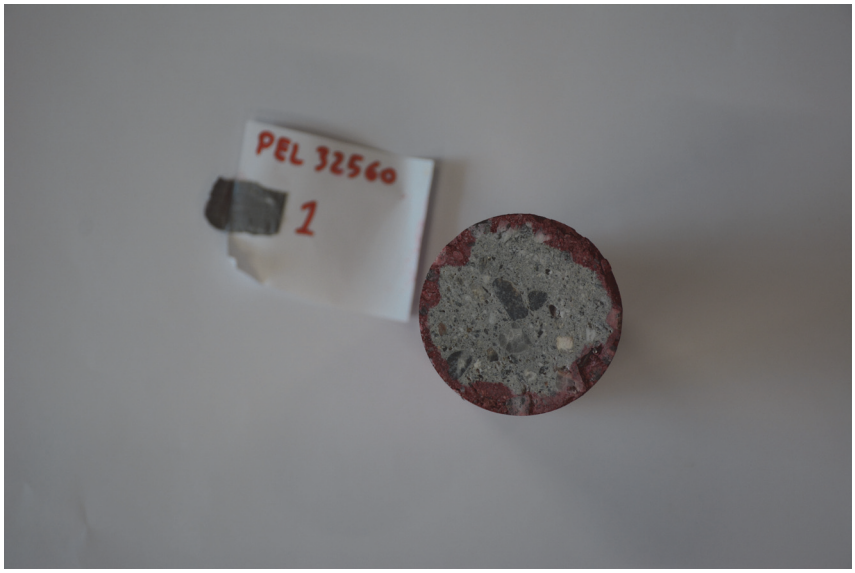


**Figure 82:** Penetration depth of dye on sprayed concrete core 1 from profile 32560.


**Figure 83:** Penetration depth of dye on sprayed concrete core 2 from profile 32560.

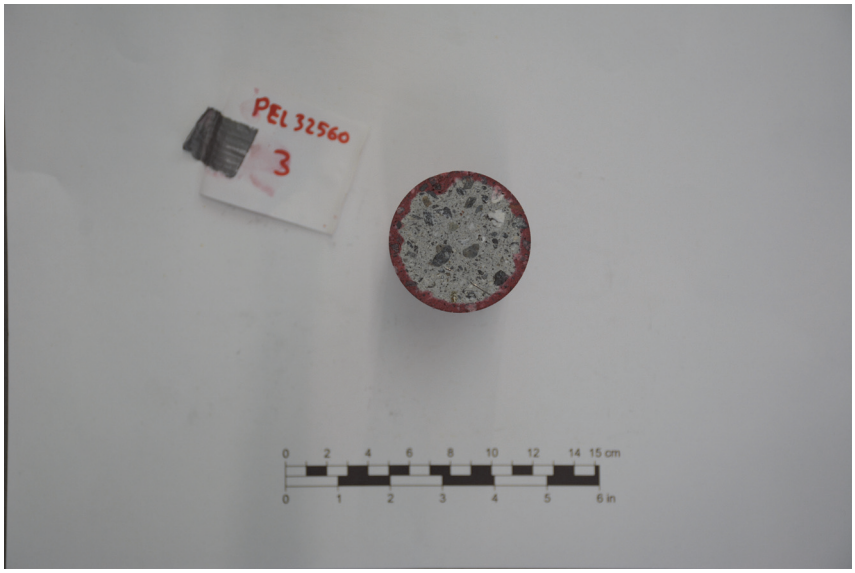


**Figure 84:** Penetration depth of dye on sprayed concrete core 3 from profile 32560.

# D Uniaxial Compressive Strength, Density and Fibre Content Testing

## D.1 Uniaxial Compressive Strength

**Table 18:** Dimensions and results from UCS testing of the cores from Longva.

| Profile nr. - sample nr. | Dimensions of sample | | Compressive strength | Slenderness (L/d) | Correction factor | Corrected cylinder comp. str. | Cube compressive strength | Age |
|---|---|---|---|---|---|---|---|---|
| | Diameter (mm) | Length (mm) | (MPa) | - | - | (MPa) | (MPa) | (days) |
| 23903 - 1 | 59.44 | 117.31 | 63.2 | 1.97 | 1.00 | 63.0 | 75.8 | 33 |
| 23903 - 2 | 59.45 | 120.66 | 58.7 | 2.03 | 1.00 | 58.7 | 70.8 | 33 |
| 23903 - 3 | 59.50 | 120.69 | 61.4 | 2.03 | 1.00 | 61.4 | 74.0 | 33 |
| 23903 - 4 | 59.56 | 113.95 | 61.9 | 1.91 | 0.99 | 61.4 | 74.0 | 33 |
| 23903 - 5 | 59.52 | 112.38 | 57.3 | 1.89 | 0.99 | 56.7 | 68.5 | 33 |
| 23910 - 1 | 59.44 | 120.34 | 66.4 | 2.02 | 1.00 | 66.4 | 79.8 | 32 |
| 23910 - 2 | 59.44 | 111.87 | 58.8 | 1.88 | 0.99 | 58.1 | 70.2 | 32 |
| 23910 - 3 | 59.53 | 120.37 | 67.6 | 2.02 | 1.00 | 67.6 | 81.2 | 32 |
| 23910 - 4 | 59.49 | 120.52 | 62.4 | 2.03 | 1.00 | 62.4 | 75.1 | 32 |
| 23910 - 5 | 59.44 | 120.53 | 67.5 | 2.03 | 1.00 | 67.5 | 81.1 | 32 |
| 23917 - 1 | 59.52 | 121.14 | 56.8 | 2.04 | 1.00 | 56.8 | 68.6 | 30 |
| 23917 - 2 | 59.56 | 121.12 | 58.3 | 2.03 | 1.00 | 58.3 | 70.4 | 30 |
| 23917 - 3 | 59.42 | 107.77 | 58.0 | 1.81 | 0.98 | 56.9 | 68.8 | 30 |
| 23917 - 4 | 59.60 | 121.23 | 55.5 | 2.03 | 1.00 | 55.5 | 67.1 | 30 |
| 23917 - 5 | 59.62 | 121.25 | 58.8 | 2.03 | 1.00 | 58.8 | 71.0 | 30 |

**Table 19:** Dimensions and results from UCS testing of the cores from Fjørtofta.

| Profile nr. - sample nr. | Dimensions of sample | | Compressive strength | Slenderness (L/d) | Correction factor | Corrected cylinder comp. str. | Cube compressive strength | Age |
|---|---|---|---|---|---|---|---|---|
| | Diameter (mm) | Length (mm) | (MPa) | - | - | (MPa) | (MPa) | (days) |
| 32450 - 1 | 59.58 | 99.35 | 31 | 1.67 | 0.97 | 29.9 | 37.4 | 57 |
| 32450 - 2 | 59.58 | 85.67 | 36 | 1.44 | 0.94 | 33.8 | 42.0 | 57 |
| 32450 - 3 | 59.52 | 99.33 | 37.5 | 1.67 | 0.97 | 36.2 | 44.7 | 57 |
| 32450 - 4 | 59.57 | 111.91 | 29.3 | 1.88 | 0.99 | 29.0 | 36.4 | 57 |
| 32450 - 5 | 59.54 | 111.92 | 38.8 | 1.88 | 0.99 | 38.4 | 47.3 | 57 |
| 32500 - 1 | 59.58 | 74.83 | 61.5 | 1.26 | 0.91 | 56.0 | 67.7 | 50 |
| 32500 - 2 | 59.60 | 60.29 | - | 1.01 | - | - | - | 50 |
| 32500 - 3 | 59.64 | 50.01 | - | 0.84 | - | - | - | 50 |
| 32500 - 4 | 59.65 | 59.8 | 67.5 | 1.00 | 0.85 | 57.4 | 69.3 | 50 |
| 32500 - 5 | 59.6 | 50.25 | - | 0.84 | - | - | - | 50 |
| 32560 - 1 | 59.65 | 122.51 | 47.5 | 2.05 | 1.00 | 47.5 | 57.9 | 42 |
| 32560 - 2 | 59.52 | 122.50 | 50.5 | 2.06 | 1.00 | 50.5 | 61.3 | 42 |
| 32560 - 3 | 59.64 | 122.63 | 52.3 | 2.06 | 1.00 | 52.3 | 63.4 | 42 |
| 32560 - 4 | 59.44 | 122.61 | 50.7 | 2.06 | 1.00 | 50.7 | 61.6 | 42 |
| 32560 - 5 | 59.43 | 101.85 | 53.2 | 1.71 | 0.97 | 51.7 | 62.7 | 42 |

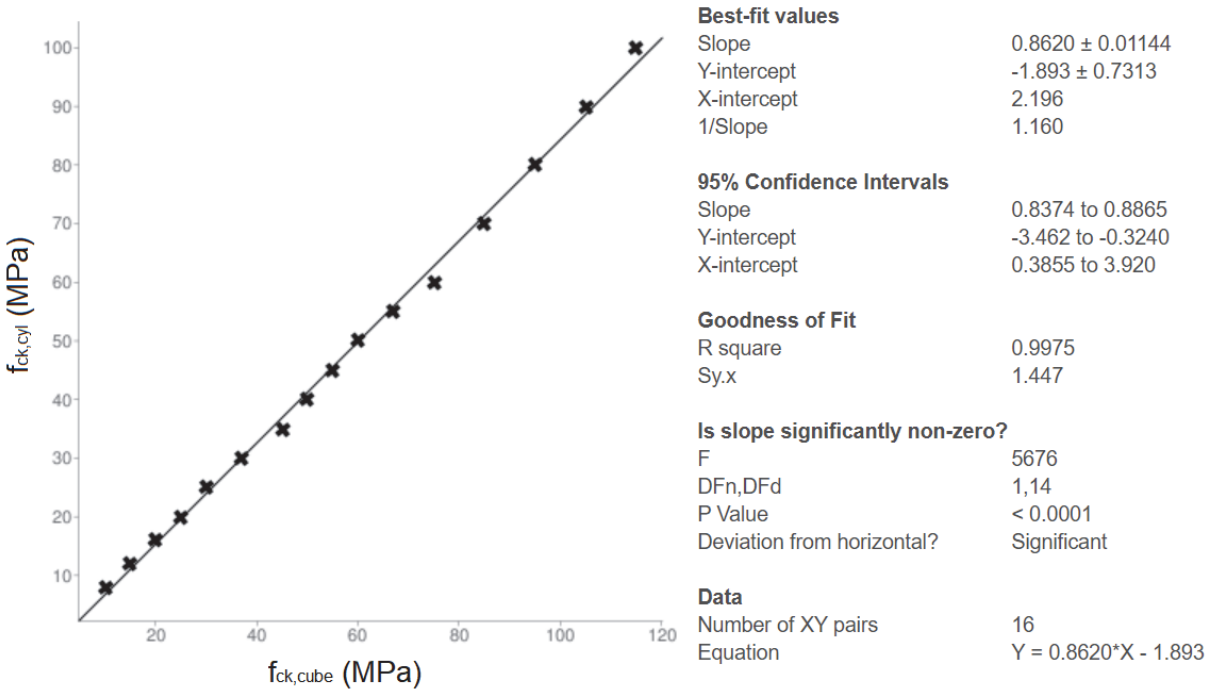


**Figure 85:** Linear regression of the data in table 11. Used to convert cylinder strength to cube strength and vice versa.

## D.2 Density

**Table 20:** Dimensions and density of cores from Longva.

| Profile nr. - sample nr. | Length (mm) | Diameter (mm) | Weight (g) | Volume ($cm^3$) | Density ($kg/m^3$) |
|---|---|---|---|---|---|
| 23903 - 1 | 117.31 | 59.44 | 752.78 | 325.5 | 2313 |
| 23903 - 2 | 120.66 | 59.45 | 773.22 | 334.9 | 2309 |
| 23903 - 3 | 120.69 | 59.50 | 780.19 | 335.6 | 2325 |
| 23903 - 4 | 113.95 | 59.56 | 728.69 | 317.5 | 2295 |
| 23903 - 5 | 112.38 | 59.52 | 718.14 | 312.7 | 2297 |
| 23910 - 1 | 120.34 | 59.44 | 764.75 | 333.9 | 2290 |
| 23910 - 2 | 111.87 | 59.44 | 704.24 | 310.4 | 2269 |
| 23910 - 3 | 120.37 | 59.53 | 767.89 | 335.0 | 2292 |
| 23910 - 4 | 120.52 | 59.49 | 763.54 | 335.0 | 2279 |
| 23910 - 5 | 120.53 | 59.44 | 762.63 | 334.5 | 2280 |
| 23917 - 1 | 121.14 | 59.52 | 754.19 | 337.1 | 2238 |
| 23917 - 2 | 121.12 | 59.56 | 763.79 | 337.5 | 2263 |
| 23917 - 3 | 107.77 | 59.42 | 673.05 | 298.8 | 2252 |
| 23917 - 4 | 121.23 | 59.60 | 758.82 | 338.2 | 2244 |
| 23917 - 5 | 121.25 | 59.62 | 768.29 | 338.5 | 2270 |

**Table 21:** Dimensions and density of cores from Fjørtofta.

| Profile nr. - sample nr. | Length (mm) | Diameter (mm) | Weight (g) | Volume ($cm^3$) | Density ($kg/m^3$) |
|---|---|---|---|---|---|
| 32450 - 1 | 99.35 | 59.58 | 601.70 | 277.0 | 2172 |
| 32450 - 2 | 85.67 | 59.58 | 517.19 | 238.9 | 2165 |
| 32450 - 3 | 99.33 | 59.52 | 603.71 | 276.4 | 2184 |
| 32450 - 4 | 111.91 | 59.57 | 676.51 | 311.9 | 2169 |
| 32450 - 5 | 111.92 | 59.54 | 690.47 | 311.6 | 2216 |
| 32500 - 1 | 74.83 | 59.58 | 464.83 | 208.6 | 2228 |
| 32500 - 2 | 60.29 | 59.60 | 372.14 | 168.2 | 2213 |
| 32500 - 3 | 50.01 | 59.64 | 308.74 | 139.7 | 2210 |
| 32500 - 4 | 59.80 | 59.65 | 373.83 | 167.1 | 2237 |
| 32500 - 5 | 50.25 | 59.60 | 307.39 | 140.2 | 2193 |
| 32560 - 1 | 122.51 | 59.65 | 773.05 | 342.4 | 2258 |
| 32560 - 2 | 122.50 | 59.52 | 771.24 | 340.8 | 2263 |
| 32560 - 3 | 122.63 | 59.64 | 770.37 | 342.6 | 2249 |
| 32560 - 4 | 122.61 | 59.44 | 771.92 | 340.2 | 2269 |
| 32560 - 5 | 101.85 | 59.43 | 636.55 | 282.5 | 2253 |

## D.3 Fibre Content

**Table 22:** Dimensions and fibre content of the cores from Longva.

| Profile nr. - sample nr. | Length (mm) | Diameter (mm) | Weight (g) | Volume ($cm^3$) | Fibre weight (g) | Fibre content ($kg/m^3$) | % Fibre (%) |
|---|---|---|---|---|---|---|---|
| 23903 - 1 | 117.31 | 59.44 | 752.78 | 325.5 | 5.6 | 17.2 | 0.74 |
| 23903 - 2 | 120.66 | 59.45 | 773.22 | 334.9 | 5.9 | 17.7 | 0.77 |
| 23903 - 3 | 120.69 | 59.50 | 780.19 | 335.6 | 6.8 | 20.4 | 0.88 |
| 23903 - 4 | 113.95 | 59.56 | 728.69 | 317.5 | 5.4 | 16.9 | 0.74 |
| 23903 - 5 | 112.38 | 59.52 | 718.14 | 312.7 | 3.9 | 12.5 | 0.54 |
| 23910 - 1 | 120.34 | 59.44 | 764.75 | 333.9 | 9.4 | 28.1 | 1.23 |
| 23910 - 2 | 111.87 | 59.44 | 704.24 | 310.4 | 7.7 | 24.9 | 1.10 |
| 23910 - 3 | 120.37 | 59.53 | 767.89 | 335.0 | 8.9 | 26.7 | 1.16 |
| 23910 - 4 | 120.52 | 59.49 | 763.54 | 335.0 | 10.0 | 29.8 | 1.31 |
| 23910 - 5 | 120.53 | 59.44 | 762.63 | 334.5 | 9.3 | 27.9 | 1.22 |
| 23917 - 1 | 121.14 | 59.52 | 754.19 | 337.1 | 4.9 | 14.4 | 0.64 |
| 23917 - 2 | 121.12 | 59.56 | 763.79 | 337.5 | 5.0 | 14.9 | 0.66 |
| 23917 - 3 | 107.77 | 59.42 | 673.05 | 298.8 | 4.1 | 13.6 | 0.60 |
| 23917 - 4 | 121.23 | 59.60 | 758.82 | 338.2 | 5.5 | 16.4 | 0.73 |
| 23917 - 5 | 121.25 | 59.62 | 768.29 | 338.5 | 4.6 | 13.5 | 0.60 |

**Table 23:** Dimensions and fibre content of the cores from Fjørtofta.

| Profile nr. - sample nr. | Length (mm) | Diameter (mm) | Weight (g) | Volume ($cm^3$) | Fibre weight (g) | Fibre content ($kg/m^3$) | % Fibre (%) |
|---|---|---|---|---|---|---|---|
| 32450 - 1 | 99.35 | 59.58 | 601.70 | 277.0 | 4.2 | 15.1 | 0.70 |
| 32450 - 2 | 85.67 | 59.58 | 517.19 | 238.9 | 2.5 | 10.3 | 0.48 |
| 32450 - 3 | 99.33 | 59.52 | 603.71 | 276.4 | 3.7 | 13.3 | 0.61 |
| 32450 - 4 | 111.91 | 59.57 | 676.51 | 311.9 | 4.8 | 15.4 | 0.71 |
| 32450 - 5 | 111.92 | 59.54 | 690.47 | 311.6 | 6.1 | 19.7 | 0.89 |
| 32500 - 1 | 74.83 | 59.58 | 464.83 | 208.6 | 2.0 | 9.6 | 0.43 |
| 32500 - 2 | 60.29 | 59.60 | 372.14 | 168.2 | 1.9 | 11.2 | 0.51 |
| 32500 - 3 | 50.01 | 59.64 | 308.74 | 139.7 | 1.8 | 13.1 | 0.59 |
| 32500 - 4 | 59.80 | 59.65 | 373.83 | 167.1 | 1.9 | 11.2 | 0.50 |
| 32500 - 5 | 50.25 | 59.60 | 307.39 | 140.2 | 2.1 | 14.7 | 0.67 |
| 32560 - 1 | 122.51 | 59.65 | 773.05 | 342.4 | 7.1 | 20.9 | 0.92 |
| 32560 - 2 | 122.50 | 59.52 | 771.24 | 340.8 | 7.7 | 22.7 | 1.00 |
| 32560 - 3 | 122.63 | 59.64 | 770.37 | 342.6 | 7.7 | 22.5 | 1.00 |
| 32560 - 4 | 122.61 | 59.44 | 771.92 | 340.2 | 6.5 | 19.1 | 0.84 |
| 32560 - 5 | 101.85 | 59.43 | 636.55 | 282.5 | 6.0 | 21.4 | 0.95 |

## D.4 Residual Plots

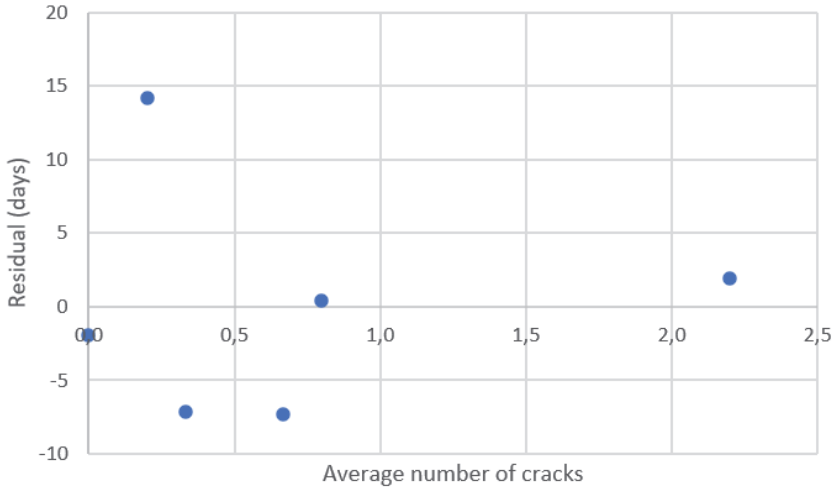


**Figure 86:** Residual plot of the regression line in figure 29 of the cracks plotted against the age of the cores.

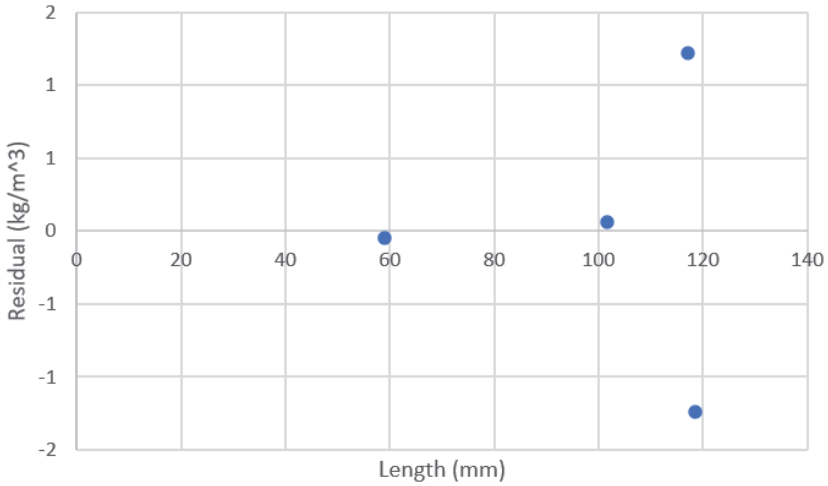


**Figure 87:** Residual plot of the regression lines in figure 39 of the fibre content plotted against the length of the cores.

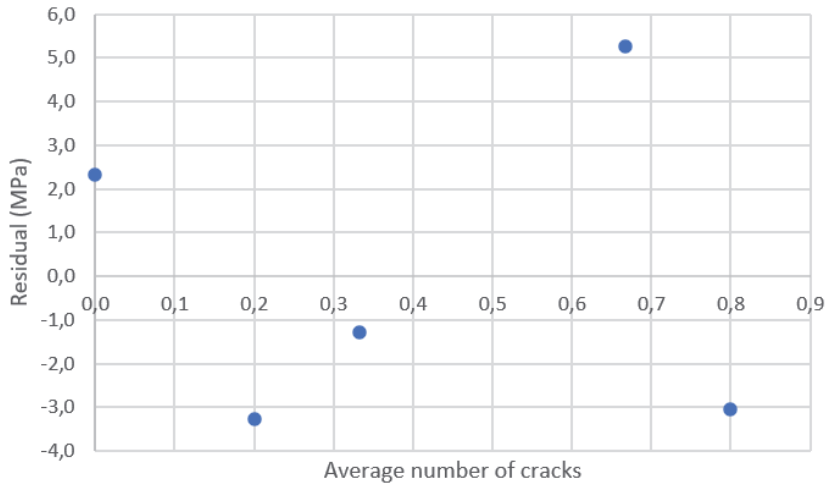


**Figure 88:** Residual plot of the regression line in figure 40 of the cracks plotted against the UCS values.

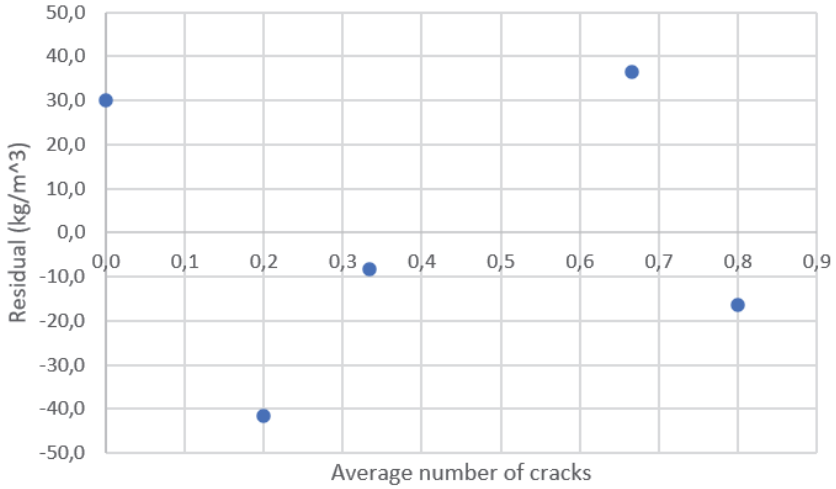


**Figure 89:** Residual plot of the regression line in figure 41 of the cracks plotted against the density measurements.

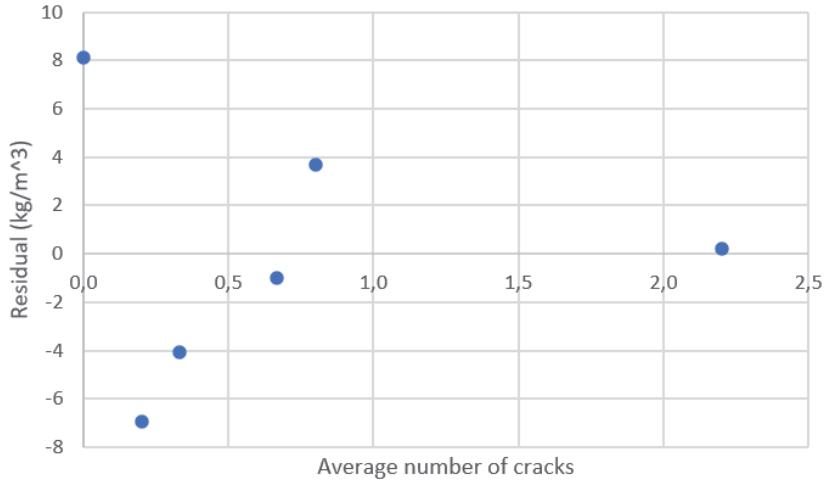


**Figure 90:** Residual plot of the regression line in figure 42 of the cracks plotted against the fibre content measurements.

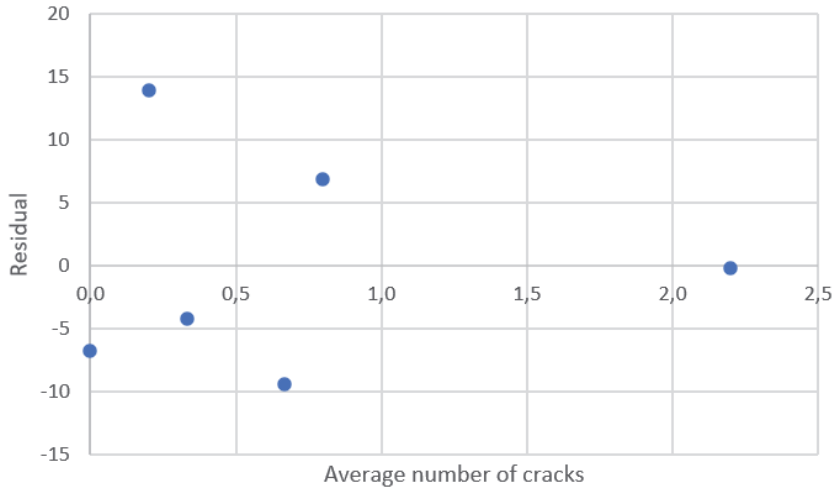


**Figure 91:** Residual plot of the regression line in figure 43 of the cracks plotted against the Q-values.

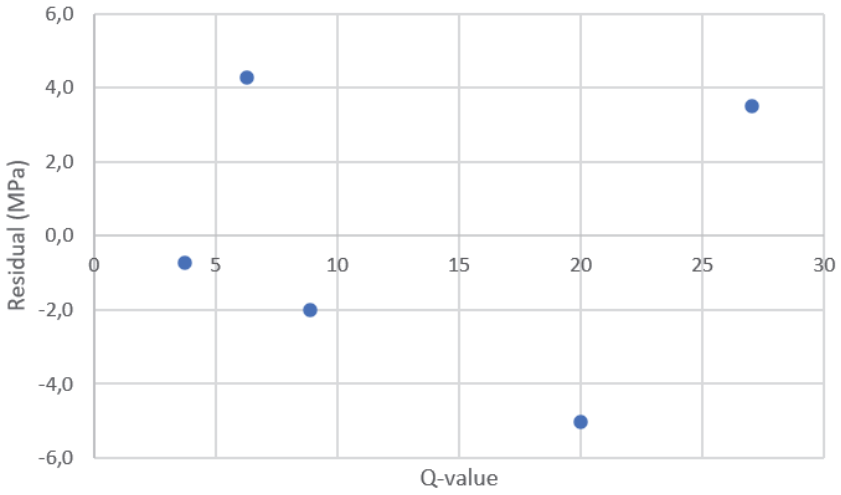


**Figure 92:** Residual plot of the regression line in figure 44 of the Q-values plotted against the UCS values.

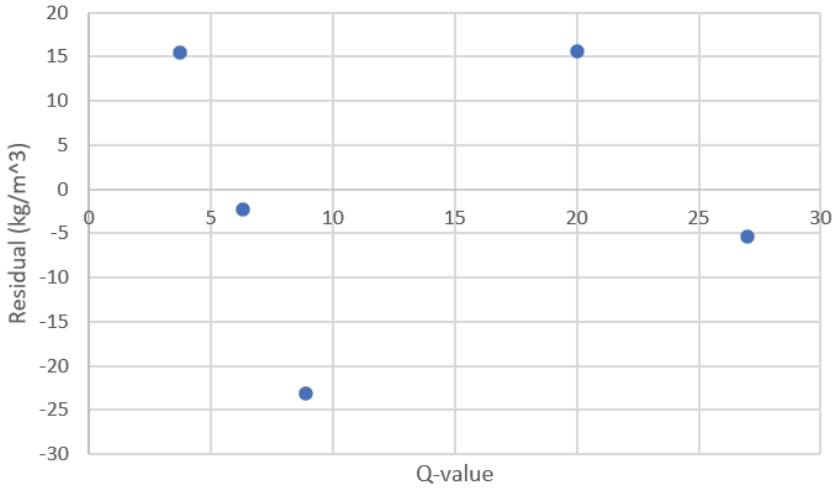


**Figure 93:** Residual plot of the regression line in figure 45 of the Q-values plotted against the density.

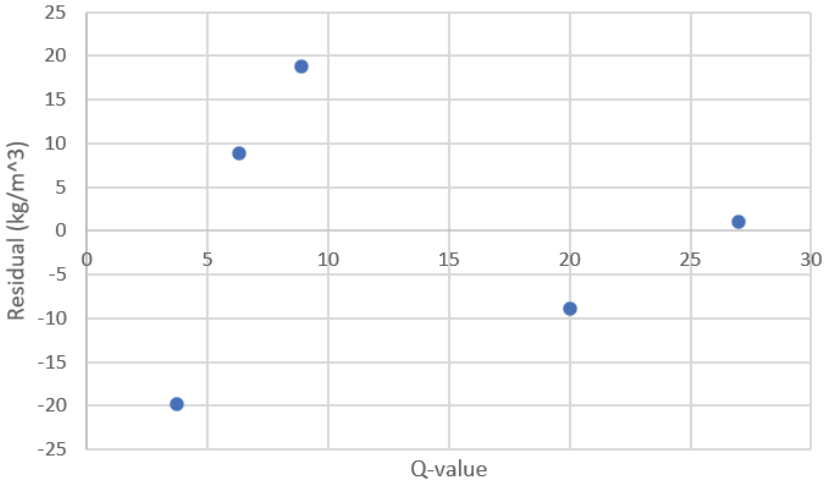


**Figure 94:** Residual plot of the regression line in figure 46 of the Q-values plotted against the deviation of the measured density from the mix design.

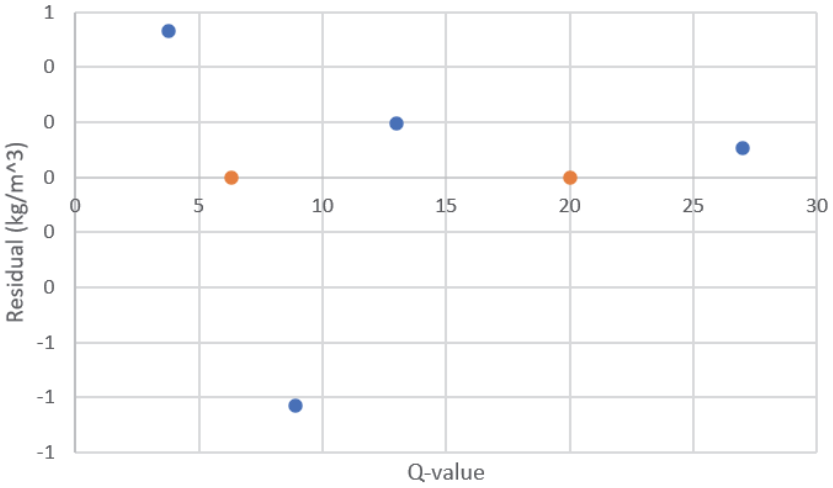


**Figure 95:** Residual plot of the regression line in figure 47 of the Q-values plotted against the fibre content.

## D.5 Photos of Cores Before Testing


**Figure 96:** All the sprayed concrete cores from profile number 23903 in Longva before the testing.

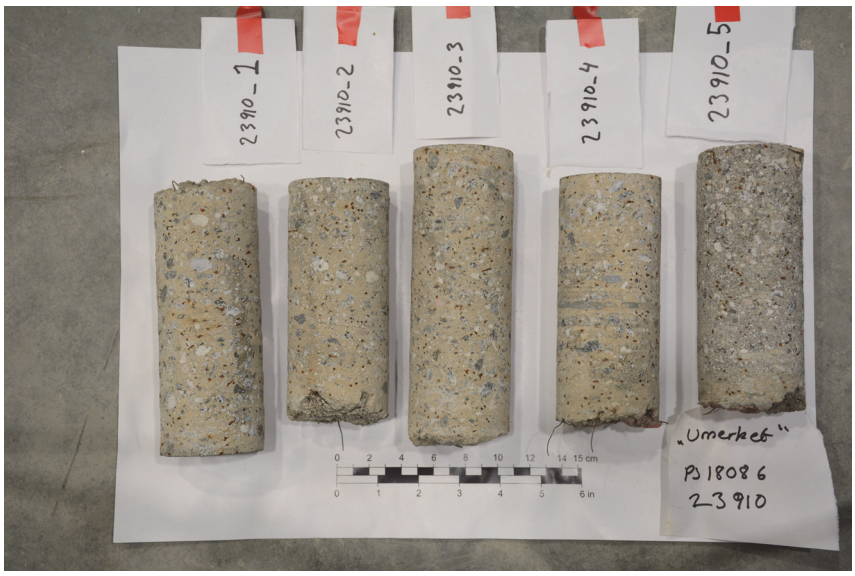


**Figure 97:** All the sprayed concrete cores from profile number 23910 in Longva before the testing.


**Figure 98:** All the sprayed concrete cores from profile number 23917 in Longva before the testing.


**Figure 99:** All the sprayed concrete cores from profile number 32450 in Fjørtofta before the testing.


**Figure 100:** All the sprayed concrete cores from profile number 32500 in Fjørtofta before the testing.


**Figure 101:** All the sprayed concrete cores from profile number 32560 in Fjørtofta before the testing.